

## REVIEW ARTICLE

[View Article Online](#)  
[View Journal](#) | [View Issue](#)

## Designing degradable hydrogels for orthogonal control of cell microenvironments

Cite this: *Chem. Soc. Rev.*, 2013, **42**, 7335Prathamesh M. Kharkar,<sup>a</sup> Kristi L. Kiick<sup>\*abc</sup> and April M. Kloxin<sup>\*ad</sup>

Degradable and cell-compatible hydrogels can be designed to mimic the physical and biochemical characteristics of native extracellular matrices and provide tunability of degradation rates and related properties under physiological conditions. Hence, such hydrogels are finding widespread application in many bioengineering fields, including controlled bioactive molecule delivery, cell encapsulation for controlled three-dimensional culture, and tissue engineering. Cellular processes, such as adhesion, proliferation, spreading, migration, and differentiation, can be controlled within degradable, cell-compatible hydrogels with temporal tuning of biochemical or biophysical cues, such as growth factor presentation or hydrogel stiffness. However, thoughtful selection of hydrogel base materials, formation chemistries, and degradable moieties is necessary to achieve the appropriate level of property control and desired cellular response. In this review, hydrogel design considerations and materials for hydrogel preparation, ranging from natural polymers to synthetic polymers, are overviewed. Recent advances in chemical and physical methods to crosslink hydrogels are highlighted, as well as recent developments in controlling hydrogel degradation rates and modes of degradation. Special attention is given to spatial or temporal presentation of various biochemical and biophysical cues to modulate cell response in static (*i.e.*, non-degradable) or dynamic (*i.e.*, degradable) microenvironments. This review provides insight into the design of new cell-compatible, degradable hydrogels to understand and modulate cellular processes for various biomedical applications.

Received 1st February 2013

DOI: 10.1039/c3cs60040h

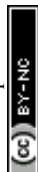
[www.rsc.org/csr](http://www.rsc.org/csr)

## 1. Introduction

Cells *in vivo* interact with biochemical and biophysical cues within their surrounding microenvironment, and such interactions influence cell behavior, function, and fate. The cell microenvironment comprises the extracellular matrix (ECM) proteins, soluble and sequestered bioactive factors, and neighboring cells. Microenvironment biochemical cues, such as receptor binding to ECM proteins or cytokines, and biophysical cues, such as modulus and fibrillar structure, play a vital role in cell fate decisions, from quiescence to activation and progenitor state to terminal differentiation. These fundamental cell–ECM interactions are highly dynamic in nature, as cells interact with and respond to ECM signals and subsequently remodel their surroundings. Understanding and harnessing this bidirectional cross talk between the microenvironment and resident cells is pivotal in strategies to regenerate tissue or regulate disease.

Although classic biomaterials, such as metals, ceramics, and synthetic polymers, have been used to successfully replace the mechanical function of tissues, such as teeth or hip and knee joints, their use as ECM mimics for tissue engineering has been limited.<sup>1</sup> Given that hydrogels demonstrate many properties similar to those of the ECM, an ever-increasing number of hydrogel-based materials have been developed to study and direct cell behavior.<sup>2</sup> Hydrogels comprise hydrophilic cross-linked polymers that contain significant amounts of water and maintain a distinct three dimensional structure.<sup>3</sup> The high water content, elasticity, and diffusivity of small molecules in these materials make them attractive candidates for mimicking soft tissue microenvironments as well as serving as reservoirs for water-soluble cytokine and growth factor delivery. Hydrogels also offer great potential to mimic the dynamic, native ECM due to the ease of tailoring their physiochemical and mechanical properties through the incorporation of degradable moieties and orthogonal chemistries.<sup>4–6</sup>

The building blocks for constructing synthetic, biomimetic microenvironments and manipulating native *in vivo* microenvironments are rapidly expanding. Synthetic ECMs have been used *in vitro* to support cells and modulate their behavior and to provide triggered, sustained release of bioactive molecules.

<sup>a</sup> Department of Materials Science and Engineering, University of Delaware, Newark, DE 19716, USA. E-mail: [kiick@udel.edu](mailto:kiick@udel.edu), [akloxin@udel.edu](mailto:akloxin@udel.edu)<sup>b</sup> Biomedical Engineering, University of Delaware, Newark, DE 19716, USA<sup>c</sup> Delaware Biotechnology Institute, University of Delaware, Newark, DE 19716, USA<sup>d</sup> Department of Chemical and Biomolecular Engineering, University of Delaware, Newark, DE 19716, USA

Additionally, hydrogels have been increasingly employed for delivering cells and therapeutics within the *in vivo* microenvironment.<sup>7–9</sup> In this review, we aim to provide a comprehensive survey of these building blocks and to overview seminal and recent works utilizing chemistries that are degradable, orthogonal, or both to permit control of biochemical or biophysical signals in the cell microenvironment (Fig. 1). Providing criteria (Section 2) and context for controlling properties in the presence of biological systems, we will summarize (i) natural

and synthetic polymers that are commonly employed as the hydrogel base (Section 3), (ii) reactive functional groups for hydrogel formation (Section 4), and (iii) degradable moieties for temporal evolution of physical or biochemical properties (Section 5). We subsequently examine how these degradable groups are being used in conjunction with orthogonal chemistries for probing and regulating cell function in regenerative medicine and integrative biology applications (Section 6).

## 2. Design considerations

Hydrogels that permit orthogonal control of multiple properties in the cell microenvironment must meet a number of biological and physical design criteria that are dictated by the intended application (Fig. 2). For example, hydrogels for three-dimensional (3D) cell culture or delivery must be crosslinked in presence of cells while maintaining cell viability; additionally, they need to mimic critical aspects of the natural ECM, such as mechanical support and degradation, to enable appropriate and desired cellular functions, such as proliferation and protein secretion.<sup>7,10,11</sup> In this section, we will address these challenges and provide perspective on key design criteria for producing cell-compatible hydrogels with properties that can be orthogonally controlled both in space and in time.

### 2.1 Biocompatibility

Biocompatibility is the first, and perhaps the most critical, parameter when considering the application of hydrogels in the cellular microenvironment. Biocompatibility is defined as the ability of a biomaterial to perform its desired function without



**Prathamesh M. Kharkar**

*Prathamesh M. Kharkar is currently pursuing a PhD in Materials Science and Engineering at the University of Delaware, where he is developing multi-mode degradable hydrogels for the controlled release of bioactive molecules under the supervision of Professor April Kloxin and Professor Kristi Kiick. He received his BS in Polymers and Coatings from the University Institute of Chemical Technology (UDCT, India), MS in Polymer Science from Joseph Fourier University (France), and subsequently worked as a research engineer under the guidance of Professor Catherine Picart at the Grenoble Institute of Technology. His main research interests include biomaterials for drug delivery and tissue engineering.*



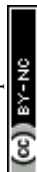
**Kristi L. Kiick**

*Kristi Kiick is a Professor of Materials Science and Engineering, Professor of Biomedical Engineering, and Deputy Dean of the University of Delaware College of Engineering. She holds a BS from UD and an MS in Chemistry (as an NSF Predoctoral Fellow) from the University of Georgia. She worked as a research scientist at Kimberly Clark Corporation before obtaining a PhD in Polymer Science and Engineering from the University of Massachusetts Amherst after completing her doctoral research as an NDSEG Fellow at the California Institute of Technology. She joined the UD faculty in 2001. Her current research is focused on combining biosynthetic techniques, chemical methods, and bioinspired assembly strategies for the production of advanced multifunctional biomaterials. Kiick's honors have included a Beckman Young Investigator Award, an NSF CAREER Award, a DuPont Young Professor Award, and induction into the College of Fellows of the American Institute for Medical and Biological Engineering.*



**April M. Kloxin**

*April M. Kloxin, PhD, is an Assistant Professor in the Department of Chemical & Biomolecular Engineering, Department of Materials Science & Engineering, and Biomedical Engineering (affiliate) at the University of Delaware. She obtained her BS (Summa Cum Laude) and MS in Chemical Engineering from North Carolina State University and PhD in Chemical Engineering from the University of Colorado, Boulder, as a NASA GSRP Fellow. She trained as a Howard Hughes Medical Institute post doctoral research associate at the University of Colorado before joining the faculty at the University of Delaware in 2011. Her research group focuses on the design of responsive biomaterials and development of controlled, dynamic models of disease and tissue repair. Kloxin's prior honors include an NSF CAREER Award, the Western Association of Graduate Schools Innovation in Technology Award, the Max S. Peters Outstanding Graduate Research Award, and the ACS Polymer Chemistry Division Excellence in Graduate Polymer Research Award.*



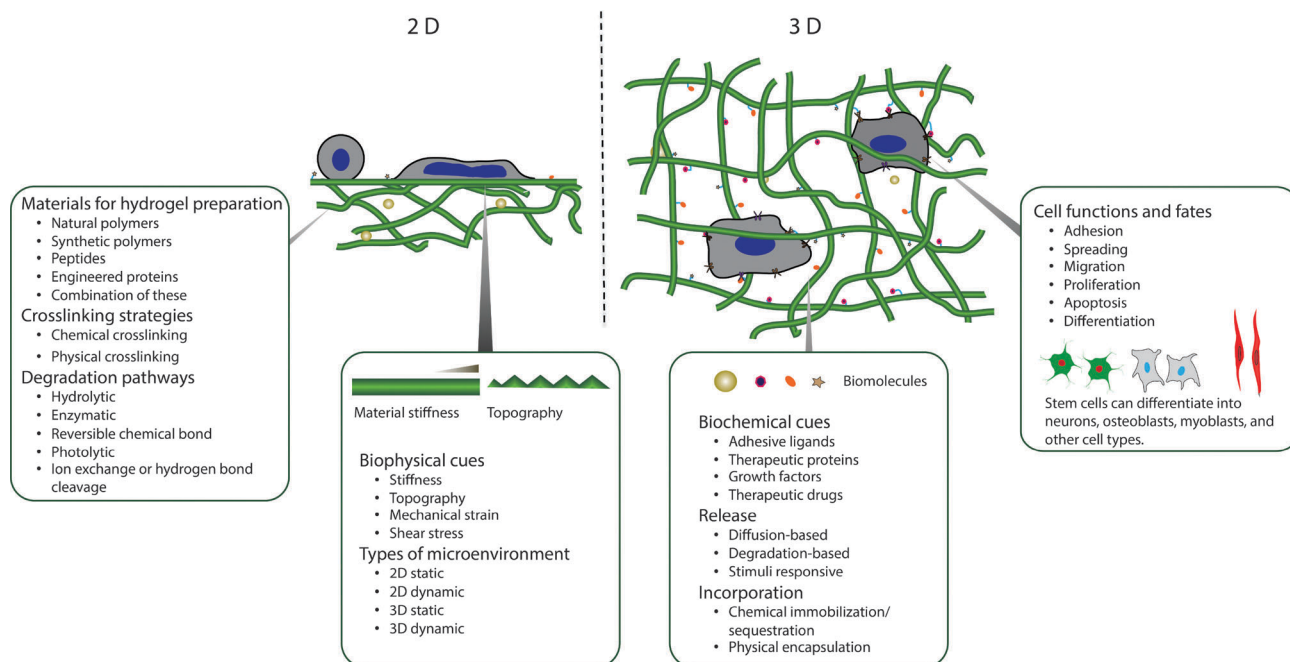


**Fig. 1** Overview. Degradable hydrogels can be used for orthogonal control of multiple properties in both two- and three-dimensional (2D and 3D) cellular microenvironments.

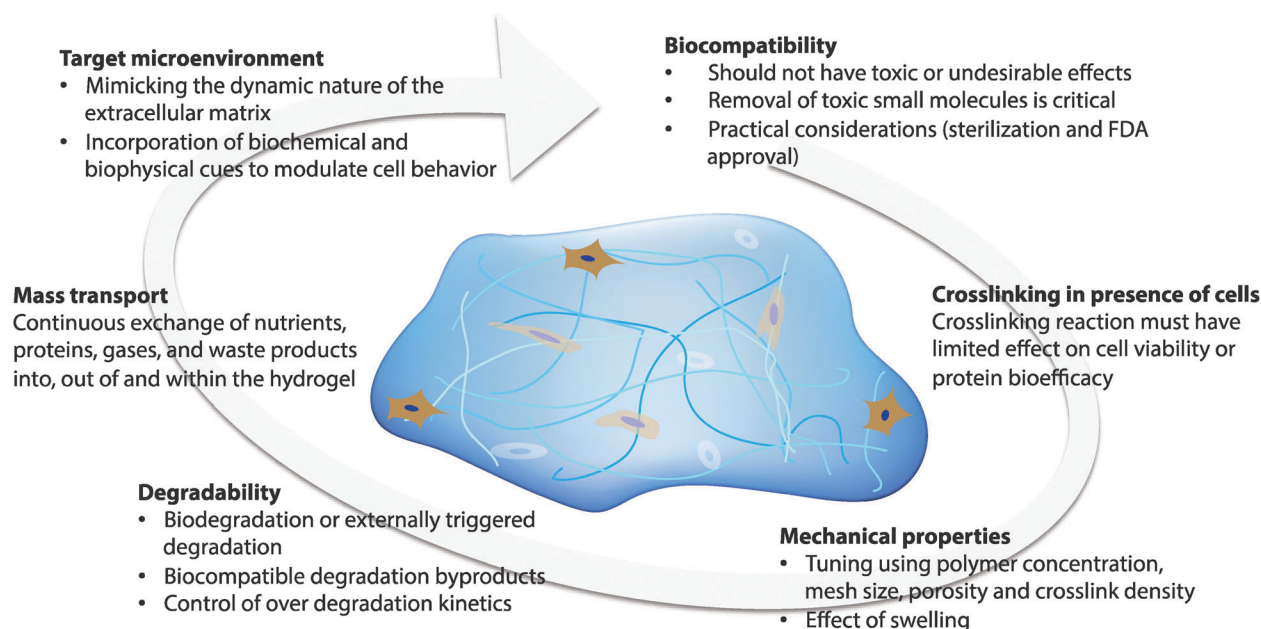
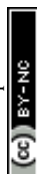


**Fig. 2** Design considerations. The design of hydrogels for orthogonal property control in cellular microenvironments is dictated by the biocompatibility, crosslinking in presence of cells or proteins, mechanical properties, degradability, mass transport properties, and target microenvironment.

eliciting any undesirable local or systemic side effects.<sup>12</sup> The hydrogel must be immunocompatible and not elicit a significant inflammatory response for use within *in vivo* microenvironments. Various naturally derived polymers (e.g., polysaccharides such as hyaluronic acid) and a few synthetic polymers (e.g., polyethylene glycol) have demonstrated adequate biocompatibility. Removal of small molecules used or generated

during hydrogel fabrication (such as unreacted monomer, initiator, and crosslinkers) is essential to consider during material design, as such molecules can be toxic to host cells both *in vivo* and *in vitro*. For example, unreacted maleimides, which are widely used in Michael-type addition reactions, are highly potent neurotoxins;<sup>13</sup> similarly, photoinitiators, such as 2,2-dimethoxy-2-phenyl-acetophenone used frequently in free-radical polymerization, can be cytotoxic.<sup>14</sup>





In addition, the hydrogel or its base components need to be simple to sterilize and should not undergo any significant functional changes during sterilization. Further, hydrogels for implantation also need to meet appropriate regulatory body (*i.e.*, FDA, EPA) guidelines. Synthetic polymers, such as PEG, PLGA, and PLA, and natural polymers, such as alginate, collagen and fibrin, have been approved for specific clinical applications by the FDA. Kim and Wright recently investigated use of FDA-approved DuraSeal™, a PEG based hydrogel used as a sealant for human spinal fluid leaks.<sup>15</sup> In a clinical trial with a total of 158 patients, it was found that DuraSeal™ spinal sealant had a significantly higher rate of intraoperative watertight dural closure (100%) compared to the control (*i.e.*, treated with traditional methods, 65%). In addition, no significant statistical differences were seen in postoperative infection and healing between the PEG hydrogel and the control group. Overall, the PEG hydrogel spinal sealant system was found to be an efficient and safe adjunct to suturing for watertight dural repair. Such biocompatible and clinically tested hydrogels (*i.e.*, DuraSeal™, Evolence®, TachoSil™, Tisseel Artiss™, Tegagel™), which are commercially available, cost effective, easy to use and have a stable shelf life (ranging from 6 months to 36 months) along with well defined *in vivo* stability, hold potential for bioengineering applications, such as wound healing, tissue engineering, 3D cell culture and vascular surgeries.<sup>16</sup>

## 2.2 Crosslinking in presence of cells

The ability to form hydrogels in the presence of cells and cargo molecules is critical for creating three-dimensional, controlled microenvironments *in vitro* and offers several advantages *in vivo*, including the ability to mold the gel to the shape of the defect site and delivery in a minimally invasive way. The chemical transformations involved in hydrogel formation, however, can be damaging to cells, and such effects must be considered for both *in vitro* and *in vivo* microenvironments. For example, free radicals can cause damage to cell membranes or detrimental loss of the pericellular matrix during cell isolation and encapsulation.<sup>17,18</sup> Sudden localized changes in temperature, pH, and free radicals during gelation also can affect the activity of cargo molecules (*e.g.*, oxidation of protein) or cell function or viability.<sup>19</sup> However, the incorporation of cells in pre-formed hydrogels is often restricted, since the average mesh size of most hydrogels is much smaller than a cell's diameter; consequently, cells often are introduced within liquid hydrogel precursor solutions.<sup>20</sup> By selecting an appropriate gelation mechanism, cells can be encapsulated in hydrogels without significantly altering their viability or activity.<sup>21–23</sup> Different chemistries for hydrogel formation in the presence of cells and their cytocompatibility will be discussed in detail within Section 4.

## 2.3 Mechanical properties

The success of cell-compatible hydrogels in a given bioengineering application is usually coupled with achieving appropriate mechanical properties. For example, tissue formation can depend on the mechanical properties of the hydrogel scaffold (*e.g.*, load bearing capability until cells have produced their own

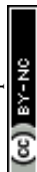
functional ECM);<sup>24,25</sup> in cell-encapsulation applications, control of the mechanical properties of the hydrogel can determine the therapeutic efficacy of the transplanted cells.<sup>26</sup> It is well accepted that these effects are the result of the mechanical properties of the hydrogel substrate influencing cellular responses, including cell migration, proliferation, and differentiation; for example, the seminal work of Discher and coworkers demonstrated that stem cell lineage specification depends on optimal outside-in signaling of hydrogel matrix elasticity.<sup>27,28</sup> Polymer concentration, the stoichiometry of reactive groups, and crosslinking density are all commonly used to tune the mechanical properties of cell-compatible hydrogels and accordingly to control the cellular microenvironment.<sup>29–31</sup> The mechanism and design considerations associated with mechanotransduction were recently reviewed by Chen and coworkers,<sup>32</sup> and relevant examples within the context of degradable cell microenvironments will be presented in Sections 5 and 6.

## 2.4 Degradation

Cell-compatible hydrogels can be designed to degrade *via* ester hydrolysis, enzymatic hydrolysis, photolytic cleavage or a combination of these mechanisms with varying degrees of control and desired degradation rates depending on the application. In tissue engineering applications, degradation provides space for proliferating cells and allows infiltration of blood vessels.<sup>33,34</sup> In controlled 3D cell culture applications, degradation can enable cell proliferation, migration, and synthetic matrix remodeling to better mimic the native ECM and understand *in vivo* cell behaviors.<sup>2</sup> In controlled drug and gene delivery applications, degradation permits spatiotemporal control of the release of cargo molecules.<sup>35</sup> Release kinetics are dictated primarily by surface erosion or bulk degradation rates when the hydrogel mesh size is smaller than the hydrodynamic radius of the cargo molecule, and by diffusion when mesh size is larger than the hydrodynamic radius of cargo molecule. For example, Hennink and coworkers demonstrated zero-order release of entrapped proteins from  $\beta$ -cyclodextrin and cholesterol-derivatized PEG hydrogels,<sup>36</sup> in which the protein release was controlled by surface erosion and dissolution. Ideally, degradation kinetics are well controlled and stable, and the generated byproducts from degradation are biocompatible without eliciting any potential side effects, such as cytotoxicity, inflammation, or immunological or foreign body responses. An optimum balance between degradability and mechanical properties, such as elastic modulus and matrix integrity, is vital to ensure the proper functionality of the hydrogel within the desired timespan.

## 2.5 Mass transport

Appropriate mass transport properties, matching those of native tissues, are essential for many bioengineering applications. In tissue engineering and cell encapsulation, continuous exchange of nutrients, proteins, gases (*i.e.*, O<sub>2</sub> and CO<sub>2</sub>) and waste products into, out of, or within the hydrogel is vital for survival and proliferation of encapsulated cells. For controlled delivery of bioactive cargo (*i.e.*, therapeutics, proteins) where initial burst is undesirable, restricted free diffusion is essential. Hydrogel matrix



permeability is thus an important design parameter, given that mass transport in these materials is controlled primarily by diffusion. The permeability of the scaffold is also correlated with the mechanical properties of the hydrogel network and its swelling properties, and as expected, variation in the permeability is a widely employed strategy for controlling cargo release.<sup>37–39</sup> For a comprehensive review of the mass transport and diffusivity of bioactive molecules through hydrogel, readers are referred to reviews by Peppas and coworkers<sup>10,40</sup> and Lin and Metters.<sup>41</sup>

## 2.6 Microenvironment

A major, and still mainly unaddressed, challenge in designing cell-compatible hydrogels is the ability to mimic the dynamic nature of the extracellular matrix (ECM). Spatiotemporal control over biological interactions at the material–cell interface, whether that material is native ECM or an engineered hydrogel, mediate cell proliferation, adhesion, migration, and receptor–ligand binding events. The challenge of controlling these interactions is particularly vexing, given that the ECM is a complex environment comprising a plethora of structural ECM proteins (such as collagen, fibronectin, laminin, and elastin), polysaccharides (such as hyaluronic acid, proteoglycans, and glycosaminoglycans), and various growth factors, enzymes, and inhibitors.<sup>42</sup> Bidirectional cross talk between the microenvironment and resident cells is termed ‘dynamic reciprocity’,<sup>43,44</sup> and opportunities to generate matrices capable of this reciprocity are afforded by multiple strategies, among the most recent being the rational incorporation of degradable chemistries in hydrogel networks (Section 4) and their application in controlled microenvironments (Section 6).

Several recent publications have addressed the importance of incorporating ECM components into hydrogel matrices to mimic the native cellular microenvironment for cell survival, proliferation, and differentiation.<sup>45–49</sup> For a comprehensive review of engineering hydrogels as extracellular matrix mimics, readers are referred to reviews by Geckill *et al.*<sup>50</sup> and Tibbitt *et al.*,<sup>2</sup> and for reviews of engineering matrices specifically for directing stem cells, readers are directed to Marklein *et al.*<sup>51</sup>

Natural polymers such as polysaccharides serve as ideal building blocks for preparing hydrogels that can mimic aspects of the structural and biological properties of the cellular microenvironment. For instance, proteoglycans are one of the vital components of articular cartilage, and use of glycosaminoglycan (GAG) hydrogels, such as those based on hyaluronic acid or chitosan, as a scaffold can be useful for cartilage tissue engineering.<sup>52</sup> Moreover, as shown in Table 1, the mechanical properties, water content, and inherent chain flexibility of polysaccharide-based hydrogels help to mimic the natural ECM. In addition, such polymers can be degraded by naturally occurring cell-secreted enzymes in the cellular microenvironment, mimicking the dynamic nature of the ECM. Further, the specific cell–surface receptors for polysaccharides are known and have been extensively studied. For example, in the case of hyaluronic acid (HA), a non-sulfated glycosaminoglycan found in the ECM, both cluster of differentiation (CD) 44 and the receptor for hyaluronan-mediated motility (RHAMM) are known to enable cell adhesion and proliferation on HA.<sup>53</sup> However, limited tunability of degradation kinetics, relatively poor mechanical properties, batch-to-batch variations from manufacturers, or potential immunogenic reactions can restrict the application of natural polymer based hydrogels.<sup>54</sup> Synthetic polymers afford tunable mechanical properties and a large scope of chemical modification, including the introduction of degradable or biochemical moieties. Commercial availability, coupled with great flexibility in the working range of pH, ionic strength, and chemical conditions, make synthetic polymers excellent candidates for hydrogel preparation. However, purely synthetic materials often exhibit inferior biocompatibility and biodegradability in comparison to naturally derived materials, which may limit their use in applications where targeted and specific biological activity is desired. Hence, many combinations of natural and synthetic polymers have been studied for developing hydrogels with orthogonal property control in the cellular microenvironment. In this section, we will limit the discussion to several widely used natural and synthetic polymer building blocks used in controlled microenvironments.

## 3. Materials for hydrogel preparation

Cell-compatible hydrogels have been prepared using a variety of polymeric materials, which can be divided broadly into two categories according to their origin: natural or synthetic.<sup>7</sup>

### 3.1 Hydrogels from natural polymers

**3.1.1 Hyaluronic acid.** Hyaluronate or HA is a non-sulfated GAG in the ECM that is distributed throughout connective, epithelial, and neural tissues. This GAG is composed of alternating

**Table 1** Selecting materials for hydrogel preparation. Comparison of natural and synthetic polymers typically used for preparation of cell compatible hydrogels

Feature/function	Natural polymers	Synthetic polymers
Biocompatibility	Polymer dependent	Polymer dependent
Bioactivity ( <i>i.e.</i> cell specific receptor)	Possible	Limited
Inherent biodegradability	✓✓	✓
Tunability of degradation kinetics	✓	✓✓
Degradation byproducts	Biocompatible	Potentially harmful
Flexibility for chemical modification	✓	✓✓
Flexibility of working range ( <i>i.e.</i> pH and ionic strength)	✓	✓✓
Tuning of mechanical properties	✓	✓✓
Commercial availability	✓	✓✓
Batch to batch variations	Likely	Controlled



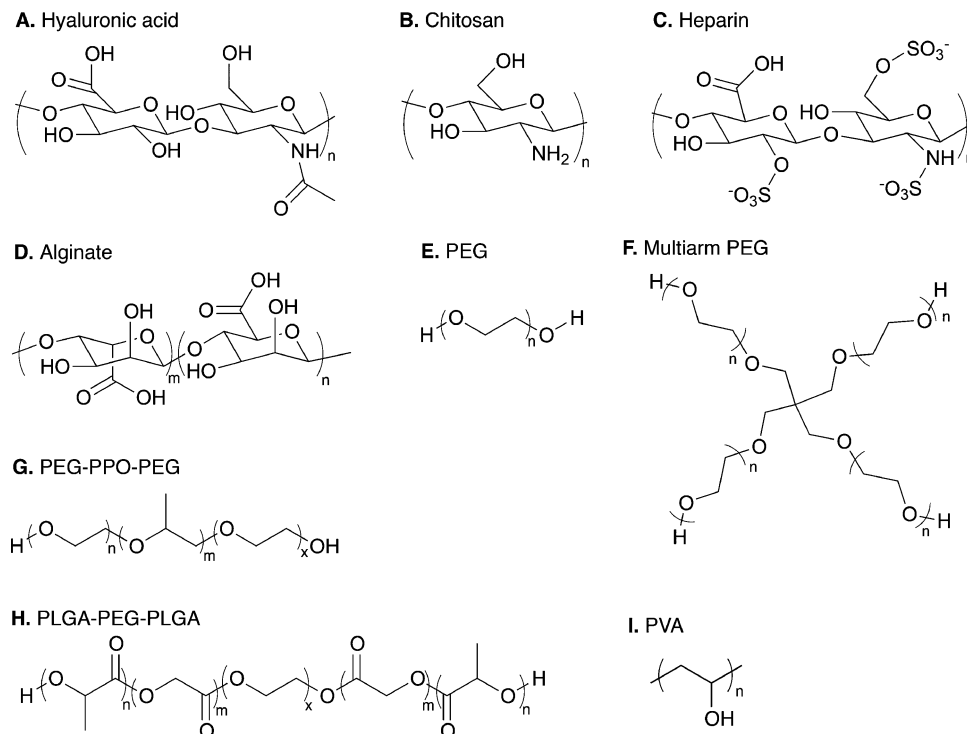


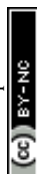
**Fig. 3** Range of natural and synthetic polymer building blocks. Molecular structures of typical polymer repeat units used for preparation of cell compatible hydrogels: (A) hyaluronic acid, (B) chitosan, (C) heparin, (D) alginate, (E) linear poly(ethylene glycol) (PEG), (F) four-arm PEG, (G) poly(ethylene glycol)-*b*-poly(propylene oxide)-*b*-poly(ethylene glycol) (PEG-PPO-PEG), (H) poly(lactic acid-co-glycolic acid)-*b*-poly(ethylene glycol)-*b*-poly(lactic acid-co-glycolic acid) (PLGA-PEG-PLGA), and (I) poly(vinyl alcohol).

disaccharide units of D-glucuronic acid and N-acetyl-D-glucosamine linked together with  $\beta$ -1,4 and  $\beta$ -1,3 glycosidic bonds (Fig. 3A).<sup>55</sup> HA is inherently biocompatible and non-immunogenic and degrades in the presence of hyaluronidase as well as in the presence of reactive oxygen species. HA is a critical component of the ECM and plays an important role in various biological processes, including wound healing, angiogenesis, and activation of various signaling pathways that direct cell adhesion, cytoskeletal rearrangement, migration, proliferation, and differentiation.<sup>56–59</sup> Although concerns over batch-to-batch variation and the possibility of contamination with endotoxins and pathogenic factors persist, recent developments in recombinant technology have significantly improved the quality of commercially-available HA.<sup>60,61</sup> However, the rapid degradation of HA in the presence of hyaluronidase can hinder its usefulness in certain applications. For example, approximately one-third of the typical fifteen grams of HA found in a human is degraded and re-synthesized daily.<sup>62</sup> Limited control over HA degradation kinetics (*i.e.*, rapid degradation) can lead to precipitate changes in mechanical properties, such as hydrogel stiffness, which may be undesirable in certain bioengineering applications.

HA can be modified with thiols, haloacetates, dihydrazides, aldehydes, or carbodiimide functional groups to allow cross-linking into hydrogels.<sup>63</sup> HA-based hydrogels have shown excellent potential for biomedical engineering applications, such as tissue engineering,<sup>64–66</sup> valve regeneration,<sup>67,68</sup> controlled delivery,<sup>69–72</sup> and controlling stem cell behavior.<sup>73,74</sup> For example, Jia and

coworkers synthesized HA- and heparin-based spherical hydrogel particles with an inverse emulsion polymerization, creating inherently bioactive delivery vehicles (due to inductive role of HA in chondrogenesis) for controlled growth factor (BMP-2) release (Fig. 4).<sup>75</sup> Additionally, Elia *et al.* used HA-based degradable hydrogels embedded within electrospun silk for sustained release of encapsulated cargo molecules (anti-inflammatory steroid drugs and proteins) over 45 to 400 minutes.<sup>72</sup> Such approaches that utilize simple fabrication techniques and tuning of release kinetics make HA hydrogels attractive candidates for tissue regeneration and sustained therapeutic delivery. For a comprehensive overview of HA hydrogels, readers are referred to recent reviews by Burdick and Prestwich<sup>63</sup> and by Jia and coworkers.<sup>46</sup>

**3.2.2 Chitosan.** Chitosan, the deacetylated derivative of chitin, is a linear polycationic polysaccharide composed of randomly distributed  $\beta$ -(1-4)-linked D-glucosamine and N-acetyl-D-glucosamine (Fig. 3B). The structural units of chitosan are similar to those of GAGs of the ECM.<sup>76</sup> It can be degraded by various mechanisms, including surface erosion, enzymatic degradation through chitosanase and lysozyme, and dissolution.<sup>77</sup> By using appropriate crosslinking chemistries and densities, the degradation kinetics can be tuned. The inherent properties of chitosan, such as excellent cytocompatibility, biodegradation, minimal foreign body response, and antimicrobial properties, make chitosan-based hydrogels attractive candidates for engineering applications, including wound-healing, bioactive molecule delivery and soft tissue engineering.



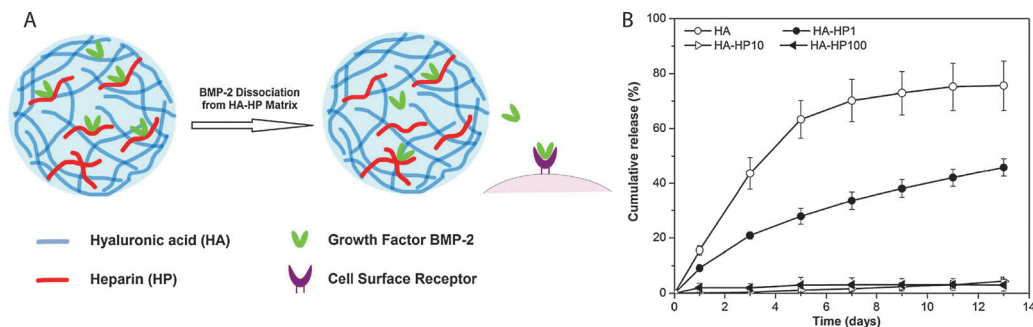


**Fig. 4** Hyaluronic acid hydrogels for controlled release applications. (A) HA/heparin hydrogel particles were synthesised by inverse emulsion polymerization and amount of heparin in hydrogel particle was varied. BMP-2 was subsequently loaded. (B) The addition of heparin to HA hydrogel particles influenced the *in vitro* release of BMP-2 from hydrogels with higher heparin content, with less than 5% of loaded BMP-2 released over 13 days (HA-HPx, x = micrograms of heparin per milligram in hydrogel particles). Reprinted from Xu *et al.*<sup>75</sup> with permission from Elsevier. Copyright (2011).

The large number of accessible hydroxyl and amine groups in chitosan provide numerous possibilities to create hydrogels *via* chemical crosslinking.<sup>78</sup> These functional groups can react with many bifunctional small molecule crosslinkers, such as glutaraldehyde, formaldehyde, genepin, diethyl squarate and diacrylate, to form chemically crosslinked hydrogels.<sup>79</sup> In addition, incorporation of new functionalities along the backbone chain (*i.e.*, those susceptible to the Schiff base reaction, disulfide bonding or Michael-type additions, Section 4) can be used for *in situ* gel formation. Chitosan-based hydrogels can be used for the controlled delivery of drugs,<sup>79,80</sup> proteins,<sup>80</sup> and growth factors<sup>81</sup> as well as the encapsulation of living cells,<sup>81,82</sup> the controlled differentiation of stem cells,<sup>83,84</sup> and applications in tissue engineering.<sup>85–88</sup> For example, Bellamkonda and coworkers recently reported chitosan-based photocrosslinkable, degradable hydrogels for neural tissue engineering application (Fig. 5).<sup>88</sup> Chitosan was functionalized with amino-ethyl methacrylate for network formation *via* photoinitiated radical polymerization.

The cytocompatible hydrogel enhanced differentiation of primary cortical neurons by ~30% and enhanced dorsal root ganglia neurite extension by about two-fold in 3D *in vitro* studies, as compared to an agarose-based hydrogel control. In principle, such hydrogels additionally can be used to control cell behavior and lineage specific differentiation by incorporation of growth factors since the gel formation chemistry does not alter the active end groups on chitosan, which allow bioactive molecule binding.

**3.2.3 Heparin.** Heparin is a heterogeneous GAG, consisting of  $\alpha$ -L-iduronic acid,  $\beta$ -D-glucuronic acid, and  $\alpha$ -D-glucosamine residues (Fig. 3C). Heparin has the highest negative charge density of any known biological macromolecule giving rise to ionic interactions with bioactive molecules such as proteins, growth factors, and cytokines.<sup>89,90</sup> Such noncovalent interactions of heparin in many cases serve not only to sequester the proteins, but also to control their biological activity (*e.g.*, enhancing cell receptor affinity).<sup>89</sup> Heparin and heparan sulfate mediate a

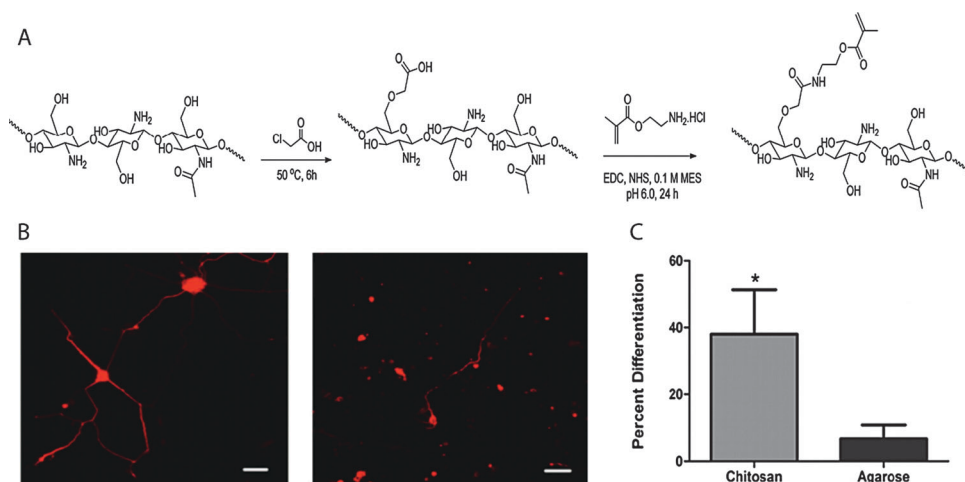


**Fig. 5** Chitosan-based hydrogels for neural tissue engineering. (A) Schematic of synthesis of methacrylated chitosan. Methacrylated chitosan (0.5 to 2% w/v) hydrogels were crosslinked in the presence of cells by photoinitiated free radical polymerization (Irgacure photoinitiator with 365 nm light). (B) E-18 rat cortical neurons were immobilized within chitosan and agarose (Seaprep<sup>®</sup>) hydrogels for investigating neuronal survival and differentiation. The cells clumped into groups and displayed extensive neurite outgrowth in chitosan hydrogels (left), as compared to agarose hydrogels (right), indicating enhanced neuron function within the chitosan matrices (scale bar, 50  $\mu$ m). (C) Neurite outgrowth quantification ( $p < 0.05$ ). Reprinted from Valmikinathan *et al.*<sup>88</sup> with permission from The Royal Society of Chemistry. Copyright (2012).



number of biological interactions, such as cell adhesion, cell proliferation, or cell surface binding of lipase and other proteins that are critical in developmental processes, blood coagulation, angiogenesis, viral invasion, and tumor metastasis.<sup>91</sup> Moreover, heparin and heparan sulfate protect proteins from degradation, regulate protein transport through basement membranes, and mediate internalization of proteins.<sup>92</sup> However, potential adverse effects of heparin, a potent anticoagulant include bleeding, thrombocytopenia, osteoporosis, alopecia, and priapism, and are related to this wide variety of biological activities.<sup>93–95</sup> Such undesirable effects may limit the use of heparin in certain *in vivo* applications.

Physically and chemically crosslinked heparin-based hydrogels have been employed for the investigation of cell function and fate,<sup>96–99</sup> cell encapsulation,<sup>100–103</sup> and controlled bioactive molecule delivery.<sup>29,104–106</sup> For instance, Kiick and coworkers used heparin-based hydrogels to modulate cell response in a 2D *in vitro* experiment.<sup>96</sup> To modulate cell adhesion and response, hydrogels with different moduli were prepared using the Michael addition reaction between combinations of maleimide-functionalized heparin, thiol functionalized PEG and maleimide functionalized PEG. Such systems, with the ability to tune biochemical and mechanical properties, make heparin based hydrogels promising candidates for controlling adventitial fibroblast remodeling of blood vessels. In another example, Tae and coworkers took advantage of heparin-based hydrogels to stably bind fibrinogen and collagen type I on a hydrogel surface using heparin binding affinity by physisorption.<sup>98</sup> The hydrogels were prepared by a Michael-type addition reaction using thiolated heparin and PEG diacrylate. The significant physisorption of proteins on the heparin hydrogel, as compared to a control PEG hydrogel, led to enhanced fibroblast adhesion and proliferation. Such approaches can be used to adhere cells on selective heparin hydrogel surfaces for applications such as biosensors, cell culture, and tissue engineering. Additionally, Werner and coworkers recently reported use of heparin-based hydrogels for cell replacement therapies in the neurodegenerative diseases.<sup>99</sup> By tuning the mechanical and biological properties of the PEG-heparin hydrogels, neural stem cell differentiation and axo-dendritic outgrowth were modulated. *In vivo* stability and excellent histocompatibility make such hydrogel systems attractive candidates for neuronal cell replacement therapies. For a comprehensive overview of heparin hydrogels, readers are referred to a recent book chapter by McGann and Kiick.<sup>89</sup>

**3.2.4 Alginate.** Alginate is a hydrophilic, cationic polysaccharide consisting of (1–4)-linked  $\beta$ -D-mannuronate (M) and its C-5 epimer  $\alpha$ -L-guluronate (G) residues (Fig. 3D). It is obtained from brown algae, and depending upon the algae source, it may consist of blocks of similar or strictly alternating residues. Alginate-based hydrogels are biocompatible and undergo physical gelation in the presence of divalent cations. Despite these advantages, the uncontrolled degradation of physically crosslinked alginate hydrogels upon the loss of divalent cations can hinder their stability. Covalent crosslinking with various crosslinkers, such as adipic acid dihydrazide and lysine, can be employed to overcome this uncontrolled

degradation. A lack of cell-specific interactions, however, can limit the use of alginate hydrogels in bioengineering applications; an attractive approach to induce bioactivity for cell culture is by covalent incorporation of bioactive ligands such as RGD-containing peptides. An additional challenge for alginate hydrogels *in vivo* is that the alginate macromolecule itself is difficult to break down under physiological conditions, and the molecular weight of released alginate strands is typically above the renal clearance threshold.<sup>107,108</sup> However, partially oxidized alginate, which undergoes biodegradation, can be utilized to overcome these limitations.<sup>109</sup>

Alginate-based hydrogels have been used for in drug delivery,<sup>110–112</sup> tissue engineering,<sup>113–115</sup> wound healing,<sup>116–118</sup> cell encapsulation,<sup>119,120</sup> and as adhesion barriers.<sup>121</sup> For instance, recently Kim *et al.* employed alginate-based hydrogels for delivering differentiated adipogenic cells for adipose tissue engineering.<sup>115</sup> Oxidized alginate (susceptible to hydrolysis) was coupled with an adhesion peptide and crosslinked with calcium sulfate to encapsulate cells *in vivo*. The injected cell-laden hydrogels led to the formation of soft, semitransparent adipose tissue after 10 weeks in male nude mice highlighting the ability of degradable alginate hydrogels to deliver cells and generate living tissue *via* a minimally invasive injection.

**3.2.5 Fibrin.** Fibrin is a fibrous, non-globular protein that is an important element of the provisional extracellular matrix. It forms hydrogels by the enzymatic polymerization of its precursor, fibrinogen, *via* thrombin-mediated cleavage of fibrinopeptide A in the presence of factor XIII.<sup>122</sup> Fibrinogen molecules are composed of two sets of disulfide-bridged  $\alpha$ -,  $\beta$ -, and  $\gamma$ -chains.<sup>123</sup> The proteinase inhibitor, aprotinin, can control the degradation rate of these biocompatible and cell-adhesive hydrogels. Further, fibrin can promote cell migration, proliferation, and adhesion.<sup>124,125</sup> Although recent improvements in hydrogel formation have been reported with the use of additional salt during gelation,<sup>126,127</sup> the fast gelation time and restricted mechanical properties still limit the use of fibrin-based hydrogels. Nevertheless, fibrin-based hydrogels have been used for wound healing,<sup>127,128</sup> controlled delivery,<sup>129,130</sup> and tissue engineering.<sup>127,131</sup> For example, Scotti *et al.* reported enhanced synthetic activity of chondrocytes encapsulated in fibrin hydrogels.<sup>131</sup> It was found that DNA content remained stable, indicating limited cell death or proliferation, and indices of cartilage matrix production, such as GAG and collagen II content, increased.

**3.2.6 Other natural polymers.** Discussion of natural polymers for hydrogel preparation in this section mainly has been limited to HA, chitosan, heparin, alginate, and fibrin, owing to scope of the article. However, other natural polymers, such as collagen, gelatin, chondroitin sulfate, agarose, carrageenan, dextran, and silk, have been utilized for variety of bioengineering applications, including cartilage, neural, spinal cord, skin and vocal cord tissue engineering as well as therapeutic and controlled delivery. Readers are directed to recent reviews by Slaughter *et al.*<sup>10</sup> for collagen based hydrogels, Vlierberghe *et al.*<sup>132</sup> for collagen, gelatin, and chondroitin sulfate based hydrogels, Perale *et al.*<sup>133</sup> for alginate and collagen based hydrogels, and Kaplan and coworkers<sup>134,135</sup> for silk based hydrogels.





### 3.2 Hydrogels from synthetic polymers

**3.2.1 Poly(ethylene glycol).** Poly(ethylene glycol) (PEG), also known as poly(ethylene oxide) (PEO) or poly(oxyethylene) (POE) depending upon the molecular weight of the polymer, is the hydrophilic non-degradable polymer of ethylene oxide (Fig. 3E and F). It lacks any protein binding sites, and due to its hydrophilic and uncharged structure, it forms highly hydrated layers that restrict protein adsorption.<sup>136</sup> The excellent biocompatibility and low toxicity of PEG-based hydrogels make them ideal candidates for various biomedical applications, and PEG-containing formulations have been approved by the FDA for several medical applications, including use as laxatives, solvents in liquid formulations, conjugates to therapeutic proteins, and lubricants.<sup>137–139</sup> Acute, short and long-term toxicology of PEG with oral, intraperitoneal and intravenous administration routes have been thoroughly reviewed.<sup>140,141</sup> Low molecular weight PEGs ( $M_w < 1$  kDa) can be oxidized *in vivo* into toxic diacids and hydroxyl acid metabolites,<sup>142</sup> but high molecular weight PEGs ( $M_w > 5$  kDa) show little or no metabolism.<sup>140</sup>

PEG macromolecules can be functionalized easily *via* its hydroxyl end groups to yield numerous homofunctional or heterofunctional terminal groups, including thiols,<sup>143</sup> vinyl sulfones,<sup>144</sup> maleimides,<sup>29,145</sup> acrylates<sup>146,147</sup> allyls,<sup>148</sup> and norbornenes.<sup>149,150</sup> The PEG hydrogels have been widely used as blank slates for the presentation of biophysical and biochemical cues in tissue engineering,<sup>151–154</sup> cell encapsulation,<sup>155–157</sup> controlled stem cell differentiation,<sup>158–160</sup> and bioactive molecule delivery applications.<sup>152,161–163</sup> For a comprehensive overview of PEG hydrogels, readers are referred to recent reviews by Lin and Anseth<sup>35</sup> for controlled delivery applications and by Papavasiliou *et al.*<sup>164</sup> for tissue engineering applications.

A large number of PEG copolymers have been utilized for drug delivery, such as non-biodegradable triblocks of PEG and polypropylene oxide (PPO) (PEG-*b*-PPO-*b*-PEG, Pluronic<sup>TM</sup>) and hydrolytically degradable block polymers of PEG, polylactic acid (PLA), and polylactic acid-*co*-glycolic acid (PLGA), as shown in Fig. 3G. For example, H. Chang *et al.* investigated the effect on an active form of an antitumor drug, topotecan (TPT), which was encapsulated in an amphiphilic PEGA-PEG-PLGA hydrogel matrix for controlled release.<sup>165</sup> Due to the increased  $pK_a$  of the carboxylate groups as a result of the hydrophobic interactions between the amphiphilic polymer matrix and TPT, the active form content of TPT was increased by about 40%, as compared to free TPT in PBS solution under physiological conditions. Further, the release was sustained for 5 days with only a mild initial burst release.

**3.2.2 Poly(vinyl alcohol).** Poly(vinyl alcohol) (PVA), as shown in Fig. 3I, is commercially obtained by partial or complete hydrolysis of poly(vinyl acetate). The extent of hydrolysis and the molecular weight of the macromolecule can be used to tune its hydrophilicity and solubility, and the pendant hydroxyl groups can act as biomolecule attachment sites. Due to its low protein adsorption and excellent biocompatibility, PVA has been used in soft contact lenses, eye drops, tissue adhesion barriers, and cartilage replacement applications.<sup>166</sup> For a comprehensive

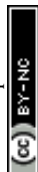
overview of PVA hydrogels in biomaterial applications, readers are referred to recent reviews by Baker *et al.*<sup>166</sup> and Alves *et al.*<sup>167</sup>

PVA-based hydrogels can be formed by chemical crosslinking using various chemistries discussed in Section 4, such as click chemistry,<sup>168,169</sup> radical polymerization,<sup>170–172</sup> and Schiff base reaction.<sup>173,174</sup> The hydrogels also can be formed by physical crosslinking *via* methods such as cryogenic gelation and hydrogen bonding,<sup>175–177</sup> and PVA hydrogels formed *via* these methods have been successfully used for tissue engineering and regenerative medicine applications.<sup>176,178–180</sup> For instance, Samal *et al.* prepared hybrid hydrogels consisting of PVA, chitosan, and multiwalled carbon nanotubes (MWCNT) by the physical freeze-drying method.<sup>176</sup> The incorporation of MWCNT improved the mechanical strength, structural coherence, and electrical conductivity of the hydrogel matrix and could influence cell behavior due to biophysical and electrostimulating cues. The hydrogel matrix showed excellent biocompatibility while retaining the inherent properties of PVA, chitosan, and MWCNT, indicating its potential for biomedical applications.

**3.3.3 Other synthetic polymers.** Poly(hydroxyethyl) methacrylate (PHEMA), a hydrophilic, water-stable polymer, was the base material for one of the first hydrogels to be successfully used for ophthalmic applications (*e.g.*, contact lenses).<sup>181</sup> While PHEMA hydrogels are stable under physiological conditions, their controlled degradation can be achieved by incorporation of hydrolytically or enzymatically cleavable linkages, such as polycaprolactone,<sup>182,183</sup> and collagenase-cleavable peptide sequences.<sup>184,185</sup> Another poly(acrylate) derivative, poly(*N*-isopropylacrylamide) (PNIPAAm), a thermoresponsive polymer with lower critical solution temperature (LCST) of approximately 32 °C, has been utilized for preparing responsive hydrogels for tissue engineering and drug delivery applications.<sup>186–188</sup> For a comprehensive review of strategies to improve the thermosensitivity of PNIPAAm hydrogels, readers are referred to a review by Zhang *et al.*<sup>189</sup>

Polyphosphazene, an organometallic polymer with a phosphorous–nitrogen backbone and organic side groups, can degrade under physiological conditions into nontoxic molecules, such as  $H_3PO_4$  and  $NH_4^+$ . The inorganic backbone undergoes hydrolytic degradation, where the rate of degradation is dictated by the side chain structures.<sup>190</sup> Polyphosphazene hydrogels can be prepared *via* physical crosslinking (*i.e.*, ionic interaction using divalent ions), or chemical crosslinking *via* glucosyl or glyceryl side groups.<sup>191</sup> Readers are referred to a recent review by Allcock for a comprehensive review of polyphosphazene,<sup>192</sup> but we note here that polyphosphazene based hydrogels have been used for bioactive molecule delivery and drug delivery.<sup>193,194</sup>

Polyesters, such as PLA, polyglycolic acid (PGA), and polycaprolactone (PCL), also have been used for the preparation of cell-compatible hydrogels. Polyester-based polymers offer inherent biodegradability due to ester hydrolysis under physiological conditions. Thus, using combinations of polyesters with other synthetic or natural polymers, the rate of hydrogel degradation can be tuned as per application requirements. For a comprehensive overview of polyester-based hydrogels, readers are referred to a review by Tomas and coworkers.<sup>195</sup>



## 4. Material functionalization for hydrogel formation

The stable crosslinking of hydrogels is essential to prevent uncontrolled dissolution of macromolecular chains in aqueous cellular microenvironments. Numerous chemical and physical crosslinking strategies have been utilized for the preparation of cell-compatible hydrogels (Fig. 6). Chemical crosslinking strategies

covalently couple reactive functional groups for hydrogel formation using chain or step growth reactions, including free radical chain polymerization, click reactions, reactions of Schiff bases, and carbodiimide-mediated activation reactions. Physical crosslinking strategies utilize non-covalent interactions between functional groups, such as ionic interactions, electrostatic interactions, hydrogen bonding, crystallization, hydrophobic interactions, and protein interactions.

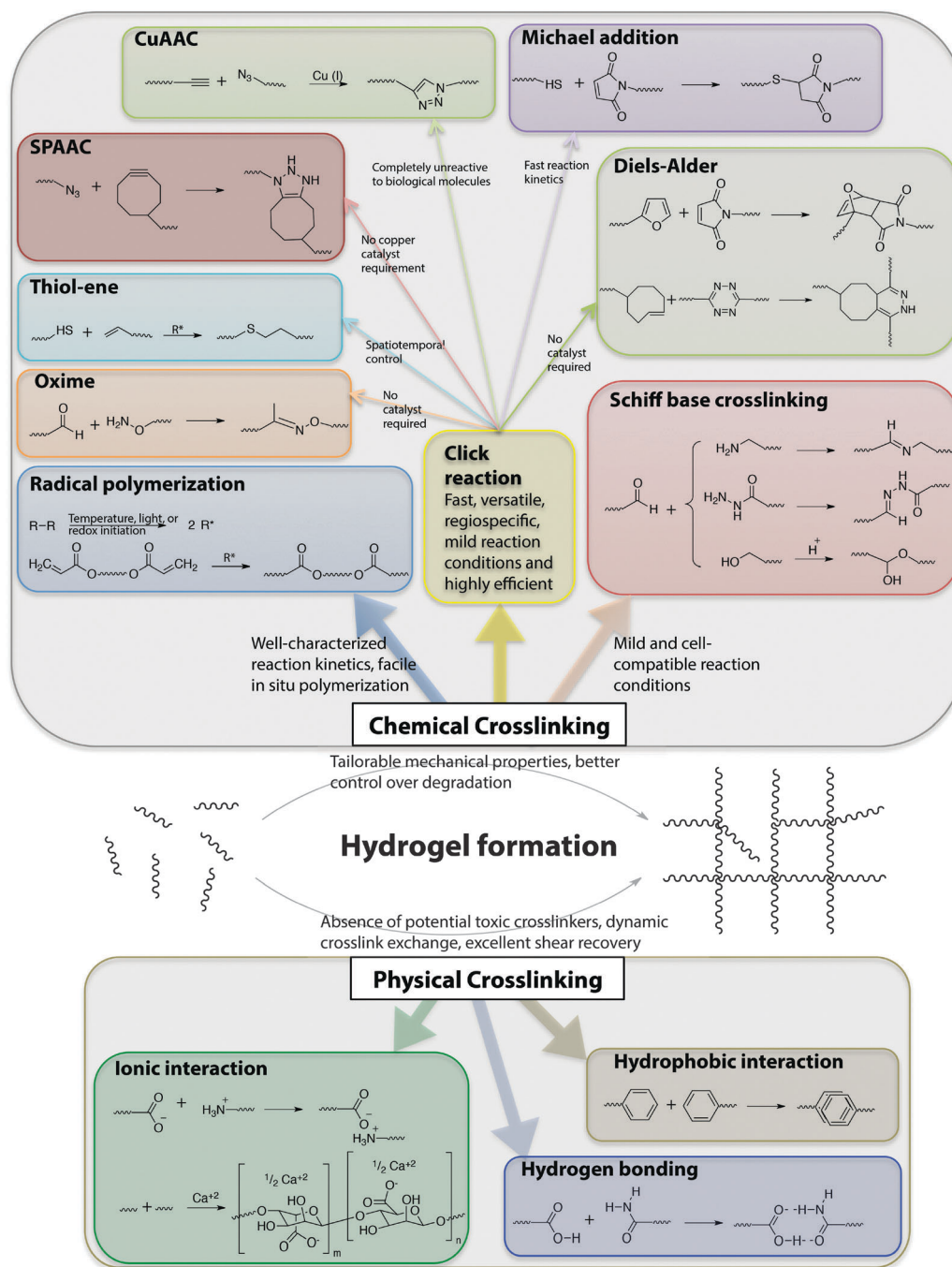


**Fig. 6** Chemical functional groups for hydrogel formation. A wide range of functional groups is available for either hydrogel formation or modification post-polymerization. Functional group selection depends on several factors related to the application of interest, including the desired initiation mechanism, the specificity and speed of the reaction, and the stability of the resulting bond under various solution conditions.



The crosslink concentration, or density, dictates various physical properties of hydrogels, including elasticity, diffusivity, water content, and mesh size. In addition, the degree of crosslinking influences the hydrogel degradation rate, and hence, precise control over hydrogel crosslinking is highly desirable. Further, for control of the properties of the cell microenvironment, hydrogel formation in the presence of cells or proteins is often required, and it is thus essential to choose a cytocompatible crosslinking method for preparing these applications.

#### 4.1 Chemically crosslinked hydrogels

**4.1.1 Radical polymerization.** Radical polymerization involves the formation of free radicals *via* decomposition of an initiator by light, temperature, or redox reaction.<sup>196</sup> The successive reaction of multifunctional free radical building blocks leads to the formation of a polymer network. Free radicals can be used to initiate hydrogel formation by different polymerization mechanisms: chain growth, step growth, or mixed mode (a combination of chain and step) polymerization.<sup>197</sup> Hydrogel formation by free radical polymerization offers advantages such as well-characterized reaction kinetics and facile *in situ* polymerization in presence of cells with spatiotemporal control.<sup>198</sup> However, free radicals can be transferred to proteins, affecting their bioactivity, or transferred to biomolecules present in the ECM, affecting cell viability.<sup>19,199</sup> These exothermic reactions also can cause a local increase in temperature,<sup>200</sup> where temperature rise must be minimized to maintain cell viability and function. Despite these challenges, free radical polymerization *via* chain growth mechanisms is a well-established method for cell encapsulation; however, the heterogeneous nature of the chain polymerization mechanism leads to a distribution of polymer chain molecular weights and thus molecular-level inhomogeneity within the network. Inhomogeneity in network can dramatically reduce the mechanical strength of hydrogels.<sup>201</sup> The widespread use of free radical chain polymerization for hydrogel formation partly arises from the availability of many hydrophilic meth(acrylate)-functionalized building blocks. Historically, radical polymerization of hydroxyethyl methacrylate (HEMA) using ethylene dimethacrylate (EDMA) as a crosslinker was extensively studied for commercial-scale manufacturing of flexible contact lenses.<sup>181</sup> A large number of macromolecules, such as HA,<sup>67,202–204</sup> chitosan,<sup>193,205</sup> and PEG,<sup>205,206</sup> are easily functionalized with vinyl end groups and can undergo radical polymerization to form hydrogels in presence of appropriate initiators. For example, Morelli and Chiellini functionalized Ulvan, a sulfated polysaccharide from green seaweed, with methacryloyl groups.<sup>207</sup> The biocompatible hydrogel network was formed *via* radical polymerization using UV irradiation in the presence of methacrylic anhydride or glycidyl methacrylate.

A significant advantage of radical polymerization methods is that, when used in conjunction with a photoinitiator, they can provide spatiotemporal control over hydrogel formation and *in situ* properties.<sup>14,208</sup> For instance, Guvendiren and Burdick demonstrated short and long-term cellular response to a dynamic microenvironment using methacrylated hyaluronic

acid.<sup>208</sup> The methacrylated HA was crosslinked with a dithiol *via* the Michael-type addition, creating a low modulus hydrogel, and subsequently *via* free radical chain polymerization of the remaining methacrylates, increasing the crosslink density and modulus of the hydrogel at time points of interest. Human mesenchymal stem cells (hMSCs) that were cultured on these hydrogel substrates spread from cell areas of  $\sim 500$  to  $3000\ \mu\text{m}^2$  and exhibited greater traction over a timescale of hours during stiffening (with  $E$  increasing from 3 to 30 kPa). The cell response to matrix stiffening was found to vary over 2 weeks in culture; an increased population of terminally differentiating hMSCs was present over time and was no longer responsive to variations in the mechanical properties of the hydrogel.

Alternatives such as controlled chain polymerization have been employed for hydrogel preparation to provide more control of hydrogel properties;<sup>209–211</sup> however, potential cytotoxicity of the unremoved metal catalysts employed during these methods can restrict their use in the cell microenvironment. Free radical step growth polymerization recently has emerged as an alternative hydrogel formation strategy that provides a more homogeneous network structure and enables spatiotemporal control of hydrogel formation;<sup>212</sup> recent developments in this area (*e.g.*, thiol-ene click reactions) will be discussed in Section 4.1.2.3.

**4.1.2 Click chemistry.** Click reactions, broadly defined, are a class of reactions that are fast, versatile, regiospecific, and highly efficient.<sup>213</sup> Click reactions usually yield a single product, leaving no reaction byproducts, and occur under mild conditions. After the introduction of click reactions by Sharpless,<sup>213</sup> the copper(I)-catalyzed azide-alkyne cycloaddition (CuAAC) has been widely used for the facile synthesis of new molecules, polymers, and hydrogels.<sup>214</sup> Over the past decade, several reactions have been observed to have 'click' reaction attributes while not requiring a metal catalyst, including the radical addition of thiols to select alkenes and alkynes, Michael-type addition of thiols to maleimides, Diels-Alder reactions between dienes and dienophiles, and oxime reactions between aminoxy groups and aldehydes or ketones (Table 2).<sup>215</sup> Click reactions are attractive tools for synthesizing cell-compatible hydrogels, which can be used for controlled cell culture, tissue engineering, and controlled release applications.<sup>216–219</sup> Advantages such as fast reaction kinetics, high regio- and chemo-selectivity, mild reaction conditions, and facile tuning of structural and mechanical properties using stoichiometry make click reactions highly useful for synthesizing cell-compatible hydrogels.<sup>169,220,221</sup>

**4.1.2.1 Azide-alkyne cycloadditions.** Copper(I)-catalyzed azide-alkyne cycloadditions (CuAAC) unite two unsaturated reactants, azides and alkynes, to form triazoles.<sup>222</sup> CuAAC click reactions have been extensively used for crosslinking both natural<sup>223–225</sup> and synthetic<sup>169,217,226</sup> polymer-based hydrogels. One advantage of this class of reactions is that both azides and alkynes are almost completely unreactive toward biological molecules.<sup>227</sup> Their limitations include alkyne homocoupling, difficulties removing residual heavy metal catalyst, and the biocompatibility of the resulting 1,2,3-triazoles. In particular,

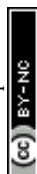


**Table 2** Click reactions for hydrogel for hydrogel formation. Comparison of important click reactions typically used for formation of cell compatible hydrogels

Click reactions	Reacting functional groups	Reaction conditions <sup>221</sup>	Key features	Applications
CuAAC	Azide and alkyne	pH 4–12, reaction time <1 h, Cu catalyst required	– Bioorthogonal – Reversible – Difficulties with complete removal of cytotoxic Cu	Cell encapsulation and delivery, <sup>217</sup> drug delivery, <sup>223,224</sup> 2D cell culture <sup>225</sup>
SPAAC	Cyclooctyne and azide	pH 7.4, reaction time <1 h	– No catalyst required	Cell encapsulation, <sup>230,231</sup> 3D cell culture <sup>216,218</sup>
Diels–Alder	Conjugated diene and substituted alkene	pH 5.5–6.5, reaction time <8 h	– No catalyst required – Longer reaction time than most of the other click reactions	Cell encapsulation and release, <sup>234</sup> controlled cargo delivery <sup>235</sup>
Inverse electron demand Diels–Alder	Dienophile and diene	pH 7.4, reaction time <5 min	– Faster rate of reaction than many other Cu-free click reactions – No catalyst required no catalyst required	Live cell imaging, <sup>238</sup> drug targeting, <sup>239</sup> cell surface protein labeling <sup>240</sup>
Thiol–ene	Thiol and unsaturated functional group (radical mediated)	pH 6–8, reaction time <1 h	– Spatiotemporal control possible with select chemistries and using a photoinitiator	Cell encapsulation, <sup>149,150</sup> degradable 3D cell culture <sup>147,246</sup>
Michael addition	Thiol and $\alpha,\beta$ -unsaturated carbonyl group	pH 6–8, reaction time <30 min	– No catalyst required – Reversible	Cell encapsulation, <sup>157,160,250</sup> controlled cargo delivery <sup>29,248</sup>
Oxime	Aminooxy and aldehyde/ketone	pH 6–8, reaction time <30 min	– No catalyst required	Cell encapsulation, <sup>251</sup> protein immobilization <sup>253</sup>

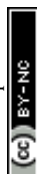
use of toxic and unstable Cu catalysts can limit applicability in cellular microenvironments. Nevertheless, Piluso *et al.* recently reported the preparation of HA-based hydrogels *via* CuAAC click crosslinking of alkyne-functionalized HA.<sup>225</sup> The elastic modulus of the resulting HA hydrogels was tuned between 0.5 to 4 kPa by varying the stoichiometry, length, and rigidity of an azide-functionalized crosslinker. In this case, limited toxicity was observed with L292 cells encapsulated in these hydrogels, indicating their potential as biomaterials.

Copper-free strain-promoted azide–alkyne cycloaddition (SPAAC) reactions have emerged to address issues with copper toxicity in biological systems.<sup>228</sup> Ring strain, as well as electron-withdrawing fluorine substituents in some cases, promotes rapid reaction of cyclooctynes with azides in the absence of the Cu catalyst.<sup>229</sup> Owing to the absence of the catalyst, SPAAC click chemistry has been used to crosslink hydrogels in the presence of cells to form controlled cellular microenvironments.<sup>216,218,230,231</sup> For instance, Zheng *et al.* reported use of a SPAAC strategy to create hydrogels by functionalizing PEG with 4-dibenzocyclooctynol.<sup>231</sup> The versatility and biocompatibility of this strategy allowed hMSC encapsulation, maintaining their viability as assessed using a live-dead imaging-based cytotoxicity assay (~90% viability after 24 h). In a broader context, such an approach can be useful for cell delivery, in which cells are hypersensitive to presence of Cu during crosslinking. In another example, DeForest *et al.* used SPAAC click chemistry for hydrogel formation followed by a thiol–ene reaction for photoaddition of three-dimensional biochemical patterns with micrometer scale resolution and in the presence of fibroblasts (>90% viability at post 24 h encapsulation).<sup>218</sup> Specifically, an enzymatically degradable peptide sequence was incorporated

into the hydrogel *via* SPAAC reaction, and the adhesion ligand was incorporated in the hydrogel network *via* cytocompatible thiol–ene photolithographic patterning. The cells selectively adhered to regions in which the RGD motif was presented and subsequently degraded the hydrogel matrix through cleavage of the enzymatically degradable linker, leading to localized cell proliferation. In principle, such approaches can be used to study cell behavior in spatio-temporally controlled 3D microenvironments.

**4.1.2.2 Diels–Alder reactions.** The Diels–Alder (DA) reaction is a well-established solution-based reaction that has also been utilized for hydrogel formation. DA reactions involve addition of conjugated dienes to substituted alkenes to form substituted cyclohexenes.<sup>215,232</sup> The efficient and facile DA reaction occurs under mild reaction conditions and does not require an initiator, which is advantageous for crosslinking hydrogels in the presence of cells. However, the reactions are slow, which could be a limitation in certain applications. The DA reaction has been utilized for the preparation of various hydrogels for bioengineering applications.<sup>233–235</sup>

Shoichet and coworkers recently demonstrated the use of a Diels–Alder click reaction to create stable and biocompatible hyaluronic acid hydrogels (Fig. 7).<sup>234</sup> The carboxylic acid group of HA was reacted with furfurylamine to create furan-functionalized HA, and the modified HA was crosslinked with a maleimide PEG crosslinker to form a hydrogel. The mechanical and degradation properties of these hydrogels were modulated using the furan to maleimide molar ratio. *In vitro* studies with a cancer cell line, MDA-MB-231, demonstrated the cytocompatibility of these Diels–Alder HA-PEG hydrogels, and a high level of cell viability was maintained over 2 weeks (>98%, live-dead assay after 14 days).





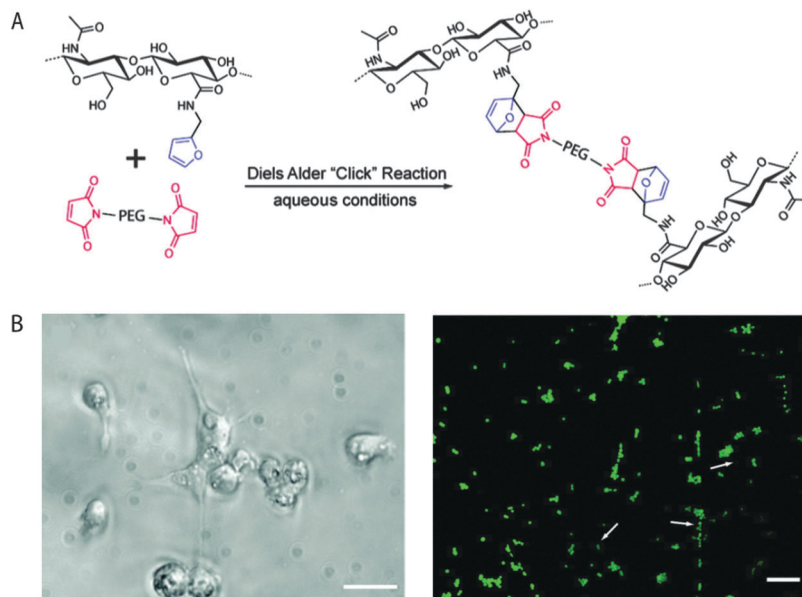


**Fig. 7** Diels–Alder click reaction for forming degradable hydrogels. (A) Schematic of hydrogel formation using Diels–Alder reaction between furan groups of HA and maleimide groups present on a PEG macromer. (B) Brightfield image of MDA-MB-231 cells (left), which are known to interact with HA via CD 44 receptor. Cells were seeded on HA/PEG hydrogels and after 14 days adopted a flattened or elongated morphology, indicating cell adhesion (scale bar, 20  $\mu\text{m}$ ). Cell viability was assessed using a live/dead assay (right, live cells in green, dead cells indicated by arrows) signifying a high level of cell survival (>98%), after 14 days (scale bar, 60  $\mu\text{m}$ ). Reprinted from Nimmo *et al.*<sup>234</sup> with permission from American Chemical Society. Copyright (2011).

Using a similar approach, Marra and coworkers prepared HA-based hydrogels for controlled release application.<sup>235</sup> HA was functionalized with either a maleimide or a furan group and crosslinked in PBS at 37 °C within ~40 minutes. Insulin (negatively charged) or lysozyme (positively charged) were encapsulated as model proteins within these HA-based hydrogels. The release profiles showed slight or no burst release depending upon the protein, owing to electrostatic interactions. In addition, the hydrogels were cytocompatible and maintained the viability of the entrapped cells. Taken together, these recent examples indicate that the Diels–Alder crosslinking for creating cell-compatible hydrogels is a promising strategy for soft tissue engineering, regenerative medicine and controlled release applications.

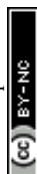
Fox and coworkers created an inverse-electron-demand Diels–Alder reaction, reacting a *trans*-cyclooctene with dipyrrolyltetrazine.<sup>236</sup> As compared to any other Cu-free click reaction, the rate of this reaction was an order of magnitude higher ( $k = 10^3 \text{ M}^{-1} \text{ s}^{-1}$ ).<sup>237</sup> Using a similar approach, reactions of tetrazines with other alkenes such as norbornene<sup>238</sup> and cyclobutene<sup>239</sup> have also been reported. In principle, such reactions could be valuable for crosslinking cell-compatible hydrogels. Additionally, the inverse-electron-demand Diels–Alder reaction has been used for cell surface protein labeling indicating their bioorthogonality.<sup>240</sup>

**4.1.2.3 Thiol–ene reactions.** Thiol–ene reactions typically involve reaction of thiols with unsaturated functional groups, such as unactivated alkenes, maleimides, acrylates, and norbornenes. Thiol–ene reactions can proceed by free radical addition, Michael-type nucleophilic addition, or a combination of these mechanisms depending on the reaction conditions.

Thiol–ene reactions share many attributes with classical click reactions: thiol–ene reactions proceed rapidly under mild conditions, have high orthogonality, yield a single regioselective product, and do not yield any byproducts. Hence, reactions that proceed by either mechanism are commonly referred as thiol–ene click reactions. For a comprehensive review of thiol–ene click reactions, readers are referred to recent reviews Hoyle *et al.*<sup>241</sup> and Kade *et al.*<sup>242</sup>

Gress *et al.* were the first to identify the radical-mediated thiol–ene reaction as a click reaction.<sup>243</sup> This radical-mediated thiol–ene coupling has since emerged as a highly attractive reaction for hydrogel formation and modification due to its high efficiency, ease of photoinitiation, and orthogonality with numerous functional groups.<sup>241,244</sup> The reaction offers advantages, such as spatiotemporal control over crosslinking and the possibility of conducting crosslinking in the presence of cells. Rydholm *et al.* reported the use of thiol–acrylate mixed mode free radical photopolymerization for the formation of hydrolytically degradable PEG hydrogels.<sup>147</sup> The mechanical properties and degradation profiles were modulated with thiol concentration. Use of photoinitiation enables controlled polymerization both spatially and temporally. In addition, thiols and acrylates also can photopolymerize in absence of a photoinitiator, which could prove useful for *in situ* crosslinking in the presence of cells.<sup>241</sup>

Fairbanks *et al.* have utilized a thiol–norbornene reaction to synthesize enzymatically degradable PEG hydrogels.<sup>245</sup> Four-arm PEG was functionalized with norbornene end groups, and thiol-containing chymotrypsin- or MMP-degradable peptides were used for crosslinking. The step-growth mechanism ensured homogeneity in the resulting hydrogel network, and



the crosslinking reaction did not significantly affect the viability of encapsulated hMSCs. Shih and Lin have recently shown the hydrolytic degradability of similar thiol–norbornene PEG hydrogels *via* ester hydrolysis under neutral or mildly basic conditions.<sup>246</sup> Taken together, degradation properties of these hydrogels can be modulated with the degree of crosslinking and the crosslinking peptide sequence, making them promising for tissue engineering applications in which fine control over degradation is desired.<sup>247</sup>

Nucleophilic Michael-type addition reactions between thiols and electron deficient ‘ene’s, such as maleimides, methacrylates,  $\alpha,\beta$ -unsaturated ketones, acrylonitrile, and crotonates, are another type of thiol–ene click reaction. Due to the mild reaction conditions, numerous hydrogels have been prepared *via* Michael-type addition in the presence of cells without significantly altering cell viability.<sup>157,160,248–250</sup> For example, Phelps *et al.* used 4-arm PEG macromers functionalized with maleimide end groups and dithiol-containing protease-cleavable peptides to form hydrogels.<sup>157</sup> The mechanical properties of the hydrogels were modulated using appropriate polymer concentrations to mimic the modulus of the native ECM. Further, these PEG hydrogels maintained cell viability during gel formation and promoted the spreading of encapsulated C2C12 cells. Kiick and coworkers have employed Michael-type additions in the production of a variety of hydrogels. In one example, polypeptide-PEG hybrid hydrogels were produced *via* the reaction of the cysteine (CYS) residues of the polypeptide with vinyl sulfone (VS) functionalized PEG (Fig. 8).<sup>250</sup> Resilin-like polypeptides (RLP) were employed owing to the outstanding elastomeric properties of natural resilin for cardiovascular tissue engineering application and to provide bioactivity to inherently inert PEG hydrogels. Depending upon

the molecular weight of the RLP and the stoichiometric ratio (CYS:VS), the storage modulus of the hydrogel was modulated from  $G' \sim 2.6$  kPa to 12 kPa. Encapsulated AoAFs adopted a spread morphology over 7 days and maintained their viability within *in vitro* culture in these hydrogels. These recent examples demonstrate the versatility of Michael-type addition reactions to crosslink hydrogels in presence of cells for soft tissue and cardiovascular tissue engineering.

**4.1.2.4 Oxime reactions.** Oxime reactions between aminoxy and aldehyde or ketone functional groups have recently been classified as click reactions owing to their fast reaction kinetics, orthogonality to various functional groups found in the cell microenvironment, and lack of catalyst. Recently, Grover *et al.* utilized oxime click reactions to synthesize cytocompatible PEG hydrogels.<sup>251</sup> Eight-arm PEG was functionalized with aminoxy groups and crosslinked with glutaraldehyde. By varying the polymer concentration and stoichiometric ratio of aminoxy to aldehyde, hydrogel mechanical properties and water content were modulated. This click reaction permitted encapsulation of murine MSCs, maintaining cell viability and metabolic activity. However, glutaraldehyde has been observed to undergo various structural rearrangements in solution depending on the pH, influencing the reaction mechanisms and potentially influencing the ‘click’ nature of this reaction.<sup>252</sup> Maynard and coworkers used oxime click reaction and CuAAC to immobilize different proteins in PEG-hydrogel constructs.<sup>253</sup> PEG was functionalized with aminoxy and alkyne groups in order to conjugate ketoamide–myoglobin and azide-modified ubiquitin as model proteins for surface patterning. While the orthogonality of these two reactions is clear, many proteins and cells present free amines in solutions, such as hydrophilic lysines along the

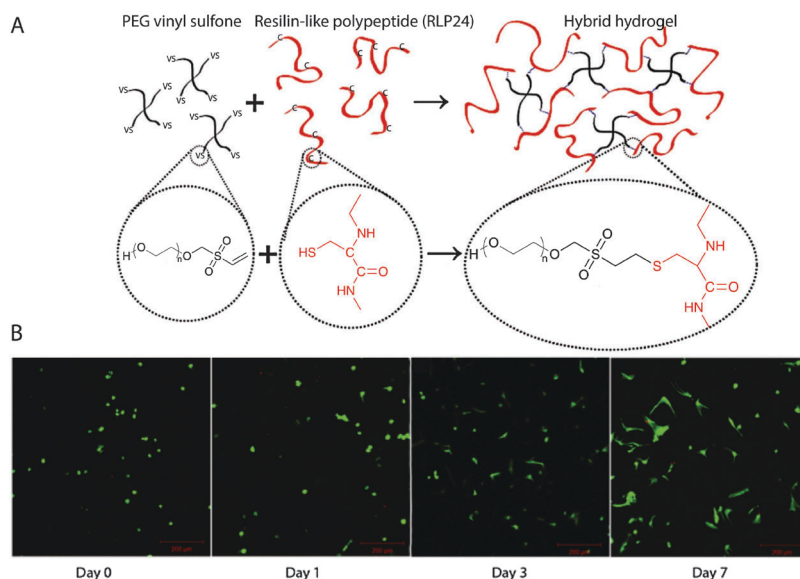


**Fig. 8** Michael-type addition reaction for hydrogel formation. (A) Schematic of hydrogel formation using the Michael-type addition reaction between vinyl sulfone groups of 4-arm PEG and cysteine residues present on the RLP. (B) Human aortic adventitial fibroblasts (AoAFs) were encapsulated during hydrogel formation and cell viability was evaluated *via* live/dead staining (fluorescent laser scanning confocal microscopy). AoAFs remained viable throughout the experiment, adopting a spread morphology (scale bar, 200 μm). Image reprinted from McGann *et al.*<sup>250</sup> with permission from John Wiley and Sons publishing. Copyright (2013).



backbone of ECM proteins and growth factors; consequently, the specificity of the oxime reaction for orthogonal gel formation should be evaluated based on the protein and application of interest. In principle such an approach can be extended for numerous possible combinations of proteins in adjacent regions of a single plane or in multilayer constructs to modulate cell behavior.

**4.1.3 Schiff base crosslinking reactions.** Schiff base crosslinking involves the reaction of macromolecules containing alcohol, amine, or hydrazide functionalities with aldehydes to form a hydrogel network. Due to the mild reaction conditions, this strategy has been utilized to prepare cell-compatible hydrogels for cell encapsulation and controlled drug delivery applications.<sup>64,254</sup> For example, Tan *et al.* synthesized *N*-succinyl-chitosan by introduction of succinyl groups at the *N*-position of the glucosamine units and also prepared hyaluronic acid with aldehyde functionality *via cis*-diol bond cleavage.<sup>64</sup> The chitosan-HA hydrogel was prepared with Schiff base linkages and exhibited a gelation time of  $\sim 1$ –4 minutes. The hydrogel supported cell adhesion, and encapsulated bovine articular chondrocytes were found to have regular spherical morphology, indicating the potential of this chemistry for tissue engineering applications. While a promising tool, many proteins present hydrophilic free amines (*e.g.*, lysines) or alcohols (*e.g.*, serine and tyrosine) in solution, as discussed with oxime reactions; the specificity of Schiff base crosslinking for orthogonal gel formation should be examined based on the desired application.

## 4.2 Physically crosslinked hydrogels

Noncovalent interactions, such as ionic interactions, crystallization, hydrophobic interactions, electrostatic interactions, hydrogen bonding, or combinations of these, can be used for physically crosslinking of macromolecules to obtain cell-compatible hydrogels.<sup>255–262</sup> Self-assembled amphiphilic block copolymers, proteins, peptides, and polypeptides typically form hydrogels *via* physical crosslinking.<sup>121,263–266</sup> Physically crosslinked hydrogels afford simple network formation, without the use of any potentially toxic chemical crosslinkers or initiators. In addition, their dynamic crosslink exchange, shear-thinning flow, and excellent shear recovery can be attractive for use as injectable hydrogels for therapeutic delivery.<sup>121,261</sup> However, potential limitations include insufficient mechanical strength for some applications due to the weakness of the physical interactions and limited control over their degradation rates, presenting possible challenges for controlled cell culture. Here, physical crosslinking methods used to design cell-compatible hydrogels from ‘off the shelf’ polymers (*e.g.*, alginate, PVA), block copolymers, and peptide–proteins are discussed along with potential applications for orthogonal property control in cellular microenvironments.

Ionic interactions have been extensively used to physically crosslink commercially available polysaccharides, such as alginate and chitosan, to form hydrogels.<sup>258–260</sup> The use of ionic interactions offers the possibility of biodegradation since ionic species present in cellular microenvironments can competitively bind, leading to dissociation of the hydrogel network. Matyash *et al.* used physical crosslinking with divalent cations such as

$\text{Ca}^{2+}$  to prepare alginate-based hydrogels that were biocompatible and facilitated neurite outgrowth.<sup>260</sup> Hydrogels can also be created by the formation of crystallites, which act as physical crosslinks for network formation. As in the example above (Section 3.2.2), PVA can form a highly elastic hydrogel when subjected to a freeze-thawing process to form crystallites, and such hydrogels have been used for various bioengineering applications, such as controlled drug delivery.<sup>175,255,262</sup> For example, Abdel-Mottaleb *et al.* used three cycles of freeze-thawing to prepare PVA hydrogels for topical delivery of Fluconazole within the dermal microenvironment.<sup>255</sup> The hydrogels were stable up to 6 months and effective in the topical treatment of skin infections.

Multiblock copolymers or graft copolymers can also be physically crosslinked for hydrogel formation. For example, Hunt *et al.* developed hydrogels with tunable physical and chemical properties using ionic coacervation upon mixing of two ABA triblock polymers, poly(allyl glycidyl ether-*b*-ethylene glycol-*b*-allyl glycidyl ether) with an oppositely charged poly(allyl glycidyl ether)-*block*, as shown in Fig. 9.<sup>257</sup> Non-covalent interactions of the positively charged (ammonium and guanidinium) and negatively charged (sulfonate, carboxylate) ABA triblock copolymers resulted in the formation of polymer-dense coacervate domains leading to network formation. The ionic interactions were efficient, specific, and sensitive to polymer concentration, pH and presence of salt. Such an approach highlights the use of ionic interactions for preparing highly tunable and dynamic physically crosslinked hydrogels with superior mechanical properties and ease of synthesis, which can be potentially used as 3D cell scaffolds.

Polypeptides and proteins represent another important class of biocompatible polymers that can be physically crosslinked upon the formation of secondary structures (*i.e.*,  $\alpha$ -helix and  $\beta$ -sheet) that drive intermolecular association. Peptide based hydrogels have been synthesized for potential applications in controlled release, 3D cell culture, and tissue regeneration.<sup>121,264,267–270</sup> For example, Yan *et al.* recently prepared  $\beta$ -hairpin peptide-based hydrogels *via* self-assembly for osteoblast encapsulation.<sup>121</sup> The effect of shear flow on the preformed, injectable  $\beta$ -hairpin hydrogel was investigated. The gel that was directly in contact with the syringe wall experienced a velocity gradient, while the central, plug-flow region experienced little to no shear. The study demonstrated that the shear thinning of preformed hydrogels did not significantly affect encapsulated cell viability. Further, Heilshorn and coworkers used tryptophan and proline-rich peptide domains for preparing mixing-induced, two component hydrogels (MITCH) for effective encapsulation of cells within 3D hydrogels.<sup>269</sup> In addition to peptide–peptide interactions, specific peptide–polysaccharide interactions also can be utilized for physically crosslinking hydrogels.<sup>271</sup>

Klick and coworkers employed noncovalent interactions between heparin-modified PEG polymers and a heparin-binding growth factor (VEGF) to create bioresponsive hydrogels.<sup>272</sup> The VEGF–LMWH interactions were confirmed by the increase in hydrogel modulus by addition of VEGF to PEG–LMWH ( $G'(\omega) > 10$  Pa in presence of VEGF,  $\sim 1$  Pa in absence of VEGF) measured using optical tweezer microrheology. The hydrogels significantly eroded after day 4, and released approximately 80% of VEGF by day



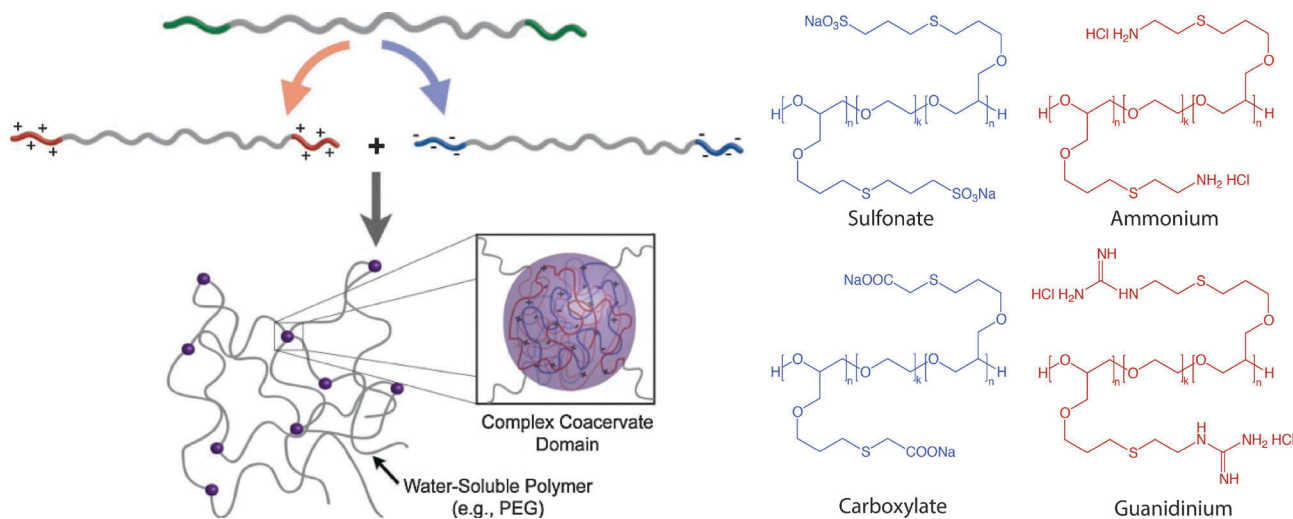


**Fig. 9** Block copolymer assembly for hydrogel formation. Multiblock copolymer based hydrogels have been prepared with coacervate crosslinking by mixing equimolar dilute solution of negatively charged (sulfonate, carboxylate) and positively charged (ammonium, guanidinium) ionic ABA triblocks. Image reprinted from Hunt *et al.*<sup>257</sup> with permission from John Wiley and Sons publishing. Copyright (2011).

10 in presence of VEGFR-2 (a VEGF receptor), as compared to PBS (~30% release over same time period). The released VEGF was bioactive, and the hydrogels were biocompatible, as confirmed by *in vitro* experiments (cell proliferation assay and live-dead staining, respectively). VEGF-LMWH interactions were further studied for their cell-responsive nature employing two different cell types: porcine aortic endothelial (PAE) cells overexpressing VEGFR-2 and PAE cells that were not equipped with VEGFR-2 transcript.<sup>273</sup> The hydrogels were eroded by day 4, and VEGF release was greater in presence of VEGFR-2 expressing cells. Such physically crosslinked hydrogels offer novel targeting strategies depending upon cell surface receptor-ligand interactions and could be used for sustained and targeted delivery of VEGF to promote angiogenesis.

## 5. Engineering degradation

Many cellular processes are influenced by spatiotemporal changes in the cell microenvironment. In hydrogel microenvironments, temporal control of matrix properties is easily achieved through selective incorporation of degradable moieties, enabling examination of how property changes influence cell function and fate. Additionally, as discussed in Section 2, controlled degradation of hydrogels is highly desirable for biomedical applications, including soft tissue engineering to promote cell secretory properties and enable tissue elaboration and therapeutic delivery to allow tunable, controlled release locally or systemically. Degradation can be achieved by forming hydrogels with degradable polymer backbones, degradable crosslinks, degradable pendant groups, or reversible non-covalent interactions. This section will focus on degradation kinetics and modes of degradation.

### 5.1 Controlling degradation rates

The desired rate of network degradation is dictated by the final application of cell-compatible hydrogels. For controlled release of bioactive molecules, rapid degradation can lead to an initial

burst or rapid release of cargo, generating large bioactive molecule concentrations which may be desirable, out of a biologically-relevant range, or even toxic depending on the application. For tissue engineering scaffolds and controlled cell culture applications, degradation affects the hydrogel crosslink density and mechanics and hence cell behavior,<sup>274</sup> where ideally the rate of degradation should match the rate of new tissue formation. To control degradation and the temporal properties of the cell microenvironment, hydrogel degradation rates can be tuned by careful selection of network chemistries, degradation kinetics, and network connectivity, which influence crosslink density and mass loss. A brief overview of the general 'handles' for modulating degradation is provided here while in-depth discussion related to specific degradation chemistries is provided in Section 5.2.

Degradation rates are influenced by the chemical nature of the polymer network backbone chain. The number and type of degradable linkages and the local environment surrounding the degradable moieties alter cleavage kinetics. For example, groups present along the polymer backbone or its side chains such as esters, succinimide-thioether linkages, and nitrobenzyl ethers can be degraded *via* hydrolytic,<sup>275–277</sup> *via* retro-Michael reaction<sup>249,278</sup> and photolytic<sup>143,279,280</sup> degradation mechanisms, respectively. The covalent bond cleavage kinetics will influence the overall rate of hydrogel degradation. For example, Jo *et al.* studied the effect of adjacent charged amino acids on the hydrolysis rate of ester bonds and the resulting degradation rate of PEG acrylates modified with cysteine-containing oligopeptides.<sup>281</sup> The positively charged arginine caused a six-fold increase in ester hydrolysis, as compared to negatively charged aspartic acid, and similarly release of covalently linked bovine serum albumin (BSA) was influenced by the rate of degradation.

Hydrogel degradation rates can be tuned by optimizing network connectivity and mesh size. Increased crosslinking density typically leads to smaller mesh size, increased modulus,





and slower degradation, owing to an increased number of cleavable bonds that must be broken for network mass loss and erosion.<sup>282</sup> Decreased mesh size also can limit accessibility of the degradable moiety within the hydrogel to larger molecules, such as enzymes, owing to a reduced diffusion rate.<sup>162</sup> In such cases, release of cargo molecules will be slower as well due to hindered diffusion.

Encapsulated cells, cell secreted enzymes, and growth media can influence degradation rates for chemically or physically crosslinked hydrogels.<sup>283,284</sup> Additionally, the degradation products can influence cell proliferation and differentiation. For instance, Lampe *et al.* studied the effect of degradable macromer content on neural cell metabolic activity, proliferation and differentiation using PEG and poly(lactic acid) copolymer based hydrogels.<sup>285</sup> It was found that the neural cell survival, proliferation and metabolic functions immediately after encapsulation were improved in hydrogels prepared with increasing degradable macromer content, suggesting a beneficial impact of lactic acid released during degradation.

Degradation rates can be investigated using bulk property measurements, such as the *in vitro* monitoring of hydrogel swelling, mass loss, mechanical properties, or solubilization or the *in vivo* imaging and analysis of implanted materials. Hydrogel degradation rate also can be studied by monitoring direct bond cleavage or monitoring degradation products (*i.e.*, uronic acid release due to HA degradation).<sup>286</sup> Methods for assessing hydrogel degradation rates are well covered within a recent review by Peppas *et al.*<sup>7</sup>

## 5.2 Modes of degradation

Hydrogels can degrade through surface erosion, bulk degradation, or a combination of the two depending upon the type and number of degradable linkages. At high crosslinking density, restricted diffusion of water and enzyme may preferentially lead to surface erosion. Bulk degradation, typically observed in hydrogels owing to their high water content and relatively high diffusivity, occurs when cleavable groups present throughout the bulk as well as on surface degrade simultaneously.

Physically crosslinked hydrogels can degrade by processes that reverse the gelation mechanism or disturb the non-covalent interactions of the crosslinks. For example, calcium cross-linked alginate hydrogels are known to degrade *in vitro* due to ion-exchange processes between  $\text{Ca}^{2+}$  ions, present within hydrogel network, and  $\text{Na}^+$  ions of buffered solutions.<sup>108</sup> Further, stereo-complexed hydrogels formed using amphiphilic copolymers of PLA and PEG can be degraded by disruption of the aggregate packing.<sup>287</sup>

Chemically crosslinked hydrogels can be degraded *via* several mechanisms, including cleavage of the backbone chain, crosslinker, or pendant groups (Fig. 10). Hydrogels prepared using polymers with degradable functional groups within the backbone chain are degraded into smaller segments of the original polymer depending upon the location of the degradable groups. A large number of hydrogels include degradable crosslinkers, such as peptides, proteins, or polymers that contain chemically labile moieties. Such hydrogel networks degrade

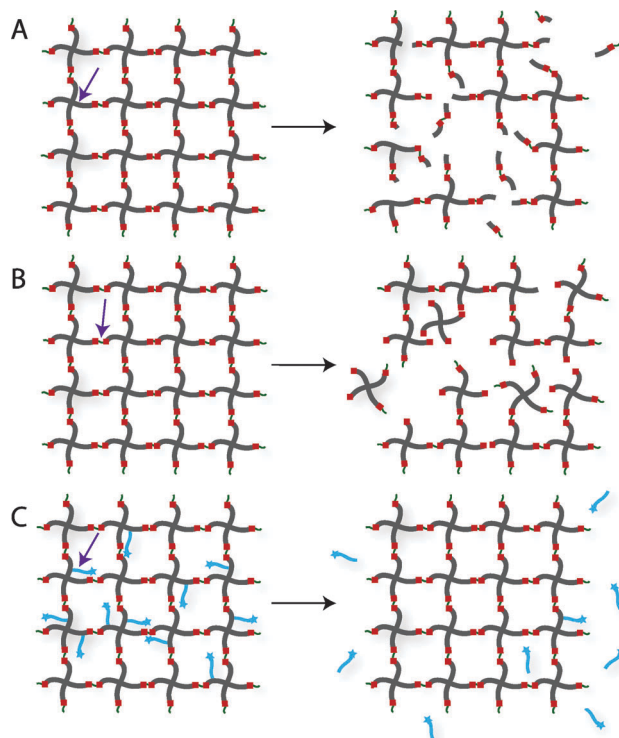


**Fig. 10** Degradation strategies for controlling hydrogel-based cell microenvironments. Chemically crosslinked hydrogels can be degraded *via* cleavage of (A) the polymer backbone, (B) crosslinker or (C) pendant group depending upon the chemistry used for hydrogel formation (choice of polymer, crosslinker, and crosslinking mechanism).

into high molecular weight polymer backbone chains and degradation products from the crosslinker. Polymer chains also can be end-capped with degradable functional groups followed by the addition of reactive functionalities, thus creating cross-linkable degradable macromers. After crosslinking and degradation, the hydrogel network is degraded into the components that comprise the polymer network backbone; for example, in the case of PEG-PLA diacrylate hydrogels, the degradation products are PEG, polyacrylate, and lactic acid. Chemically crosslinked hydrogels often are degraded through hydrolysis, enzymatic cleavage, reversible click reactions, or photolytic degradation (Fig. 11). To engineer hydrogel degradability, it is essential to understand the types of cleavable groups and modes of degradation, their byproducts, and factors affecting degradation rates. These modes of degradation are briefly discussed below with respect to their use in cell-compatible hydrogels.

**5.2.1 Enzymatic degradation.** Cell-mediated enzymatic cleavage is of particular importance for the degradation of hydrogels composed of natural polymers, proteins, or peptide linkages. For instance, Kane and coworkers incorporated alginase-loaded PLGA microspheres in an alginate hydrogel.<sup>288</sup> The rate of hydrogel degradation was tuned by the activity of alginase released from microspheres, as mammalian cells do not produce alginase. Further, these degradable alginate hydrogels enhanced neural progenitor cell expansion rates *in vitro* as compared to control non-degradable hydrogels.



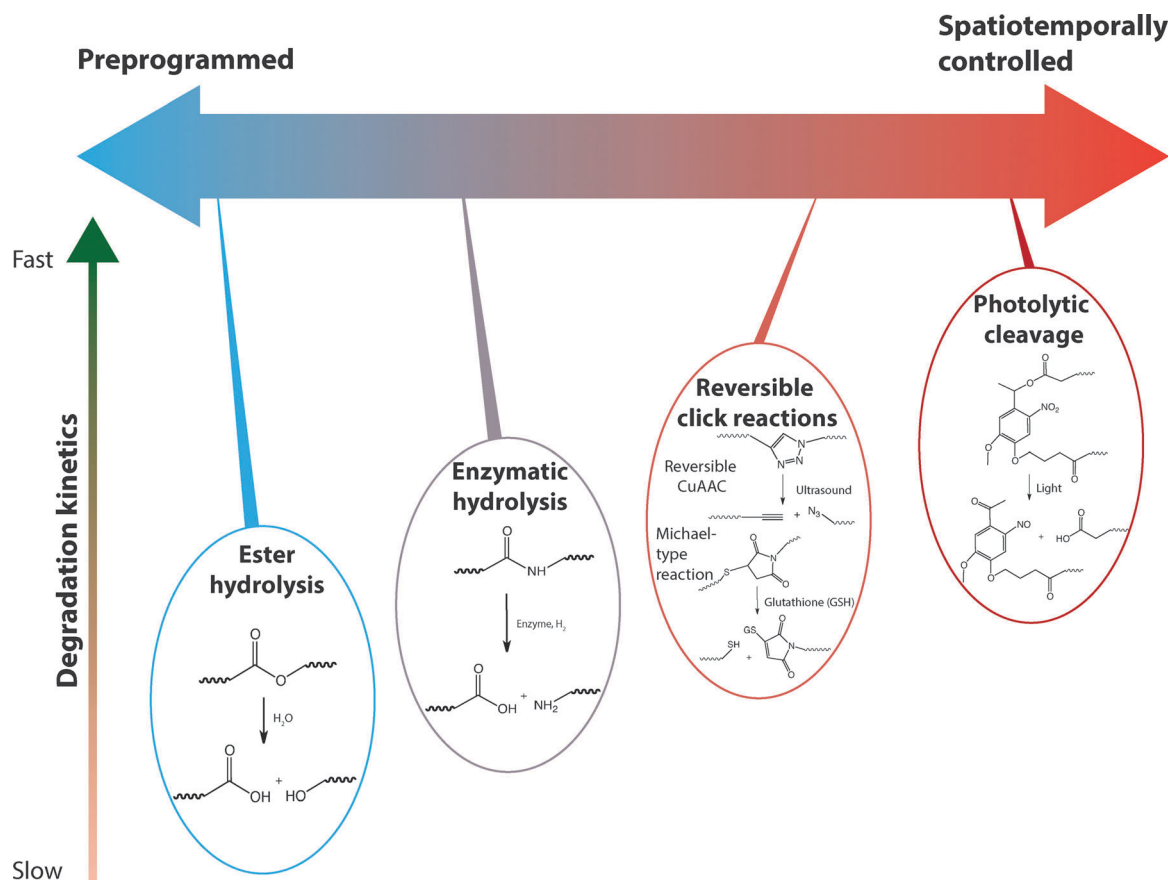


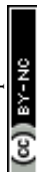
**Fig. 11** Selection of labile groups to control degradation rates. Chemically crosslinked hydrogels can be engineered to degrade at a preprogrammed, cell-dictated, or user-defined rate with varying degrees of spatiotemporal control.

Enzymatically degradable hydrogels also have been utilized for targeted drug delivery since the concentration of enzyme is dependent upon cell and tissue types, enabling local triggered drug release. For instance, the concentration of hyaluronidase is known to be substantially higher in various carcinomas,<sup>289</sup> and enzymatically-degradable HA-based hydrogels can be used as site-specific therapeutic delivery vehicles. HA-based hydrogels degrade in the presence of hyaluronidase, a family of enzymes that catalyze the hydrolysis of C–O, C–N and C–C bonds. Lee *et al.* prepared a HA-tyramine based injectable hydrogel for protein delivery in which the release of the cargo molecule was partially dependent on hydrogel degradation *via* hyaluronidase.<sup>286</sup> Approximately 70% of the activity of released lysozyme, a model cargo protein, was retained *in vitro*. In principle, such an approach can be used for sustained, local therapeutic protein release to inhibit tumor growth.

Parameters such as pH, local ionic strength, enzyme concentration, and temperature may change degradation profiles due to their influence on the specificity of enzyme–substrate complex formation. The crosslinking density and pore size of the hydrogel also can influence the hydrogel degradation rate. For instance, Aimetti *et al.* reported use of a human neutrophil elastase (HNE) sensitive peptide for crosslinking PEG hydrogels using thiol–ene photopolymerization.<sup>162</sup> The gels were engineered to degrade *via* surface erosion by limiting diffusion of

HNE inside the hydrogel network *via* a high crosslink density and small mesh size; upon erosion, a physically entrapped protein was released. Surface degradation was investigated using mass loss and swelling ratio measurements, and the release of the model encapsulated protein, BSA, was modulated by changing peptide  $k_{\text{cat}}$  values with amino acid substitutions, HNE concentration, and peptide crosslinker concentration.

Incorporation of protein- or peptide-based linkages, which are susceptible to proteases as noted in the example above, is a powerful way to control hydrogel degradation both synthetically and *in situ*.<sup>150,162,290–292</sup> For instance, Patterson and Hubbell prepared PEG hydrogels with protease-sensitive peptides through Michael-type addition reactions.<sup>290</sup> When incubated with MMP1 and MMP2, the hydrogel samples degraded *via* enzymatic hydrolysis with variable rates depending upon the peptide sequence used (MMP1  $k_{\text{cat}} \sim 0.1$  to  $7.9 \text{ s}^{-1}$ , MMP2  $\sim k_{\text{cat}} 0.30$  to  $5.6 \text{ s}^{-1}$ ). Encapsulated fibroblasts showed increased spreading and proliferation when cultured in three-dimensions within hydrogels crosslinked using more rapidly degrading peptides. The results highlighted the possibility of engineering hydrogel degradability in response to specific MMPs that are overexpressed in relevant cell type(s) of interest. For example, endothelial cells predominantly express MMP-2 and MMP-9,<sup>293</sup> and thus MMP-2 and MMP-9 sensitive hydrogels can be used to promote endothelial cell invasion for angiogenesis. Further,



enzymatically degradable hydrogels have been employed for wound healing<sup>294,295</sup> and bone regeneration.<sup>296,297</sup>

**5.2.2 Hydrolytic degradation.** A myriad of synthetic hydrogels have been engineered to degrade through hydrolysis of ester linkages within the network backbone or crosslinker, where ester cleavage produces a carboxylic acid and an alcohol. In hydrolytically degradable hydrogels, crosslinking density, local pH, and polymer network chemistry, including backbone molecular weight, crystallinity, and hydrophobicity, influence the degradation rate. Recently, Zhang *et al.* reported use of a biodegradable triblock copolymer poly( $\epsilon$ -caprolactone-*co*-lactide)-*b*-poly(ethylene glycol)-*b*-poly( $\epsilon$ -caprolactone-*co*-lactide) hydrogel as a post-operative intestinal adhesion barrier.<sup>275</sup> The hydrogel retained its integrity for approximately 6 weeks *in vivo* and eventually degraded by ester hydrolysis without significant cytotoxicity. Patenaude and Hoare synthesized hydrolytically degradable thermoresponsive hydrogel using aldehyde and hydrazide functionalized PNIPAAm.<sup>298</sup> The rate of hydrolysis of the hydrazone linkages in acidic microenvironment varied from 2 to 6 hours, leading to complete degradation of cell-compatible hydrogels, and extrapolation of kinetic data predicted degradation on the order of several months under physiological conditions.

**5.2.3 Reversible click reactions.** Click chemistries offer several advantages in hydrogel network formation as discussed in Section 4; however, the application of reversible click reactions as a simple approach to engineer degradability near physiological conditions has been restricted. A few of the click reactions, namely CuAAC and Michael-type additions, have been investigated for their reversibility.

Bielawski and coworkers reported a novel strategy through which the 1,3-dipolar cycloaddition reaction was reversed (Fig. 12).<sup>299</sup> 2,2'-(1*H*-1,2,3-triazole-1,4-diyl)diethanol was condensed with 2-bromoisobutyl bromide for preparing bifunctional initiator; this initiator was used to prepare triazole-centered poly(methyl acrylate) *via* Cu-mediated single electron transfer

living radical polymerization of methyl acrylate. Ultrasound techniques were employed to cause chain scission near the center of the polymer and thus generate the respective azide and alkyne precursors. An optimal polymer molecular weight, triazole location in the chain, and sonication time were determined. The liberated alkyne and azide components subsequently were able to undergo the 1,3-dipolar cycloaddition reaction in the presence of a copper(i) catalyst. Such unclicking approaches could be used to prepare hydrogels capable of degradation under applied mechanical force.

In another example, Baldwin and Kiick recently reported use of a retro click reaction to engineer the degradation rates of heparin-functionalized hydrogels prepared using thiol-based Michael-type addition reactions between multifunctional PEG thiols and maleimide-modified heparin.<sup>249,278</sup> Differences in the  $pK_a$  of the mercaptoacids used to functionalize PEG led to differences in hydrogel degradation rate within a reducing environment (*i.e.*, in the presence of glutathione), owing to differential retro Michael-type cleavage rates of the succinimide-thioether linkage; the more rapid equilibration of an aryl thioether succinimide product with its reactant aryl-thiol modified PEGs and maleimide-functionalized heparin resulted in the capture of the liberated maleimide by the exogenous glutathione (GSH). The choice of mercaptoacid also was used to control the release of bioactive molecules *in vitro*. The intracellular concentration of GSH, a tripeptide of glutamic acid, cysteine, and glycine, is known to be significantly higher than the extracellular concentration,<sup>300</sup> and the GSH content of carcinoma cells also is elevated, owing to the role of GSH in regulating mutagenic mechanisms, DNA synthesis, and growth.<sup>301,302</sup> Since the rate of degradation and release of cargo molecules from these gels depend upon the local reducing environment, this degradation strategy is promising for intracellular or site-specific controlled drug delivery.

Another exciting class of reversible click reactions is retro Diels–Alder cycloreversion, which can be an attractive tool to modulate hydrogel degradation. Early examples of incorporating this reversible reaction chemistry within the crosslinks of hydrogels exhibited significant network degradation at temperatures above 60 °C, potentially limiting their translation into controlled cell microenvironments.<sup>303,304</sup> However, recent work incorporating furan-functionalized pendant peptides within PEG-maleimide-based hydrogels demonstrates controlled release of these peptide tethers under physiological conditions.<sup>305</sup> While higher temperatures (up to 80 °C) increased release, physiological temperature was adequate for significant tether release (~40%), and dexamethasone released by this mechanism was shown to promote osteogenic differentiation of encapsulated hMSCs.<sup>305</sup> This class of reversible click reactions is promising for predictable, tunable control of cell microenvironment properties.

**5.2.4 Light-mediated degradation.** Photolabile monomers and polymers engineered to cleave under cytocompatible irradiation conditions allow spatiotemporal control of hydrogel degradation and *in situ* property tuning.<sup>306</sup> Anseth and coworkers developed photodegradable hydrogels for cell culture by creating an acrylated nitrobenzyl ether-derived

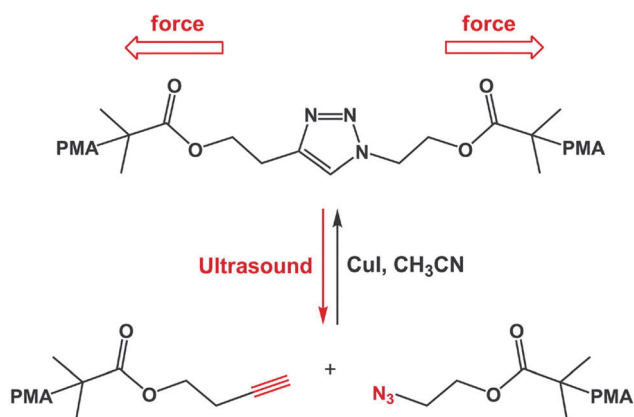


**Fig. 12** Ultrasound-induced retro [3+2] cycloaddition of an embedded triazole moiety. Triazole bond formation can be reversed by the application of mechanical force, resulting in azide and alkyne functional groups. The generated azide and alkyne moieties of the functionalized poly(methyl acrylate) (PMA) were subsequently 'clicked' (Cu, CH<sub>3</sub>CN) to form the triazole-based starting material. Image reprinted from Brantley *et al.*<sup>299</sup> with permission from Nature publishing group. Copyright (2011).



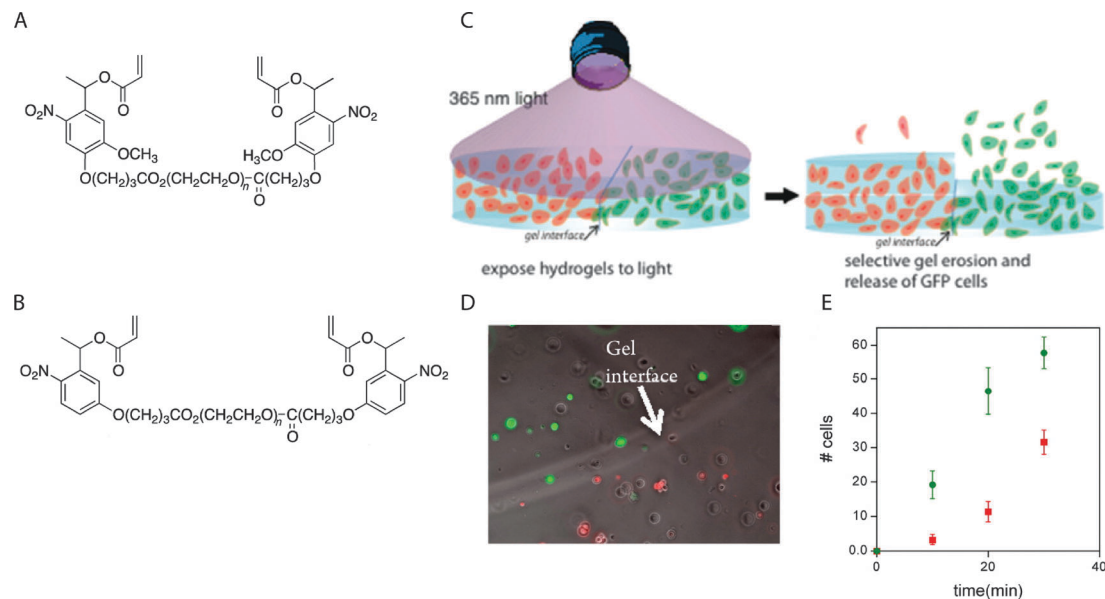


**Fig. 13** Selective cell release via photodegradation using differences in reactivity of *o*-nitrobenzyl groups. (A), (B) *o*-Nitrobenzyl linkers with different degradation kinetics were used to vary the degradation rate of adjacent hydrogels. (C) RFP-expressing hMSCs and GFP-expressing hMSCs were encapsulated within hydrogels made with (A) or (B), where the two hydrogels were in direct contact with each other (RFP = red fluorescent protein, GFP = green fluorescent protein). (D) The interface between hydrogels containing RFP- and GFP-expressing hMSCs was observed using optical microscopy. (E) Gels were exposed to light (10 mW cm<sup>-2</sup> at 365 nm, 30 minute total duration), resulting in a biased release of one cell population over another ( $R_{\text{GFP}}/R_{\text{RFP}} \sim 2.4$ ) which was consistent with the degradation rate constants of (A) and (B) ( $k_{\text{app A}}/k_{\text{app B}} \sim 2.5$ ). Image reprinted from Griffin *et al.*<sup>280</sup> with permission from American Chemical Society. Copyright (2012).

moiety with a pendant carboxylic acid that could be attached to poly(ethylene glycol) (PEG)-bis-amine or amine-terminated peptides to create a photocleavable cross-linking diacrylate macromer (PEG-diPDA) or a photoreleasable pendant peptide tether, respectively.<sup>205</sup> The PEG-diPDA hydrogels degraded when irradiated with cytocompatible doses of long wavelength UV, visible, or two-photon IR light (365, 405, and 740 nm, respectively), enabling precise control over hydrogel degradation profiles *in situ*. Hydrogel photodegradation and the corresponding change in crosslink density led to an increase in the mesh size and decrease in the polymer density surrounding the cells, promoting encapsulated hMSC spreading as compared to non-irradiated control hydrogels.<sup>279</sup> In addition, photolabile RGDS containing hydrogels were found to influence the integrin expression on the surface of cells, where temporal modulation enhanced hMSC differentiation. Griffin and Kasko recently incorporated *o*-nitrobenzyl groups with varying cleavage kinetics within the backbone of PEG hydrogels (Fig. 13).<sup>280</sup> The hydrogels were formed using redox polymerization in presence of hMSCs and were selectively photodegraded to release specific stem cell population. Such an approach can be used for cell encapsulation and on-demand release of therapeutic cells for regenerative medicine and wound healing applications.

In a complementary light-mediated approach, Anseth and coworkers used photoinitiators to degrade disulfide-bonded PEG hydrogels.<sup>307</sup> When irradiated, the photoinitiator created free radicals through heterolytic decomposition, attacking the disulfide bonds and resulting in hydrogel degradation. In principle, this photoinitiated disulfide bond degradation could be conducted in the presence of cells in conjunction

with cytocompatible disulfide gel formation.<sup>308</sup> Almutairi and coworkers recently reported synthesis of polymer containing a pendant photocleavable group, 4-bromo-7-hydroxycoumarin (Bhc).<sup>309</sup> Upon photolysis with cell and tissue compatible near infrared irradiation, the polymer undergoes a triggered cascade of cyclization reactions, leading to degradation of the polymer backbone with potential applications for controlled release *in vivo* within deep tissues.

## 6. Orthogonal property control

### 6.1 Biochemical cues

Bioactive molecules, such as proteins, cytokines, growth factors, and therapeutic drugs, have been extensively used to provide biochemical cues that modulate cell adhesion, migration, differentiation, and proliferation. Spatial and temporal presentation of such biochemical cues can mimic the dynamic nature of the native cellular microenvironment *in vitro* or enable site-specific regulation of cellular functions within *in vivo* microenvironments. Significant advances have been made in improving hydrogel properties for spatiotemporal controlled presentation of bioactive molecules. Current technologies have demonstrated the potential of hydrogels for controlled, sustained, and local delivery of bioactive molecules, and the static or dynamic presentation of insoluble biochemical signals, such as immobilized integrin binding peptide sequences or sequestered growth factors. However, some challenges remain for improving the clinical applicability and spatiotemporal functionality of hydrogels for controlled presentation of bioactive molecules. For controlled release, issues with encapsulation efficacy, the stability of





encapsulated proteins and sensitive bioactive molecules, and long-term delivery of hydrophobic molecules persist; for insoluble cues, difficulties persist with the dynamic presentation of multiple cues with high spatial resolution.

For controlled incorporation or presentation of bioactive molecules, one must consider factors such as the mechanism of release, the triggering mechanism, and the ability to control spatiotemporal presentation or release, in addition to the design considerations discussed in Section 2. The release of cargo molecules can be controlled by diffusion, degradation (surface or bulk erosion), the cleavage of a tether, or a combination of these mechanisms, where the bioactive molecules are chemically immobilized, sequestered or physically encapsulated in the hydrogel network. Here, we present several recent advances in the design and production of cell-compatible hydrogels, including the controlled presentation of bioactive molecules and the manipulation of mechanical and physicochemical properties.

**6.1.1 Chemical immobilization/sequestration.** Many mammalian cells are anchorage-dependent. Cellular processes such as adhesion, migration, proliferation, and differentiation are now known to be regulated by signals from cell–substrate interactions.<sup>51,310,311</sup> Hence, one of the most vital features

for the adaptation of cells to their environment is their adhesive interaction with a substrate. Integrins, members of the *trans*-membrane family of proteins, are the principle cell surface adhesion receptors that mediate cell–matrix adhesion.<sup>312</sup> Integrins mediate numerous intracellular signaling pathways, such as calcium channels, kinases, and phosphatases, and also recruit intracellular signaling reagents, influencing cellular functions such as motility and tissue invasion.<sup>313</sup> Cellular adhesion can be controlled by tethering proteins or their analogs directly to the polymer network, entrapping these molecules, sequestering them from serum, or by manipulating the hydrophobicity of the network.

One of the most successful techniques for promoting cell adhesion in cell-compatible hydrogels is to incorporate peptide-based analogs of native ECM components, such as RGD, YIGSR, and IKVAV, into the hydrogel matrix.<sup>314–317</sup> The RGD (*Arg-Gly-Asp*) sequence is found in a number of extracellular proteins, including fibrinogen, fibronectin, vitronectin, and laminin, and binds several integrins with varying strength.<sup>318,319</sup> For spatiotemporally controlled presentation of the RGD motif in hydrogels, DeForest and Anseth employed SPAAC and thiol–ene click chemistries (Fig. 14).<sup>320</sup> Four-arm cyclooctyne-

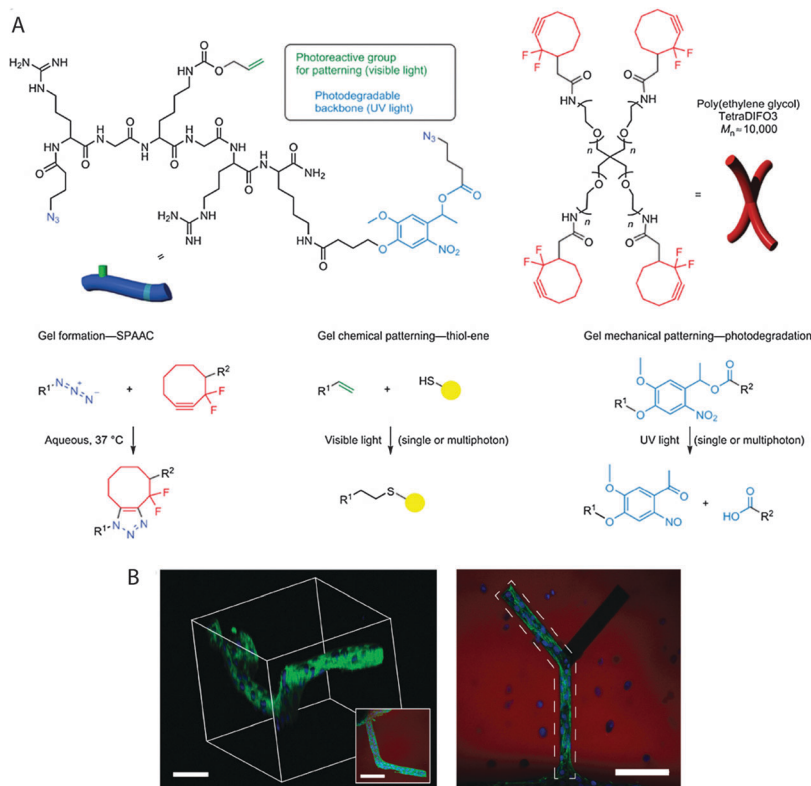
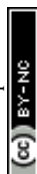


**Fig. 14** Spatiotemporal control of biochemical cues in 3D microenvironment. (A) Four-arm PEG functionalized with cyclooctyne was reacted with azide di-functionalized polypeptides via SPAAC reaction to form a hydrogel network via step-growth mechanism. A light-mediated thiol–ene reaction (cytocompatible 490–650 nm or 860 nm pulsed laser light) was used to immobilize cell adhesive thiol-functionalized peptides (RGD) using vinyl functionalities present on hydrogel network. Further, 3-D channels were degraded within the hydrogel using pulsed laser light (740 nm) via irreversible cleavage of nitrobenzyl ether moiety. (B) A cell-laden (3T3 fibroblasts) fibrin clot was encapsulated in the hydrogel (3D microenvironment). Biochemical (channel containing RGD noted by dashed polygon) and biophysical cues (photodegraded channel) were added to control 3T3 cell outgrowth in the presence of encapsulated hMSCs (right, top-down projection; left, 3D rendering). (Scale bar, 100 μm, hydrogel shown in red, F-actin in green and cell nuclei in blue) Image reprinted from DeForest *et al.*<sup>320</sup> with permission from Nature publishing group. Copyright (2011).



functionalized PEG was reacted with a bis(azide)-functionalized photodegradable polypeptide using SPAAC reaction for hydrogel formation. Thiol-containing RGD peptide was photopatterned with vinyl functionalities on the polypeptide backbone *via* a photoinitiated thiol-ene reaction using visible light. Further, fibroblast outgrowth and spreading within a photodegraded channel was directed spatially in the RGD photopatterned region. When incorporating cell-binding domains into hydrogels, it must be recognized that multiple factors, including the bulk density, domain size, and length of the spacer arm to the adhesion ligand, can influence cell adhesion and spreading. Lee *et al.* studied the effect of the spacer length in RGD-modified substrates for controlling cell phenotype in the 2D and 3D cell microenvironment *via* the use of  $G_n$ RGDSP-modified alginate hydrogels.<sup>321</sup> From measurements of the cell aspect ratio and projected area, at least four glycines ( $n = 4$ ) were required for fibroblast adhesion on the  $G_n$ RGDSP-modified alginate hydrogels.

While incorporation of bioactive peptides into a hydrogel matrix provides an interesting strategy to induce bioactivity and enhance cell adhesion and spreading, understanding the effect of such peptide incorporation on the mechanical and transport properties of the network is essential. Zustiak *et al.* demonstrated that peptide ligands influence the physical, mechanical and transport properties of PEG hydrogels and that the extent of this influence was dependent on the concentration and the amino acid sequence of a given ligand.<sup>322</sup> Incorporation of the peptide RGDS at a concentration of 300  $\mu$ M in a PEG hydrogel (10% w/v) led to an  $\sim 20\%$  decrease in the hydrogel storage

modulus ( $G'$ ), and accordingly, the calculated average network mesh size ( $\xi$ ) increased by  $\sim 1$  nm. Further, the greatest change in  $G'$  and  $\xi$  was observed for hydrogels modified with either IKVAV (10  $\mu$ M) or YIGSR (100  $\mu$ M), emphasizing the importance of the amino acid sequence and related ligand-polymer interactions. The pronounced effect of YIGSR ligands on hydrogel properties was hypothesized to arise from the formation of hydrogen bonds between the phenolic OH group of Y and the ether oxygen of the PEG polymer. The incorporation of RGDS, IKVAV or YIGSR at a concentration of 100  $\mu$ M resulted in a decrease in the diffusivity of encapsulated BSA by approximately 30%.

The process of cell adhesion is mediated through proteins. Hydrogel network hydrophobicity, which promotes protein adsorption, consequently can influence cell adhesion. Ayala *et al.* recently demonstrated the effect of matrix hydrophobicity on the adhesion, morphology, and differentiation of hMSCs using a hydrogel based on copolymers of select acryloyl amino acids (referred to generally as AA) and acrylamide (Am), as shown in Fig. 15.<sup>323</sup> Substrate hydrophobicity was systematically controlled by varying the length of pendant alkyl side chains, as assessed by contact angle measurements, without significantly altering the chemical or mechanical properties of the hydrogel. The adhesion and spreading of hMSCs were found to be non-monotonically dependent on matrix hydrophobicity. A hydrogel equipped with a 5-carbon long alkyl chain (C5) was shown to support improved cell adhesion as compared to those modified with 1–4 (C1 to C4) and 6–10 carbons (C6 to C10). Cell spreading was hypothesized to be greater on the

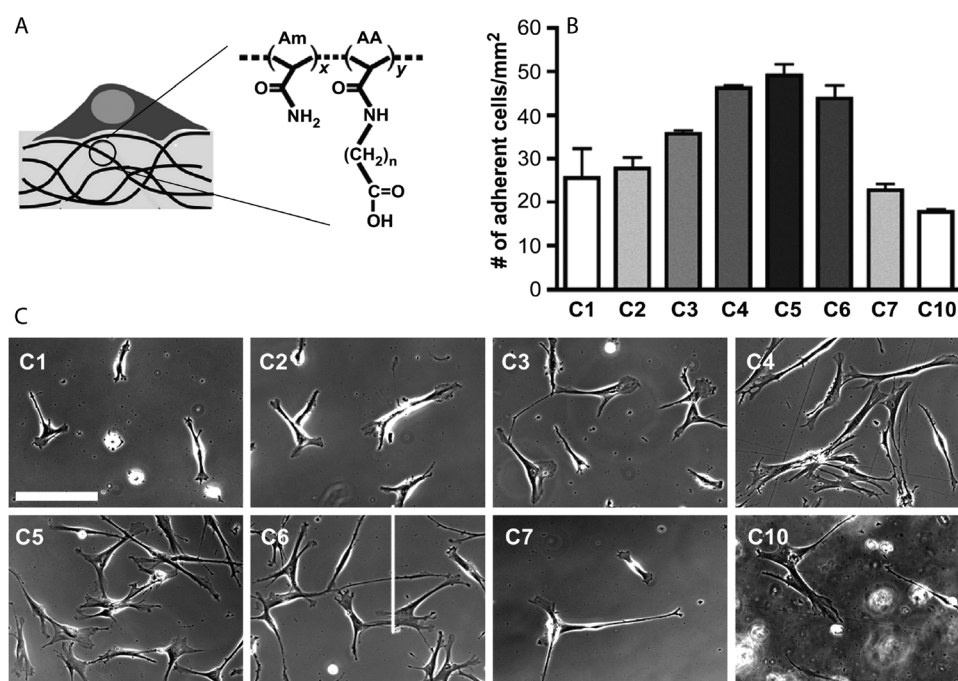


**Fig. 15** Modulation of cell adhesion and spreading in 2D microenvironment. (A) The hydrogels were prepared by copolymerizing acrylamide (Am) with acryloyl amino acid (AA) using a bis-acrylamide initiator. Depending upon the number of  $\text{CH}_2$  groups on the AA pendant chain ( $n = 1$  to 10, referred as C1, C2, ..., C10), the interfacial hydrophobicity of the hydrogel varied, with water contact angle ranging from  $26^\circ$  to  $85^\circ$  (sessile drop method,  $20^\circ\text{C}$ ). (B), (C) Non-monotonic dependence on the monomer side chain length was observed in cell adhesion and spreading of hMSCs on C1–C10 hydrogels (scale bar,  $400\ \mu\text{m}$ ). Image reprinted from Ayala *et al.*<sup>323</sup> with permission from Elsevier. Copyright (2011).



C5-containing hydrogels, as compared to the C1–C4 hydrogels, due to limitations in the accessibility of the AA side chain to fibronectin. For the hydrogels with longer alkyl chains (C6–C10), it was postulated that collapse of the hydrophobic domain into the matrix resulted in limited accessibility of the AA for binding.

In addition to controlling cell adhesion, efforts have been made to design cell-compatible hydrogels for highly directed cell migration. Cell migration is a central, highly integrated multistep process required for maintenance and development of numerous physiological processes.<sup>324,325</sup> In hydrogel networks, cell migration has been controlled using spatiotemporal gradients of selective cell adhesion ligands. Numerous experiments have shown increased cell migration with increased ligand density up to a critical value, or towards the higher ligand density in a gradient. Cell migration speed is known to have a parabolic response to ligand density.<sup>326</sup> In 2D culture, Guarnieri *et al.* studied the effect of a linear gradient of covalently immobilized RGD within PEG diacrylate-based hydrogels on the migration of fibroblasts (NIH3T3s).<sup>327</sup> It was shown that the cells moved preferentially along the direction of increasing concentration of immobilized RGD. Further, the cell migration speed increased with an increase in the magnitude of the gradient. Schwartz *et al.* studied migration of fibrosarcoma cells (HT-1080) in 3D microenvironments using enzymatically degradable PEG hydrogels.<sup>326</sup> MMP degradable peptides and RGD-containing peptides were incorporated inside the PEG hydrogel *via* thiol–ene reaction between norbornene functionalized 4-arm PEG and cysteine containing peptides. The mesh

size of the hydrogel ( $13 \pm 1$  nm) was engineered to be much smaller than the size of encapsulated cells ( $\sim 10$   $\mu$ m) to limit migration to a proteolytic mechanism. The percentage of migrating fibrosarcoma cells (HT-1080s) was found to have a parabolic response to ligand density. Further, HT-1080s were observed to migrate through a Rho kinase (ROCK)-dependent mechanism with a rounded morphology that quantitatively resembled *in vivo* migrating cancer cells. In principle, various thiol functionalized biochemical cues can be incorporated into such hydrogels to study cell migration for understanding cancer cell invasive behavior and metastasis.

The ability to promote cell survival and proliferation over desired time periods also is a critical hydrogel design feature and can be achieved by the presentation of growth factors or by controlling cell–ECM and cell–cell interactions. Growth factors are signaling polypeptides that trigger cell responses such as cell survival, migration, differentiation, or proliferation. Precise control over the presentation of proteins and growth factors in hydrogel matrices is critical for mimicking the native cellular microenvironment and promoting cell–substrate and cell–cell interactions for tissue engineering and regenerative medicine applications.<sup>328</sup>

Growth factor immobilization strategies can take advantage of either covalent tethering or affinity interactions between growth factor(s) and rationally designed hydrogels. For example, Kiick and coworkers have employed heparin-containing PEG-based hydrogels for controlling the release of basic FGF (bFGF, also known as FGF-2), using affinity of the growth factor with heparin for sequestering growth factors.<sup>29</sup> Hydrogels were

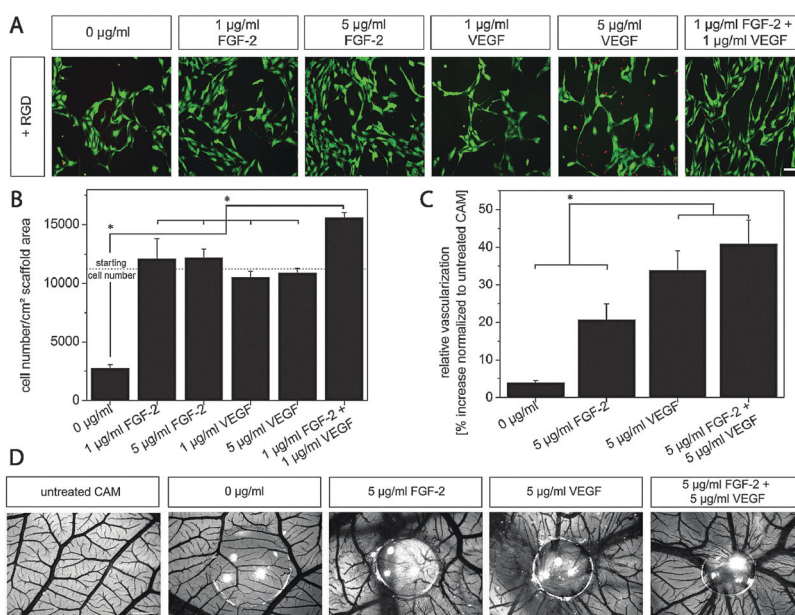
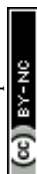


**Fig. 16** Dual growth factor delivery by sequestration in controlled cell microenvironments. (A) Human endothelial cells from the umbilical cord vein (HUVECs) on RGD-modified hydrogel substrates were presented with varying amounts of basic fibroblast growth factor (FGF-2) and vascular endothelial growth factor (VEGF) *via* sequestration. The enhanced cell survival and typical spindle-like morphology on the hydrogel substrate comprising the combination of FGF-2 and VEGF highlights the synergistic activity of both growth factors (fluorescence microscopy images after live/dead staining). (B) Further, HUVEC proliferation was enhanced by the dual presentation (MTT assay, day 3). (C) These hydrogels were placed onto the developing chicken embryo chorioallantoic membrane (CAM) from embryonic day 8 until day 12 to study the effect of growth factors on vascularization. An increased number of vessels within the site of gel transplantation was observed; (D) representative images indicate substantial angiogenic response to combined FGF-2 and VEGF delivery. Reprinted from Zieris *et al.*<sup>329</sup> with permission from Elsevier. Copyright (2011).



prepared *via* Michael-type addition chemistry using thiol-functionalized PEG and maleimide-functionalized heparin. The release of FGF-2 could be tuned as a function of polymer weight percent, polymer molecular weight, and initial cargo loading. In addition to local delivery of a single growth factor, simultaneous delivery of multiple growth factors may enhance cell response. For example, Zieris *et al.* investigated the effect of independent delivery of bFGF and VEGF from PEG-heparin hydrogels, on vascularization (Fig. 16).<sup>329</sup> Amine-functionalized PEG was chemically crosslinked with EDC/s-NHS-activated carboxylic acid groups of heparin to form the hydrogel, and growth factors were immobilized post-hydrogel formation *via* heparin interaction. It was found that the loaded concentration of the growth factor could easily be tuned as a function of the initial concentration of growth factor, and release of the cargo occurred without significant initial burst. The cell number after 3 days, determined indirectly *via* a MTT metabolic activity assay, was approximately four times higher in hydrogels with growth factors ( $\sim 10\,000$ – $12\,000$  cells  $\text{cm}^{-2}$  scaffold area) as compared to a control hydrogel that lacked growth factors ( $\sim 2700$  cells  $\text{cm}^{-2}$  scaffold area), indicating enhanced survival and proliferation in hydrogels with sequestered FGF-2 and VEGF. Quantification of chicken embryo chorioallantoic membrane (CAM) vascularization indicated a significant increase in vascularization in the presence of FGF-2, VEGF or a combination of both ( $\sim 20\%$ ,  $35\%$  and  $40\%$ , respectively) as compared to control hydrogel. Overall, the combined delivery of FGF-2 and VEGF resulted in superior pro-angiogenic effects (cell survival, proliferation, differentiation, and migration *in vitro* and CAM vascularization *in vivo*) relative to single factor delivery.

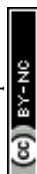
Cell-cell interactions are important for various cellular processes, including cell survival, proliferation, and differentiation, and hence designing hydrogels to promote cell-cell communication can positively impact or regulate these. Lin and Anseth recently developed functional PEG hydrogels with immobilized cell-cell communication cues in order to enhance the survival of encapsulated pancreatic  $\beta$ -cells.<sup>330</sup> A PEG-diacrylate (PEGDA) macromer and thiol-functionalized fusion proteins (EphA5-Fc receptor and ephrinA5-Fc ligand) were polymerized with a cell-compatible photoinitiator *via* mixed mode thiol-acrylate photopolymerization in the presence of a murine insulinoma cell line (MIN6). EphA-ephrinA binding is known to mediate insulin secretion in pancreatic  $\beta$ -cells and also is linked to several intracellular signaling pathways that influence cell survival.<sup>331</sup> The immobilization of these fusion proteins (200 nM) in the hydrogel resulted in more than a 100% increase in cell metabolic activity compared to hydrogels without any immobilized protein. Such an approach could be used to tailor the hydrogel microenvironment *via* incorporation of appropriate ECM components and using cell-cell communication signals to synergistically enhance cell survival for applications, including soft tissue engineering, controlled 3D cell culture, and cell delivery.

Wylie *et al.* reported simultaneous patterning of multiple growth factors, sonic hedgehog (SHH) and ciliary neurotrophic factor (CNTF), in three-dimensional hydrogels using orthogonal

physical binding.<sup>332</sup> Agarose hydrogels containing coumarin-caged thiols yielded reactive thiol groups upon two-photon irradiation; these selectively de-protected thiols subsequently served as sites for the sequential immobilization of maleimide functionalized barnase and streptavidin *via* a thiol-maleimide reaction. Barstar-SHH and biotin-CNTF were incubated in the hydrogel, for immobilization *via* their physical binding interactions with barnase and streptavidin, respectively. SHH and CNTF remained bioactive after immobilization. The hydrogel with immobilized growth factors did not show significant cytotoxicity, and in principle, such a simple approach could be used to control the spatiotemporal presentation of multiple growth factors to precisely engineer cell differentiation.

**6.1.2 Physical encapsulation and release.** Several chemotactic agents, which influence cell migration,<sup>333–336</sup> can be physically encapsulated within hydrogels. Li *et al.* studied the effect of hepatocyte growth factor (HGF), a strong chemo-attractant, and leukemia inhibitory factor (LIF), a key regulator of stem cell mobilization, on cell migration by loading these factors in PEG hydrogels and PLGA nanoparticles, respectively.<sup>336</sup> The release of HGF from the hydrogel resulted in an approximate 4-fold increase in neural stem cell (NSC) migration through cell culture inserts after 24 hours as compared to a negative control. Further, when nanoparticles containing LIF were encapsulated in hydrogels loaded with HGF, cell migration was enhanced approximately 10-fold after 36 hours, relative to the negative control of blank nanoparticles and a blank hydrogel. This strategy demonstrates the potential for using materials to control the mobilization of NSCs for regenerating central nervous system tissue.

Physical encapsulation of growth factors with stimuli responsive release enables temporal tuning of bioactive molecule concentrations in local microenvironments. The triggering mechanisms used for stimuli responsive hydrogels include pH, temperature, enzymes, externally applied light, or magnetic fields. Garbern *et al.* designed pH- and temperature-responsive injectable hydrogels using poly(*N*-isopropylacrylamide-co-propylacrylic acid-co-butyl acrylate) (*p*[NIPAAm-co-PAA-co-BA]) for sustained and local delivery of bFGF in the acidic micro-environment of ischemic myocardium.<sup>337</sup> The (*p*[NIPAAm-co-PAA-co-BA]) existed as a liquid at room temperature and pH 7.4, but reversibly formed hydrogels at 37 °C and pH 6.8. *In vivo* studies within a rat model of myocardial ischemia indicated that the bFGF could be highly localized at the site of injection when encapsulated within the responsive hydrogel. The amount of bFGF recovered at day 7 was increased by approximately 10-fold with the hydrogel delivery system as compared to delivery *via* saline injection. These *in vivo* studies also indicated an increased microvessel density and improved cardiovascular function (as measured by echocardiography) after 28 days of treatment, indicating the potential for spatiotemporal controlled delivery of the growth factor. Biochemical cues also can be used for regenerative medicine applications. For example, recently Diab *et al.* reported the use of degradable silk fibroin hydrogels for delivering growth factors, such as bone morphogenetic protein BMP-2 (Fig. 17A and B).<sup>338</sup> The





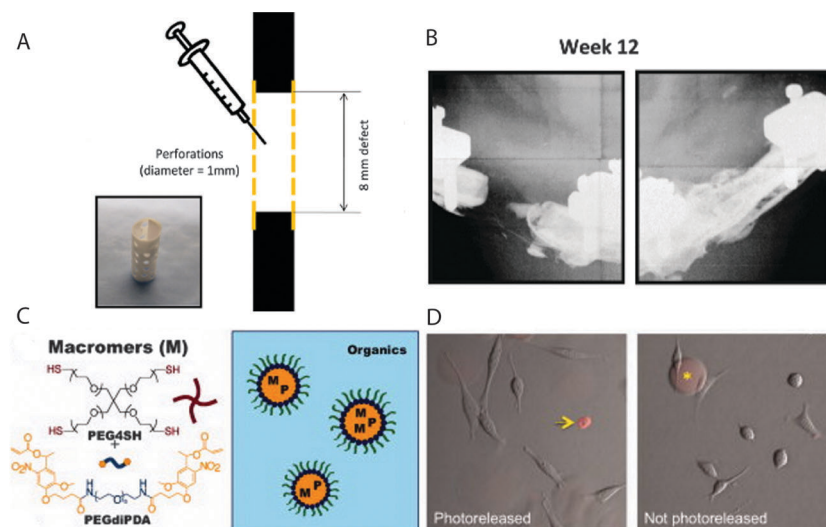


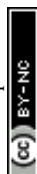
**Fig. 17** Hydrogels for delivering cargo biomolecules (therapeutic proteins, growth factors, and drugs) with pre-programmed or user-defined release behavior. (A) A degradable silk fibroin hydrogel for pre-programmed release was formed in the presence of BMP-2, using a sonication-induced gelation process, and was injected into a bone defect. (B) Enhanced bone formation was observed *in vivo* in SASCO Sprague Dawley rats injected with the silk hydrogel containing BMP-2 as compared to the control group (no growth factor) (week 12, X-ray radiography). A, B reprinted from Diab *et al.*<sup>338</sup> with permission from Elsevier. Copyright (2011). (C) Photodegradable hydrogel microparticles were synthesized by an inverse suspension polymerization of a PEG-diphotodegradable acrylate with a PEG tetrathiol (PEG4SH) *via* base-catalyzed Michael addition. (D) A model cargo protein (Annexin V) was loaded (right), and its release to 3T3 cells (left) was triggered by cytocompatible irradiation (1 min of 13.5 mW cm<sup>-2</sup> at 365 nm). C, D reprinted from Tibbitt *et al.*<sup>339</sup> with permission from John Wiley and Sons publishing. Copyright (2012).

hydrogels were prepared using a sonication-induced gelation process in a solution containing BMP-2 and injected at the large femoral segmental defect site. An initial burst was observed and about ~20–30% of cargo was released by day 4 depending upon hydrogel polymer concentration. An *in vivo* study demonstrated enhanced bone formation with hydrogels containing BMP-2 compare to control (hydrogels without BMP-2). The histological evaluation after 12 weeks indicated that the silk hydrogel was completely degraded.

For controlled release during cell culture, Anseth and coworkers recently reported photodegradable, PEG based hydrogel microspheres with entrapped cargo proteins that deliver proteins locally upon exposure to selected wavelengths of light (Fig. 17C and D).<sup>339</sup> Poly(ethylene glycol) di-photodegradable-acrylate (PEGdiPDA) was copolymerized with poly(ethylene glycol) tetrathiol (PEG4SH) *via* base-catalyzed Michael-type addition using an inverse suspension polymerization technique. Transforming growth factor beta 1 (TGF-β1), which controls proliferation, differentiation, and apoptosis, was encapsulated inside of the microspheres during hydrogel formation. The *o*-nitrobenzyl ether moiety in the PEGdiPDA was cleaved using cytocompatible irradiation (at 365 nm for less than 5 minutes), which resulted in network degradation followed by localized release of the cargo molecule. The released TGF-β1 maintained its bioactivity as demonstrated by upregulated luciferase production when applied to a reporter cell line. In principle, such an approach could be used to spatiotemporally control the release of a broad range of cargo molecules, such as growth factors, cytokines, and extracellular matrix components, within 2D and 3D cell microenvironments *via* multiple wavelengths of light.

Cell differentiation is a commonly occurring process by which a less specialized cell, a stem or progenitor cell, becomes a more specialized cell type. For example, mesenchymal stem cells can differentiate into osteoblasts, chondrocytes, or adipocytes amongst other lineages. Due to their ability to differentiate into a wide variety of cell types, stem cells represent a promising resource for tissue engineering and regenerative medicine. To take maximum advantage of pluripotency for such biomedical applications, it is crucial to understand and control the presentation of cues, such as immobilized factors, ECM signaling molecules, and substrate properties, all which can influence stem cell differentiation. Oh *et al.* studied the effect of bFGF on the proliferation and osteogenic differentiation of hMSCs encapsulated in collagen hydrogels in a 3D environment.<sup>340</sup> Sustained release of encapsulated bFGF was observed up to 30 days (with an initial burst). Enhanced osteogenic differentiation of hMSCs in the bFGF-loaded hydrogels was significant after 14 days *in vitro*, as detected by gene expression analysis. The combination of natural hydrogel networks with appropriate growth factors, and the resulting control of cell differentiation, is very promising for clinical use in the field of regenerative medicine.

Significant advances in molecular and cell biology have led to the development of increasingly powerful drugs, which can regulate specific cellular activity. To improve the efficacy, stability, and reduce potential side effects of these drugs, hydrogel-based drug carriers have been reported for controlled release applications. For comprehensive review of hydrogels for drug delivery, readers are referred to a review by Hoare and Kohane.<sup>341</sup> Other drug carriers such as microspheres and liposomes have also been incorporated in hydrogel matrices



to create composite hydrogels. Such approaches can provide superior control over the release profiles of cargo molecules and can enhance biocompatibility of the particular vehicle by its incorporation in the cell-compatible hydrogel. Wei *et al.* used a dual drug delivery system based on PVA or chitosan hydrogels with encapsulated poly(L-glutamic acid)-*b*-poly(propylene oxide)-*b*-poly(L-glutamic acid) micelles that contained aspirin or DOX as the cargo drug molecules, respectively.<sup>342</sup> The release of cargo was found to be dependent on pH and temperature with short-term release of aspirin (~75% release within 3–5 hours) and longer, sustained release of DOX (~25–75% release within 7 hours). The release of DOX was accelerated at lower pH or higher temperature, indicating the potential for localized delivery of the anti-cancer drugs in carcinoma tissue.

## 6.2 Biophysical cues

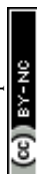
Physical properties of the cellular microenvironment, such as rigidity and topography, also play critical roles in regulating cellular functions and mediating cellular response to a variety of stimuli, such as strain and shear stress. Biophysical cues, whether inherent or applied, have been observed to affect actin cytoskeleton organization, focal adhesion assembly, and cell shape, leading to changes gene and protein expression.<sup>343</sup> These signaling processes regulate cell function and fate, such as adult stem cell differentiation. Hydrogel matrices thus can be engineered to control cell behavior by providing appropriate biophysical cues initially and upon degradation. Here, we overview cell-compatible hydrogels that have been used to manipulate cell response by providing appropriate biophysical cues in static and dynamic 2D and 3D microenvironments along with some examples. The static examples are intended to provide motivation and context for the critical microenvironment signals that regulate cellular processes. The dynamic examples highlight recent works that probe how *changes* in the cell microenvironment influence cell response utilizing orthogonal chemistries and manipulations, degradable moieties, or combinations of these to mimic the native cell microenvironment.

**6.2.1 2D static microenvironments.** Cells adhere to and exert forces against the matrix, initiating mechano-transduction, with the traction forces generated by actomyosin resulting in transmission of forces to the substrate. The substrate resists such deformation and the resulting repulsive force influences cell morphology, function, and fate. Thus, the elasticity of soft tissues (with Young's moduli ( $E$ ) that range from 0.1 kPa (*i.e.*, neural and mammary tissues) to 100<sup>+</sup> kPa (*i.e.*, connective tissues and pre-calcified bone)<sup>27</sup> impacts cellular events such as migration, morphology, and differentiation. For example, in seminal work, Engler *et al.* demonstrated the strong influence of substrate stiffness on stem cell lineage.<sup>27,344</sup> hMSCs seeded on protein-functionalized polyacrylamide (PAAm) hydrogels *in vitro* and cultured in the same medium differentiated into neurons on soft substrates, myoblasts on stiffer substrates, and osteoblasts on comparatively rigid substrates. By use of such approaches, stem cells can be precommitted *in vitro* before use within the *in vivo* microenvironment for regenerative medicine applications. Building on this work, several different substrates

have been designed to probe the role of mechano-transduction in cell function and fate within 2D culture. Recently, Discher and coworkers used ligand functionalized HA and PAAm hydrogels to study hMSC adhesion and morphology in both 2D and 3D environments, investigating if cell response to physical features is independent of matrix composition.<sup>345</sup> HA was functionalized with thiol groups and chemically crosslinked with PEG-diacrylate to form hydrogels. Young's modulus was varied from 0.1 to 100 kPa, covering a broad physiological range, by modulating crosslink density, polymer concentration, and temporal deactivation of remaining free thiol groups. hMSCs seeded on HA and PAAm hydrogels with varying elasticity exhibited an increase in cell area monotonically with increased modulus for both HA and PAAm hydrogels. Cells treated with blebbistatin, a nonmuscle myosin IIa inhibitor, had a limited cell area and aspect ratio. The results highlighted the importance of understanding biophysical cues, which can influence cell response.

Mechanical feedback from the ECM, which is required for integrin clustering and for the subsequent formation of focal adhesions, is critical for stem cell differentiation. Trappmann *et al.* studied the differentiation of hMSCs and human epidermal stem cells using collagen coated polydimethylsiloxane (PDMS) and polyacrylamide (PAAm) hydrogel surfaces.<sup>346</sup> The substrate modulus was varied from 0.1 kPa to 2300 kPa (by modulating polymer-crosslinker ratio) and from 0.5 kPa to 740 kPa for PAAm (by modulating monomer-crosslinker ratio). hMSCs seeded on all PDMS and PAAm substrate with high stiffness differentiated into bone cells, whereas epidermal stem cells differentiated only on soft PAAm substrate. The authors hypothesized that the decreased pore size of PAAm correlated with changes in substrate modulus led to variation in collagen tethering and altered differentiation; to verify this, the authors subsequently varied the collagen tethering. Epidermal cell shape and fate were influenced by the distance between the anchoring points. The absence of stiffness dependent spreading and differentiation on PDMS, apparently contradictory to previous findings of cell differentiation dependence on substrate stiffness, can be explained by the ability of seeded cells to remodel the collagen layer present on viscoelastic PDMS, diminishing their sensitivity to substrate stiffness.<sup>347</sup> This study demonstrates the importance of stem cell exerted mechanical forces on substrate-bound ECM, altering the matrix composition on these non-degradable hydrogels, and the influence of traction forces on cell-fate decisions.

Substrate stiffness can have an effect on the phenotypes of numerous other types of cells as well.<sup>27,28,348–352</sup> Robinson *et al.* recently studied the effect of substrate modulus on human vascular endothelial, smooth muscle, and fibroblastic cells using heparinized PEG hydrogels ( $G' \sim 0.3, 5.2, \text{ and } 13.7 \text{ kPa}$ ).<sup>349</sup> Maleimide-functionalized heparin was reacted with thiol-functionalized PEG to form hydrogels, and bioactivity was ensured by the incorporation of fibronectin and growth factors (bFGF or VEGF, depending upon the cell line). The substrate modulus was varied by changing polymer concentration. Differences in cell behavior (attachment, proliferation and gene expression) were observed and correlated with hydrogel modulus. For example, human vascular smooth muscle cells demonstrated



preferential growth on the relatively stiff hydrogel substrate while endothelial cells exhibited preferential growth on the soft substrates. In another example, Murphy and coworkers investigated the effect of substrate stiffness on vascular endothelial cell behavior using polyacrylamide gels with varying modulus (25, 50, and 75 kPa).<sup>353</sup> Umbilical vein (HUVEC), aorta (HAEC), saphenous vein (HSAVEC) and dermal microvasculature (HmVEC) endothelial cells were seeded on hydrogels. It was found that the differences in substrate stiffness influenced cell attachment, spreading, proliferation and migration. For example, an increase in modulus from 25 kPa to 75 kPa resulted in an approximately 75% decrease in HUVEC cell attachment after 24 h. Response to substrate stiffness was cell specific, indicating heterogeneity in the response to biophysical cues. Taken together, these examples highlight the need to determine optimal conditions (*i.e.*, range of moduli) for specific cell types in relevant biomedical applications.

In addition to the impact of substrate stiffness, cells can also sense surface topographical features that can impact cellular properties including cell morphology, adhesion, and differentiation. The native ECM exhibits numerous topographical features, including fibers and sheets with micron and sub-micron dimensions. Two-dimensional hydrogels with topographical features such as grooves and pits thus have been explored as model systems to study such cellular behavior. Poellmann *et al.* used collagen-coated polyacrylamide hydrogels with a micro-patterned array of posts with varied shape and spacing to study the morphologies of murine MSCs.<sup>354</sup> The patterned hydrogel was prepared *via* the polymerization of acrylamide at room temperature with a silicon master pattern floating on top of the prepolymer solution. The patterned posts influenced the cell orientation and the gaps between posts resulted in elongated cell bodies. In another example, Guvendiren and Burdick used micro-scale hydrogel surface wrinkles to modulate hMSC response by changing surface wrinkle size and shapes.<sup>355</sup> The hydrogels were prepared using poly(2-hydroxyethyl methacrylate) (PHEMA) and ethylene glycol dimethacrylate and photopolymerized to a PDMS master to induce surface patterning. It was found that hMSCs took the shape of the pattern, and with high aspect ratio patterns, preferentially differentiated into osteoblasts. When seeded in hexagonal patterns, hMSCs exhibited a rounded morphology and differentiated preferentially into adipocytes. This is consistent with findings of others that have shown directed hMSC differentiation *via* controlled adhesion to micropatterned features<sup>356</sup> and suggests the importance of controlled topography to modulate cell behavior, including user-desired lineage specification for regenerative medicine applications.

**6.2.2 2D dynamic microenvironments.** The ECM is highly dynamic in nature, and temporal changes in topography or modulus can affect cell behavior.<sup>208,357–359</sup> Changes in hydrogel modulus can be achieved through temporally controlled crosslinking or degradation to regulate cell micro-environment elasticity. Young and Engler developed dynamic hydrogels capable of temporal stiffness changes using collagen-coated PEG-HA hydrogels.<sup>357</sup> The hydrogel was prepared by reacting thiol-functionalized HA with acrylate-functionalized

PEG at 37 °C for one hour followed by surface attachment of type I rat tail collagen. The stiffness of their hydrogel increased from 1.9 kPa to 8.2 kPa over 450 hours post-gelation, owing to continued polymerization and crosslinking of the hydrogel. When these hydrogels were tuned to stiffen over timescales consistent with heart muscle development, up to 60% more matured muscle fibers were formed over 2 weeks for the dynamic hydrogels as compared to static polyacrylamide hydrogel controls. The hydrogels were found to be degradable *via* ester hydrolysis with slower kinetics than the continued polymerization. Such an approach can be important for *in vivo* cell-based therapeutic applications where hydrogel-based materials are designed to produce mature cells from injected precursor cells.

Frey and Wang have developed hydrogel compositions for 2D culture in which modulus can be decreased with UV irradiation and degradation, providing a method for probing cellular response to changes in substrate rigidity (Fig. 18).<sup>360</sup> Photodegradable PAAm hydrogels comprising 4-bromomethyl-3-nitrobenzoic acid (BNBA) and polyacrylamide acryl hydrate (PAAH) were prepared on glutaraldehyde-activated coverslips. UV exposure at a dose tolerated by live cells cleaved the nitrobenzyl group and the network, causing the hydrogel to soften by up to 30% (from 7.2 kPa to 5.5 kPa). Softening of hydrogel network led to reduced area of spread 3T3 fibroblasts; further, localized softening of the substrate underlying the leading edge of the cell resulted in pronounced cell retraction, suggesting that mechanosensing was localized to the anterior of polarized cells. In a complementary study, Wang *et al.* studied the deactivation of valvular myofibroblasts to dormant fibroblasts using photodegradable hydrogels.<sup>358</sup> A photodegradable PEG hydrogel (described in Section 5.2.4) was polymerized with an acrylated adhesion peptide (RGDS), and valvular interstitial cells (VICs) were seeded on this photo-responsive hydrogel. When irradiated with light, the modulus of the hydrogel was reduced from 32 kPa to 7 kPa *via in situ* photodegradation, leading to de-activation of myofibroblasts to quiescent fibroblasts, assessed by a decrease in cells positive for  $\alpha$ -smooth muscle actin stress fibers, negligible apoptosis, and changes in cell proliferation and gene expression. These approaches to dynamically control the 2D microenvironment through degradation are complementary to non-degradable approaches.<sup>361,362</sup> In principle, such approaches can be used to probe spatial and temporal response of cells to microenvironment rigidity.

**6.2.3 3D static microenvironments.** While 2D culture has been used widely to study various cellular functions, cells experience a different environment in the native ECM (3D) compared to 2D, owing to differences in cell polarization, surrounding matrix density, and 3D anisotropic presentation of various ECM-based signals. An increasing number of studies accordingly have employed 3D hydrogel microenvironments to study the effect of biophysical cues on cell phenotype and function.<sup>363–366</sup> Here, we review a couple of recent examples of cell-compatible hydrogels that have been used to study cell behavior in 3D microenvironments by providing appropriate biophysical cues.



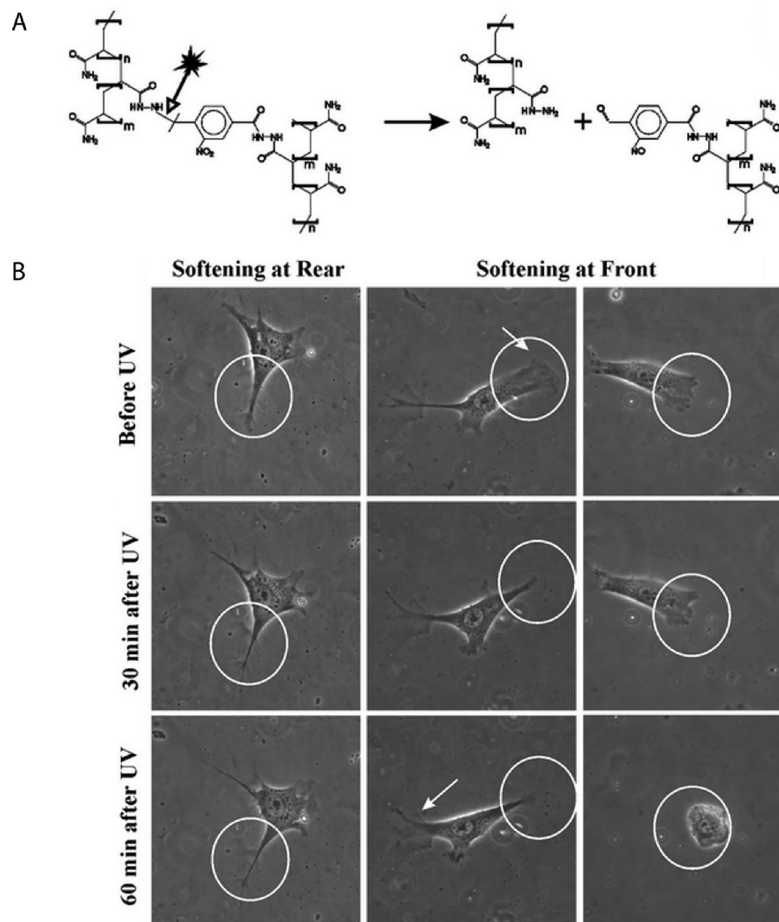


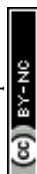
**Fig. 18** Modulation of substrate stiffness in a 2D dynamic microenvironment. (A) Incorporation of a photodegradable nitrobenzyl moiety in a hydrogel network, prepared using polyacrylamide acryl hydrate (PAAH) and a 4-bromomethyl-3-nitrobenzoic acid (BNBA) crosslinker, enabled gel degradation and softening using cytocompatible doses of UV light (365 nm). (B) Softening of the posterior substratum (rear) did not significantly alter cell spreading (left column). However, softening of the anterior substratum (front) led to reverse polarity (central column) or trapping in the softened region (right column; scale bar, 20  $\mu\text{m}$ ). Reprinted from Frey *et al.*<sup>360</sup> with permission from The Royal Society of Chemistry publishing group. Copyright (2009).

To investigate the effect of hydrogel network structure on pericellular and extracellular matrix deposition, Nicodemus *et al.* prepared PEG hydrogels at different polymer concentrations (10, 15 or 20 wt%) *via* photopolymerization of a PEG-diacrylate macromer.<sup>366</sup> Depending upon the polymer and photoinitiator concentrations, crosslink density was varied to form of hydrogels with compressive moduli varying from 60 to 590 kPa. It was found that glycosaminoglycan production was greater in the lowest crosslinked hydrogels. Further, Collagen II and VI, aggrecan, and decorin were found to be localized in the pericellular region and their presence decreased with an increase in the crosslinking. The study thus indicated that changes in hydrogel crosslinking and matrix stiffness could impact the type of tissue deposited and spatial evolution of the tissue.

Mooney and coworkers have recently studied stem cell response to substrate rigidity in three-dimensional micro-environments.<sup>367</sup> Peptide-coupled alginate, agarose, and PEG-dimethacrylate were crosslinked into hydrogel networks (*via* calcium sulfate, physical crosslinking, and free radical polymerization, respectively) in the presence of murine

mesenchymal stem cells (mMSCs). By varying the crosslink density and polymer concentration, it was possible to tune network rigidity ( $E \sim 2.5$  to 11 kPa) and the density of RGD. The commitment of encapsulated murine mesenchymal stem cells to specific differentiation lineages varied with the rigidity of the hydrogel network (*i.e.*, adipogenic and osteogenic lineage predominantly at 2.5–5 kPa and 11–30 kPa, respectively). Further, it was observed that network stiffness regulated integrin binding and adhesion ligand recognition.

To investigate the effect of a static mechanical stress gradient induced by the material geometry, Ruiz and Chen investigated hMSC differentiation in collagen hydrogel cubes formed using a PDMS mold (Fig. 19).<sup>368</sup> Initially, during 2D monolayer culture, cells seeded on the outer edges of an adhesive pattern committed to an osteogenic lineage and interior cells committed to an adipogenic lineage. Using traction force measurements, it was found that the geometry of the pattern induced mechanical stress, which influenced cell fate (high stress regions resulted in osteogenesis, low stress regions resulted in adipogenesis). This finding was translated to 3D hydrogel structures: cells near the edge of 3D cube-shaped collagen constructs differentiated down





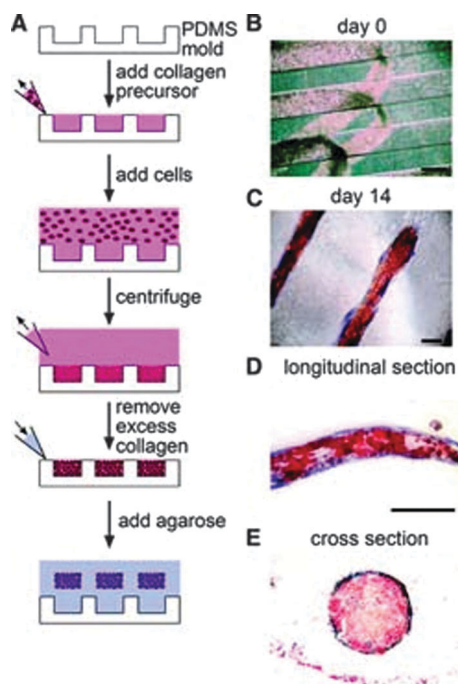


**Fig. 19** Stress gradients within hydrogels influence cell differentiation in three dimensions. (A) Schematics of the process for creating three-dimensional multicellular hydrogels and encapsulating human mesenchymal stem cells (hMSCs). Briefly, prepolymer type I collagen was added to PDMS molds and hMSCs were suspended, before polymerizing at 37 °C. Liquid agarose was added to the mold to encase the collagen hydrogel at 4 °C. (B) Phase image of hMSCs in three-dimensional structures at day 0. (C) The hydrogel constructs with encapsulated hMSCs were suspended in mixed media and after 14 days, the cells at the edge of the constructs differentiated down an osteogenic lineage (blue) and those at the center underwent adipogenesis (red) (oil droplets, alkaline phosphatase staining) (D) Longitudinal section and (E) cross-sections confirmed the patterning of lineage specification in a tension-dependent manner (scale bar, 250  $\mu\text{m}$ ). Reprinted from Ruiz *et al.*<sup>368</sup> with permission from John Wiley and Sons publishing. Copyright (2008).

an osteogenic lineage, and those at the center differentiated down an adipogenic lineage. This study highlights the importance of mechanical patterning for cell differentiation, and

hence provides important insight for designing hydrogels for regenerative medicine.

**6.2.4 3D dynamic microenvironments.** While considerable progress has been made using ECM-mimetic hydrogels to investigate microenvironmental factors that influence cell behavior, the static nature of many 3D hydrogels does not adequately capture the dynamic nature of the *in vivo* ECM. Degradable hydrogels and tunable hydrogel chemistries can be utilized to mimic and probe how temporal microenvironment changes influence cell function and fate. To spatially manipulate cellular microenvironments, Khetan and Burdick developed HA-based hydrogels capable of undergoing multiple modes of crosslinking to create differential network structures (Fig. 20).<sup>369</sup> Acrylated HA was reacted with thiol groups of MMP-degradable peptides to form a hydrogel network in the presence of hMSCs, and secondary crosslinking in select areas was carried out by exposure to UV light using photolithography. The increase in crosslink density upon secondary crosslinking led to an increase in hydrogel stiffness from 6 kPa to 15 kPa in the photopatterned hydrogels. Encapsulated hMSCs exhibited good viability in the HA-hydrogels. Cells encapsulated in the –UV regions were more highly spread and locally degraded the matrix, whereas cells in the +UV region remained rounded with a low aspect ratio. These results demonstrate that secondary crosslinking in the hydrogel network can be employed to modulate cell behavior such as cell outgrowth and spreading.

In the native ECM, the cells can migrate either *via* localized matrix degradation by matrix metalloproteinases (proteolytic migration) or *via* local deformation of the ECM (nonproteolytic, or amoeboid migration). Ehrbar *et al.* took advantage of bio-active PEG hydrogels as an artificial ECM to study the effect of matrix stiffness on migration of encapsulated mouse preosteoblastic cells (MC3T3-E1).<sup>370</sup> Using peptide conjugation, the authors synthesized PEG macromers with a glutamine-acceptor substrate (*n*-PEG-Gln), a lysine-donor substrate containing a MMP-sensitive linker (*n*-PEG-MMP<sub>sensitive</sub>-Lys), and a MMP-insensitive linker (*n*-PEG-MMP<sub>insensitive</sub>-Lys). Thrombin-activated factor XIIIa was used to initiate hydrogel formation in

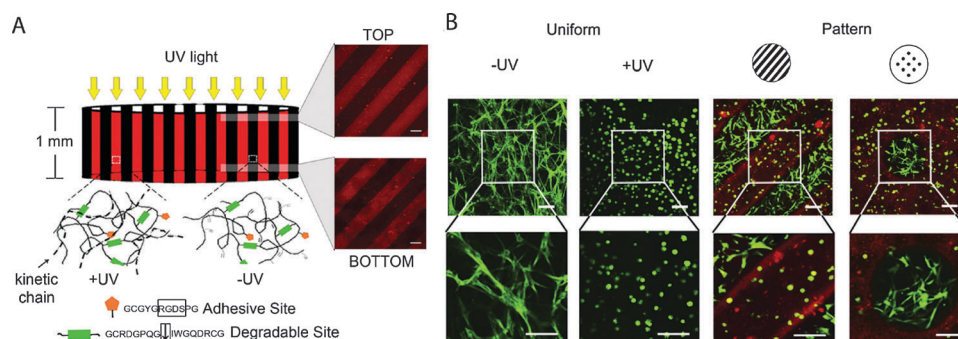


**Fig. 20** Spatiotemporal manipulation of biophysical cues in 3D cell microenvironments. (A) Hydrogels were prepared by reaction of an acrylated PEG macromer with thiol-functionalized, degradable and cell-adhesive peptides using a Michael-type addition reaction (–UV hydrogel, degradable peptide crosslinks), in the presence of an inactive photoinitiator. Using photolithography (4 min with 10 mW  $\text{cm}^{-2}$  at 365 nm), remaining acrylate groups on the PEG macromers in select regions were reacted by photoinitiated free radical polymerization, forming non-degradable covalent crosslinks (+UV hydrogel) (confocal microscopy images show top and bottom surface photopatterned with 250  $\mu\text{m}$  stripes). (B) Encapsulated hMSCs (day 14 stained with calcein) spread only in –UV regions, where the degradable peptide was used as a crosslinker (scale bar, 100  $\mu\text{m}$ ). Reprinted from Khetan *et al.*<sup>369</sup> with permission from Elsevier. Copyright (2010).

presence of cells. By varying the polymer concentration, the modulus of the hydrogel was tuned from  $\sim 100$  Pa to 500 Pa. It was found that cell migration correlated with matrix stiffness, with nonproteolytic migration dominating at lower stiffness and proteolytic migration dominating at higher stiffness.

In another example, Guo *et al.* studied hMSC migration in a controlled 3D hydrogel environment using genetically encoded photoactivatable Rac1 (PA-Rac), a member of the Rho GTPase family that stimulates actin polymerization.<sup>371</sup> Channels were photoetched in real-time using a two-photon microscope, and PA-Rac was activated within cells encapsulated in the hydrogel by local exposure to visible light, inducing directional mobility. At an optimum concentration of YRGDS (2.2 mM), the stiffness of the hydrogel was varied from 12 kPa to 50 kPa and the rate of cell migration increased with increased gel stiffness. The rate of cell migration was higher in photodegraded channels as compared to non-degraded hydrogels. The authors demonstrated the ability to modulate migration speed of encapsulated cells by providing appropriate biophysical cues (*i.e.*, matrix stiffness and degradability) in the presence of appropriate biochemical cues (*i.e.*, adhesive peptides and intracellular signaling proteins).

To investigate the role of biophysical cues in the development of branched tissues, such as kidney, lung, and mammary glands, Gjorevski and Nelson used microfabrication of collagen hydrogels to build model mammary epithelial tissue of well-controlled geometries.<sup>372</sup> The collagen matrix was further crosslinked by incubation in D-ribose at 37 °C for one week before addition of cells, which lead to an increase in matrix stiffness. The epithelial cells adopted the shape and size of the collagen cavities, fabricated using soft lithography, and formed tubules, which remained dormant until the addition of hepatocyte growth factor. Stiffening of the hydrogel network by modulating D-ribose concentration led to an increase in the magnitude of mechanical stress and enhanced branching from the tubule tips. Further, using a finite element method, branching was determined to occur only at locations where dynamic biochemical and biophysical cues reinforced each other, and the magnitude of mechanical stress at branching sites correlated with the extent of branching. Previously, using a similar a collagen-hydrogel system, Nelson *et al.* demonstrated that tissue geometry influences the site of mammary branching morphogenesis.<sup>373</sup>

Recently, Anseth and coworkers developed an enzymatically degradable and photolytically degradable hydrogel platform for spatiotemporally controlling biophysical cues in 3D microenvironments to study critical cues and mechanisms that lead to tissue development and repair.<sup>374</sup> The hydrogel was prepared using a click reaction between PEG-tetracycloctyne and photolabile, enzyme-labile diazide peptide along with an azide-functionalized integrin-binding sequence. Cells were seeded within hydrogel microwells created *via* photolithographic degradation (depth 50–200  $\mu\text{m}$ ), and a second hydrogel layer was added to encapsulate the cells within a 3D microenvironment. This platform enabled the geometry or connectivity of the local matrix to be spatiotemporally modulated in the presence of lung epithelial

cells using cytocompatible light (740 nm, pulsed laser) and cell morphology and phenotype to be easily assessed over time.

## 7. Concluding remarks

The building blocks to control biophysical and biochemical cues within artificial cell microenvironments are rapidly expanding. Hydrolytically, enzymatically, or photolytically degradable moieties have been incorporated in water-soluble monomers and polymers to afford tunable cleavage of synthetic covalently crosslinked extracellular matrices or protein-releasing depots in the presence of cells. Additionally, hydrogels that (dis)assemble based on physical interactions offer shorter-term dynamic control of cell microenvironment structure or chemistry. Within either covalently or physically formed hydrogels, orthogonal chemistries are being utilized in conjunction with degradability for controlled presentation of biochemical cues to promote desired cell behaviors, such as adhesion, spreading, or migration.

The growing number and combinations of degradable chemistries enables precise and dynamic control of the cell microenvironment. Yet, this added complexity necessitates increased development and utilization of *in situ* characterization techniques and predictive modeling to fully realize the power of these tools. Innovative approaches are needed to marry *in situ* hydrogel property characterization with real-time cell response assessment techniques.

Monitoring hydrogel degradation and property evolution *in situ* and in three-dimensions remains limited but offers great promise in correlating real-time microenvironment changes with dynamic cell response. Enzymatically cleavable peptide sequences containing Förster (or fluorescence) resonance energy transfer (FRET) fluorophore-quencher pairs have been developed to observe hydrogel degradation with confocal microscopy.<sup>375</sup> FRET techniques have also been applied to quantitatively analyze interactions at the cell-material interface and assess cell adhesion to integrin-binding peptide sequences.<sup>376,377</sup> Increased deployment of degradation models could facilitate the rational design and understanding of the complex degradation profiles that result with cleavage of multiple labile moieties. For example, individual models have been developed to describe mass loss from hydrolytically,<sup>378</sup> enzymatically,<sup>379</sup> or photolytically<sup>374,390</sup> degradable PEG hydrogels, providing insight into the gel structure, degradation mechanisms, and property evolution. As combinations of different labile chemistries are utilized, integration and expansion of these models will aid in material design and correlating property evolution with biological functions, such as the cleavage of multiple variants of photolabile *o*-nitrobenzyl ether groups for selective cell release.<sup>280</sup> Additionally, advances in techniques to monitor matrix modulus, as a measure of crosslink density and degradation, will provide further insight into complex degradation profiles and mechanisms. Recent advances include the pairing of rheometry and microfluidic sample generation plus microrheology ( $\mu^2$  rheology) to evaluate the full material history over many compositions<sup>380</sup> and microparticle barcoding using stop flow lithography to rapidly generate and assess thousands of hydrogel compositions.<sup>381</sup>



Microrheology has been also used to monitor evolution of the hydrogel modulus *in situ* during degradation.<sup>382</sup>

Focusing on monitoring cell response, cell-exerted traction forces, which vary with matrix modulus, allow in-direct monitoring of hydrogel degradation and cell function changes related to dynamic biophysical matrix cues.<sup>383,384</sup> Additionally, reporter cell lines allow real-time monitoring of transcriptional or cytoskeletal changes in response to microenvironment stimuli.<sup>385</sup> For example, cells can be engineered to produce fluorescent proteins, such as green and red fluorescent protein variants, during transcription of specific gene(s) or fluorescent cytoskeleton fusion proteins for real-time and often high-throughput monitoring of gene expression<sup>361,386,387</sup> and signal transduction,<sup>388</sup> respectively. Incorporation of reporter chemistries and utilization of *in situ* property and cell monitoring techniques such as these will advance our understanding of how degradation-induced, evolving microenvironment properties influence cell function and fate.

Last, incorporation of degradable chemistries to control hydrogel properties largely has been focused on covalent hydrogels. Hydrogels formed by physical interactions, which are increasingly designed using *de novo* principles,<sup>389</sup> can uniquely mimic aspects of the native ECM with properties that span multiple size scales. Incorporation of degradable chemistries within these physical gels or assembling peptides within covalent degradable hydrogels could offer additional handles to control the cell microenvironment and enable new experiments to understand and direct cellular processes. Further, utilization of combinations of degradable chemical linkages could afford complementary control over degradation rates and hydrogel properties. In sum, hydrogels are being designed with degradable chemistries to enable *in situ* property control and dynamically control the cell microenvironment. Degradable materials are promising tools to understand and direct complex biological systems and cell behaviors, such as cell adhesion and spreading, migration, differentiation, proliferation, and apoptosis.

## Acknowledgements

The authors gratefully acknowledge support, for related work in their laboratories, from the National Institutes of Health (Institutional Development Award (IDeA) from the National Institute of General Medical Sciences of the National Institutes of Health (P20GM103541), the INBRE program of the National Institutes of Health (P2012A01377), and the NIDCD (R01DC011377A)), the Nemours Research Foundation, and the University of Delaware Research Foundation. Additionally, the authors would like to thank Matthew Rehmann and Lisa Sawicki for feedback on earlier versions of this manuscript.

## References

- G. Chan and D. J. Mooney, *Trends Biotechnol.*, 2008, **26**, 382–392.
- M. W. Tibbitt and K. S. Anseth, *Biotechnol. Bioeng.*, 2009, **103**, 655–663.
- Biomedical Applications of Hydrogels Handbook*, ed. R. M. Ottenbrite, K. Park and T. Okano, Springer, 2010.
- R. J. Wade and J. A. Burdick, *Mater. Today*, 2012, **15**, 454–459.
- D. Seliktar, *Science*, 2012, **336**, 1124–1128.
- M. S. Rehmann and A. M. Kloxin, *Soft Matter*, 2013, DOI: 10.1039/c3sm50217a.
- N. A. Peppas, J. Z. Hilt, A. Khademhosseini and R. Langer, *Adv. Mater.*, 2006, **18**, 1345–1360.
- C. Wang, R. R. Varshney and D. A. Wang, *Adv. Drug Delivery Rev.*, 2010, **62**, 699–710.
- R. Ulijn, N. Bibi, V. Jayawarna, P. Thornton, S. Todd, R. Mart, A. Smith and J. Gough, *Mater. Today*, 2007, **10**, 40–48.
- B. V. Slaughter, S. S. Khurshid, O. Z. Fisher, A. Khademhosseini and N. A. Peppas, *Adv. Mater.*, 2009, **21**, 3307–3329.
- A. S. Hoffman, *Adv. Drug Delivery Rev.*, 2012, **64**, 18–23.
- D. F. Williams, *Biomaterials*, 2008, **29**, 2941–2953.
- A. B. Lowe, *Polym. Chem.*, 2010, **1**, 17.
- V. A. Liu and S. N. Bhatia, *Biomed. Microdevices*, 2002, **4**, 257–266.
- K. D. Kim and N. M. Wright, *Spine*, 2011, **36**, 1906–1912.
- S. V. Murphy, A. Skardal and A. Atala, *J. Biomed. Mater. Res., Part A*, 2013, **101**, 272–284.
- N. E. Fedorovich, M. H. Oudshoorn, D. van Geemen, W. E. Hennink, J. Alblas and W. J. Dhert, *Biomaterials*, 2009, **30**, 344–353.
- C. C. Lin, A. Raza and H. Shih, *Biomaterials*, 2011, **32**, 9685–9695.
- T. Vermonden, R. Censi and W. E. Hennink, *Chem. Rev.*, 2012, **112**, 2853–2888.
- F. Brandl, F. Sommer and A. Goepferich, *Biomaterials*, 2007, **28**, 134–146.
- T. P. Kraehenbuehl, L. S. Ferreira, P. Zammaretti, J. A. Hubbell and R. Langer, *Biomaterials*, 2009, **30**, 4318–4324.
- N. C. Hunt and L. M. Grover, *Biotechnol. Lett.*, 2010, **32**, 733–742.
- T. Aikawa, T. Konno, M. Takai and K. Ishihara, *Langmuir*, 2012, **28**, 2145–2150.
- S. Sundelacruz and D. L. Kaplan, *Semin. Cell Dev. Biol.*, 2009, **20**, 646–655.
- A. M. Martins, C. M. Alves, F. K. Kasper, A. G. Mikos and R. L. Reis, *J. Mater. Chem.*, 2010, **20**, 1638–1645.
- J. J. Schmidt, J. Rowley and H. J. Kong, *J. Biomed. Mater. Res., Part A*, 2008, **87**, 1113–1122.
- A. J. Engler, S. Sen, H. L. Sweeney and D. E. Discher, *Cell*, 2006, **126**, 677–689.
- D. E. Discher, P. Janmey and Y. L. Wang, *Science*, 2005, **310**, 1139–1143.
- T. Nie, A. Baldwin, N. Yamaguchi and K. L. Kiick, *J. Controlled Release*, 2007, **122**, 287–296.
- S. A. Bencherif, A. Srinivasan, F. Horkay, J. O. Hollinger, K. Matyjaszewski and N. R. Washburn, *Biomaterials*, 2008, **29**, 1739–1749.
- M. Patenaude and T. Hoare, *Biomacromolecules*, 2012, **13**, 369–378.





- 32 J. Eyckmans, T. Boudou, X. Yu and C. S. Chen, *Dev. Cell*, 2011, **21**, 35–47.
- 33 J. D. Kretlow and A. G. Mikos, *AIChE J.*, 2008, **54**, 3048–3067.
- 34 E. C. Novosel, C. Kleinhans and P. J. Kluger, *Adv. Drug Delivery Rev.*, 2011, **63**, 300–311.
- 35 C. C. Lin and K. S. Anseth, *Pharm. Res.*, 2009, **26**, 631–643.
- 36 F. van de Manacker, K. Braeckmans, N. e. Morabit, S. C. De Smedt, C. F. van Nostrum and W. E. Hennink, *Adv. Funct. Mater.*, 2009, **19**, 2992–3001.
- 37 L. M. Weber, C. G. Lopez and K. S. Anseth, *J. Biomed. Mater. Res., Part A*, 2009, **90**, 720–729.
- 38 A. Bertz, S. Wohl-Bruhn, S. Miethe, B. Tiersch, J. Koetz, M. Hust, H. Bunjes and H. Menzel, *J. Biotechnol.*, 2013, **163**, 243–249.
- 39 M. C. Du, W. X. Song, Y. Cui, Y. Yang and J. B. Li, *J. Mater. Chem.*, 2011, **21**, 2228–2236.
- 40 N. A. Peppas and A. R. Khare, *Adv. Drug Delivery Rev.*, 1993, **11**, 1–35.
- 41 C. C. Lin and A. T. Metters, *Adv. Drug Delivery Rev.*, 2006, **58**, 1379–1408.
- 42 M. Martins-Green, in *Principles of Tissue Engineering*, ed. R. Lanza, R. Langer and J. P. Vacanti, Academic Press, 2nd edn, 2000.
- 43 C. M. Nelson and M. J. Bissell, *Annu. Rev. Cell Dev. Biol.*, 2006, **22**, 287–309.
- 44 R. Xu, A. Boudreau and M. J. Bissell, *Cancer Metastasis Rev.*, 2009, **28**, 167–176.
- 45 G. D. Prestwich, *J. Controlled Release*, 2011, **155**, 193–199.
- 46 X. Xu, A. K. Jha, D. A. Harrington, M. C. Farach-Carson and X. Jia, *Soft Matter*, 2012, **8**, 3280–3294.
- 47 A. M. Ferreira, P. Gentile, V. Chiono and G. Ciardelli, *Acta Biomater.*, 2012, **8**, 3191–3200.
- 48 *Engineering Biomaterials for Regenerative Medicine: Novel Technologies for Clinical Applications*, ed. S. K. Bhatia, Springer, 2011.
- 49 Y. Lei, S. Gojgini, J. Lam and T. Segura, *Biomaterials*, 2011, **32**, 39–47.
- 50 H. Geckil, F. Xu, X. Zhang, S. Moon and U. Demirci, *Nanomedicine*, 2010, **5**, 469–484.
- 51 R. A. Marklein and J. A. Burdick, *Adv. Mater.*, 2009, **22**, 175–189.
- 52 J. K. F. Suh and H. W. T. Matthew, *Biomaterials*, 2000, **21**, 2589–2598.
- 53 B. P. Toole, *Nat. Rev. Cancer*, 2004, **4**, 528–539.
- 54 R. Langer and D. A. Tirrell, *Nature*, 2004, **428**, 487–492.
- 55 H. G. Garg and C. A. Hales, *Chemistry and biology of hyaluronan*, Elsevier, Amsterdam, Boston, 2004.
- 56 T. C. Laurent, *The chemistry, biology, and medical applications of hyaluronan and its derivatives*, Portland Press, London, Miami, 1998.
- 57 E. J. Oh, K. Park, K. S. Kim, J. Kim, J. A. Yang, J. H. Kong, M. Y. Lee, A. S. Hoffman and S. K. Hahn, *J. Controlled Release*, 2010, **141**, 2–12.
- 58 D. D. Allison and K. J. Grande-Allen, *Tissue Eng.*, 2006, **12**, 2131–2140.
- 59 A. Almond, *Cell. Mol. Life Sci.*, 2007, **64**, 1591–1596.
- 60 L. Liu, Y. Liu, J. Li, G. Du and J. Chen, *Microb. Cell Fact.*, 2011, **10**, 99.
- 61 N. Izawa, M. Serata, T. Sone, T. Omasa and H. Ohtake, *J. Biosci. Bioeng.*, 2011, **111**, 665–670.
- 62 R. Stern, *Eur. J. Cell Biol.*, 2004, **83**, 317–325.
- 63 J. A. Burdick and G. D. Prestwich, *Adv. Mater.*, 2011, **23**, H41–H56.
- 64 H. Tan, C. R. Chu, K. A. Payne and K. G. Marra, *Biomaterials*, 2009, **30**, 2499–2506.
- 65 R. Jin, L. S. M. Teixeira, A. Krouwels, P. J. Dijkstra, C. A. van Blitterswijk, M. Karperien and J. Feijen, *Acta Biomater.*, 2010, **6**, 1968–1977.
- 66 X. Jia, Y. Yeo, R. J. Clifton, T. Jiao, D. S. Kohane, J. B. Kobler, S. M. Zeitel and R. Langer, *Biomacromolecules*, 2006, **7**, 3336–3344.
- 67 K. S. Masters, D. N. Shah, L. A. Leinwand and K. S. Anseth, *Biomaterials*, 2005, **26**, 2517–2525.
- 68 D. N. Shah, S. M. Recktenwall-Work and K. S. Anseth, *Biomaterials*, 2008, **29**, 2060–2072.
- 69 R. A. Peattie, E. R. Rieke, E. M. Hewett, R. J. Fisher, X. Z. Shu and G. D. Prestwich, *Biomaterials*, 2006, **27**, 1868–1875.
- 70 J. Patterson, R. Siew, S. W. Herring, A. S. Lin, R. Guldberg and P. S. Stayton, *Biomaterials*, 2010, **31**, 6772–6781.
- 71 A. K. Jha, X. Xu, R. L. Duncan and X. Jia, *Biomaterials*, 2011, **32**, 2466–2478.
- 72 R. Elia, D. R. Newhide, P. D. Pedevillano, G. R. Reiss, M. A. Firpo, E. W. Hsu, D. L. Kaplan, G. D. Prestwich and R. A. Peattie, *J. Biomater. Appl.*, 2013, **27**, 749–762.
- 73 R. A. Marklein and J. A. Burdick, *Soft Matter*, 2010, **6**, 136.
- 74 O. A. Lozoya, E. Wauthier, R. A. Turner, C. Barbier, G. D. Prestwich, F. Guilak, R. Superfine, S. R. Lubkin and L. M. Reid, *Biomaterials*, 2011, **32**, 7389–7402.
- 75 X. Xu, A. K. Jha, R. L. Duncan and X. Jia, *Acta Biomater.*, 2011, **7**, 3050–3059.
- 76 *Chitosan-based hydrogels: functions and applications*, ed. K. Yao, J. Li, F. Yao and Y. Yin, CRC Press, 2012.
- 77 J. Zhao, in *Chitosan-based hydrogels: functions and applications*, ed. K. Yao, J. Li, F. Yao and Y. Yin, CRC Press, 2012.
- 78 M. Prabakaran, *J. Biomater. Appl.*, 2008, **23**, 5–36.
- 79 N. Bhattarai, J. Gunn and M. Zhang, *Adv. Drug Delivery Rev.*, 2010, **62**, 83–99.
- 80 S. Lü, M. Liu and B. Ni, *Chem. Eng. J.*, 2010, **160**, 779–787.
- 81 A. Sukarto, C. Yu, L. E. Flynn and B. G. Amsden, *Biomacromolecules*, 2012, **13**, 2490–2502.
- 82 K. M. Park, S. Y. Lee, Y. K. Joung, J. S. Na, M. C. Lee and K. D. Park, *Acta Biomater.*, 2009, **5**, 1956–1965.
- 83 N. D. Leipzig, R. G. Wylie, H. Kim and M. S. Shoichet, *Biomaterials*, 2011, **32**, 57–64.
- 84 S. M. Richardson, N. Hughes, J. A. Hunt, A. J. Freemont and J. A. Hoyland, *Biomaterials*, 2008, **29**, 85–93.
- 85 L. Wang and J. P. Stegemann, *Biomaterials*, 2010, **31**, 3976–3985.
- 86 K. E. Crompton, J. D. Goud, R. V. Bellamkonda, T. R. Gengenbach, D. I. Finkelstein, M. K. Horne and J. S. Forsythe, *Biomaterials*, 2007, **28**, 441–449.





- 87 Y. Zhou, G. Ma, S. Shi, D. Yang and J. Nie, *Int. J. Biol. Macromol.*, 2011, **48**, 408–413.
- 88 C. M. Valmikinathan, V. J. Mukhatyar, A. Jain, L. Karumbaiah, M. Dasari and R. V. Bellamkonda, *Soft Matter*, 2012, **8**, 1964.
- 89 C. McGann and K. Kiick, in *Engineering Biomaterials for Regenerative Medicine: Novel Technologies for Clinical Applications*, ed. S. K. Bhatia, Springer, 2011.
- 90 D. L. Nelson and M. M. Cox, *Lehninger Principles of Biochemistry*, W. H. Freeman, 4th edn, 2008.
- 91 D. L. Rabenstein, *Nat. Prod. Rep.*, 2002, **19**, 312–331.
- 92 J. Turnbull, A. Powell and S. Guimond, *Trends Cell Biol.*, 2001, **11**, 75–82.
- 93 S. Alban, in *Heparin – A Century of Progress*, ed. R. Lever, B. Mulloy and C. P. Page, Springer, 2012, vol. 207.
- 94 A. Greinacher, *Pathophysiol. Haemostasis Thromb.*, 2006, **35**, 37–45.
- 95 C. Melloni, K. P. Alexander, A. Y. Chen, L. K. Newby, M. T. Roe, N. M. A. LaPointe, C. V. Pollack, Jr., W. B. Gibler, E. M. Ohman and E. D. Peterson, *Am. Heart J.*, 2008, **156**, 209–215.
- 96 T. Nie, R. E. Akins, Jr. and K. L. Kiick, *Acta Biomater.*, 2009, **5**, 865–875.
- 97 D. S. Benoit, S. D. Collins and K. S. Anseth, *Adv. Funct. Mater.*, 2007, **17**, 2085–2093.
- 98 M. Kim, Y. J. Kim, K. Gwon and G. Tae, *Macromol. Res.*, 2012, **20**, 271–276.
- 99 U. Freudenberg, A. Hermann, P. B. Welzel, K. Stirl, S. C. Schwarz, M. Grimmer, A. Zieris, W. Panyanuwat, S. Zschoche and D. Meinhold, *Biomaterials*, 2009, **30**, 5049–5060.
- 100 M. Kim, J. Y. Lee, C. N. Jones, A. Revzin and G. Tae, *Biomaterials*, 2010, **31**, 3596–3603.
- 101 S. P. Seto, M. E. Casas and J. S. Temenoff, *Cell Tissue Res.*, 2012, **347**, 589–601.
- 102 R. Wieduwild, M. Tsurkan, K. Chwalek, P. Murawala, M. Nowak, U. Freudenberg, C. Neinhuis, C. Werner and Y. Zhang, *J. Am. Chem. Soc.*, 2013, **135**, 2919–2922.
- 103 G. Tae, Y.-J. Kim, W.-I. Choi, M. Kim, P. S. Stayton and A. S. Hoffman, *Biomacromolecules*, 2007, **8**, 1979–1986.
- 104 A. D. Baldwin, K. G. Robinson, J. L. Militar, C. D. Derby, K. L. Kiick and R. E. Akins, Jr., *J. Biomed. Mater. Res., Part A*, 2012, **100**, 2106–2118.
- 105 O. Jeon, C. Powell, L. D. Solorio, M. D. Krebs and E. Alsberg, *J. Controlled Release*, 2011, **154**, 258–266.
- 106 G. Bhakta, B. Rai, Z. X. H. Lim, J. H. Hui, G. S. Stein, A. J. van Wijnen, V. Nurcombe, G. D. Prestwich and S. M. Cool, *Biomaterials*, 2012, **33**, 6113–6122.
- 107 A. Alshamkhani and R. Duncan, *J. Bioact. Compat. Polym.*, 1995, **10**, 4–13.
- 108 C. Gao, M. Liu, J. Chen and X. Zhang, *Polym. Degrad. Stab.*, 2009, **94**, 1405–1410.
- 109 T. Boonthekul, H. J. Kong and D. J. Mooney, *Biomaterials*, 2005, **26**, 2455–2465.
- 110 Y. N. Dai, P. Li, J. P. Zhang, A. Q. Wang and Q. Wei, *Biopharm. Drug Dispos.*, 2008, **29**, 173–184.
- 111 E. Josef, M. Zilberman and H. Bianco-Peled, *Acta Biomater.*, 2010, **6**, 4642–4649.
- 112 J. Shi, X. Liu, X. Sun and S. Cao, *Polym. Adv. Technol.*, 2011, **22**, 1539–1546.
- 113 L. Zhao, M. D. Weir and H. H. Xu, *Biomaterials*, 2010, **31**, 6502–6510.
- 114 H. Zhou and H. H. Xu, *Biomaterials*, 2011, **32**, 7503–7513.
- 115 W. S. Kim, D. J. Mooney, P. R. Arany, K. Lee, N. Huebsch and J. Kim, *Tissue Eng., Part A*, 2012, **18**, 737–743.
- 116 K. Murakami, H. Aoki, S. Nakamura, S. Nakamura, M. Takikawa, M. Hanzawa, S. Kishimoto, H. Hattori, Y. Tanaka, T. Kiyosawa, Y. Sato and M. Ishihara, *Biomaterials*, 2010, **31**, 83–90.
- 117 J. O. Kim, J. K. Park, J. H. Kim, S. G. Jin, C. S. Yong, D. X. Li, J. Y. Choi, J. S. Woo, B. K. Yoo, W. S. Lyoo, J. A. Kim and H. G. Choi, *Int. J. Pharm.*, 2008, **359**, 79–86.
- 118 B. Balakrishnan, M. Mohanty, P. R. Umashankar and A. Jayakrishnan, *Biomaterials*, 2005, **26**, 6335–6342.
- 119 M. Tang, W. Chen, M. D. Weir, W. Thein-Han and H. H. Xu, *Acta Biomater.*, 2012, **8**, 3436–3445.
- 120 W. H. Tan and S. Takeuchi, *Adv. Mater.*, 2007, **19**, 2696–2701.
- 121 C. Yan, M. E. Mackay, K. Czymbek, R. P. Nagarkar, J. P. Schneider and D. J. Pochan, *Langmuir*, 2012, **28**, 6076–6087.
- 122 M. W. Mosesson, *J. Thromb. Haemostasis*, 2005, **3**, 1894–1904.
- 123 R. F. Doolittle, *Annu. Rev. Biochem.*, 1984, **53**, 195–229.
- 124 T. A. Ahmed, E. V. Dare and M. Hincke, *Tissue Eng., Part B*, 2008, **14**, 199–215.
- 125 D. J. Geer and S. T. Andreadis, *J. Invest. Dermatol.*, 2003, **121**, 1210–1216.
- 126 A. J. Man, H. E. Davis, A. Itoh, J. K. Leach and P. Bannerman, *Tissue Eng., Part A*, 2011, **17**, 2931–2942.
- 127 S. Seetharaman, S. Natesan, R. S. Stowers, C. Mullens, D. G. Baer, L. J. Suggs and R. J. Christy, *Acta Biomater.*, 2011, **7**, 2787–2796.
- 128 H. Hall, *Curr. Pharm. Des.*, 2007, **13**, 3597–3607.
- 129 M. Ahearne, C. T. Buckley and D. J. Kelly, *Biotechnol. Appl. Biochem.*, 2011, **58**, 345–352.
- 130 M. E. Kidd, S. Shin and L. D. Shea, *J. Controlled Release*, 2012, **157**, 80–85.
- 131 C. Scotti, L. Mangiavini, F. Boschetti, F. Vitari, C. Domeneghini, G. Frascini and G. M. Peretti, *Knee Surg Sports Traumatol Arthrosc.*, 2010, **18**, 1400–1406.
- 132 S. Van Vlierberghe, P. Dubruel and E. Schacht, *Biomacromolecules*, 2011, **12**, 1387–1408.
- 133 G. Perale, F. Rossi, E. Sundstrom, S. Bacchiega, M. Masi, G. Forloni and P. Veglianesi, *ACS Chem. Neurosci.*, 2011, **2**, 336–345.
- 134 K. Numata and D. L. Kaplan, *Adv. Drug Delivery Rev.*, 2010, **62**, 1497–1508.
- 135 E. M. Pritchard and D. L. Kaplan, *Expert Opin. Drug Delivery*, 2011, **8**, 797–811.
- 136 S. I. Jeon, J. H. Lee, J. D. Andrade and P. G. De Gennes, *J. Colloid Interface Sci.*, 1991, **142**, 149–158.



- 137 B. D. Cash and B. E. Lacy, *Gastroenterol. Hepatol.*, 2006, **2**, 736–749.
- 138 S. N. S. Alconcel, A. S. Baas and H. D. Maynard, *Polym. Chem.*, 2011, **2**, 1442.
- 139 G. Pasut and F. M. Veronese, *Adv. Drug Delivery Rev.*, 2009, **61**, 1177–1188.
- 140 R. Webster, E. Didier, P. Harris, N. Siegel, J. Stadler, L. Tilbury and D. Smith, *Drug Metab. Dispos.*, 2007, **35**, 9–16.
- 141 C. Fruijtier-Polloth, *Toxicology*, 2005, **214**, 1–38.
- 142 P. K. Working, M. S. Newman, J. Johnson and J. B. Cornacoff, in *Poly(Ethylene Glycol): Chemistry and Biological Applications*, ed. J. M. Harris and S. Zalipsky, Amer Chemical Soc, Washington, 1997, vol. 680, pp. 45–57.
- 143 B. D. Fairbanks, S. P. Singh, C. N. Bowman and K. S. Anseth, *Macromolecules*, 2011, **44**, 2444.
- 144 M. P. Lutolf and J. A. Hubbell, *Biomacromolecules*, 2003, **4**, 713–722.
- 145 K. M. Schultz, A. D. Baldwin, K. L. Kiick and E. M. Furst, *Macromolecules*, 2009, **42**, 5310–5316.
- 146 A. Metters and J. Hubbell, *Biomacromolecules*, 2005, **6**, 290–301.
- 147 A. E. Rydholm, C. N. Bowman and K. S. Anseth, *Biomaterials*, 2005, **26**, 4495–4506.
- 148 A. E. Rydholm, S. K. Reddy, K. S. Anseth and C. N. Bowman, *Polymer*, 2007, **48**, 4589–4600.
- 149 B. D. Fairbanks, M. P. Schwartz, A. E. Halevi, C. R. Nuttelman, C. N. Bowman and K. S. Anseth, *Adv. Mater.*, 2009, **21**, 5005–5010.
- 150 S. B. Anderson, C. C. Lin, D. V. Kuntzler and K. S. Anseth, *Biomaterials*, 2011, **32**, 3564–3574.
- 151 Y. P. Hou, C. A. Schoener, K. R. Regan, D. Munoz-Pinto, M. S. Hahn and M. A. Grunlan, *Biomacromolecules*, 2010, **11**, 648–656.
- 152 J. Kim, T. E. Hefferan, M. J. Yaszemski and L. Lu, *Tissue Eng., Part A*, 2009, **15**, 2299–2307.
- 153 H. Tan, A. J. DeFail, J. P. Rubin, C. R. Chu and K. G. Marra, *J. Biomed. Mater. Res., Part A*, 2010, **92**, 979–987.
- 154 F. P. Brandl, A. K. Seitz, J. K. Tessmar, T. Blunk and A. M. Gopferich, *Biomaterials*, 2010, **31**, 3957–3966.
- 155 C. M. Perez, A. Panitch and J. Chmielewski, *Macromol. Biosci.*, 2011, **11**, 1426–1431.
- 156 V. Chan, P. Zorlutuna, J. H. Jeong, H. Kong and R. Bashir, *Lab Chip*, 2010, **10**, 2062–2070.
- 157 E. A. Phelps, N. O. Enemchukwu, V. F. Fiore, J. C. Sy, N. Murthy, T. A. Sulchek, T. H. Barker and A. J. Garcia, *Adv. Mater.*, 2012, **24**, 64–70, 62.
- 158 D. S. Benoit, M. P. Schwartz, A. R. Durney and K. S. Anseth, *Nat. Mater.*, 2008, **7**, 816–823.
- 159 H. Park, X. Guo, J. S. Temenoff, Y. Tabata, A. I. Caplan, F. K. Kasper and A. G. Mikos, *Biomacromolecules*, 2009, **10**, 541–546.
- 160 G. A. Hudalla, T. S. Eng and W. L. Murphy, *Biomacromolecules*, 2008, **9**, 842–849.
- 161 C. T. Huynh, M. K. Nguyen, J. H. Kim, S. W. Kang, B. S. Kim and D. S. Lee, *Soft Matter*, 2011, **7**, 4974.
- 162 A. A. Aimetti, A. J. Machen and K. S. Anseth, *Biomaterials*, 2009, **30**, 6048–6054.
- 163 F. M. Andreopoulos and I. Persaud, *Biomaterials*, 2006, **27**, 2468–2476.
- 164 G. Papavasiliou, S. Sokic and M. Turturro, *Synthetic PEG Hydrogels as Extracellular Matrix Mimics for Tissue Engineering Applications*, 2012.
- 165 G. Chang, T. Ci, L. Yu and J. Ding, *J. Controlled Release*, 2011, **156**, 21–27.
- 166 M. I. Baker, S. P. Walsh, Z. Schwartz and B. D. Boyan, *J. Biomed. Mater. Res., Part B*, 2012, **100**, 1451–1457.
- 167 M. H. Alves, B. E. Jensen, A. A. Smith and A. N. Zelikin, *Macromol. Biosci.*, 2011, **11**, 1293–1313.
- 168 M. H. Alves, C. J. Young, K. Bozzetto, L. A. Poole-Warren and P. J. Martens, *Biomed. Mater.*, 2012, **7**, 024106.
- 169 D. A. Ossipov and J. Hilborn, *Macromolecules*, 2006, **39**, 1709–1718.
- 170 E. Vidović, D. Klee and H. Höcker, *J. Polym. Sci., Part A: Polym. Chem.*, 2007, **45**, 4536–4544.
- 171 N. Zhang, Y. Shen, X. Li, S. Cai and M. Liu, *Biomed. Mater.*, 2012, **7**, 035014.
- 172 A. Nilasaroya, L. A. Poole-Warren, J. M. Whitelock and P. Jo Martens, *Biomaterials*, 2008, **29**, 4658–4664.
- 173 K. Juntanon, S. Niamlang, R. Rujiravanit and A. Sirivat, *Int. J. Pharm.*, 2008, **356**, 1–11.
- 174 L. Wu and C. S. Brazel, *Int. J. Pharm.*, 2008, **349**, 144–151.
- 175 V. I. Lozinsky, L. G. Damshkaln, B. L. Shaskol'skii, T. A. Babushkina, I. N. Kurochkin and I. I. Kurochkin, *Colloid J.*, 2007, **69**, 747–764.
- 176 S. Samal, F. Chiellini, C. Bartoli, E. Fernandes and E. Chiellini, in *Hydrogels: Biological Properties and Applications*, ed. R. Barbucci, Springer, Milan, 2009, pp. 67–78.
- 177 E. Otsuka and A. Suzuki, *J. Appl. Polym. Sci.*, 2009, **114**, 10–16.
- 178 S. Bonakdar, S. H. Emami, M. A. Shokrgozar, A. Farhadi, S. A. H. Ahmadi and A. Amanzadeh, *Mater. Sci. Eng., C*, 2010, **30**, 636–643.
- 179 K. L. Spiller, J. L. Holloway, M. E. Gribb and A. M. Lowman, *J. Tissue Eng. Regener. Med.*, 2011, **5**, 636–647.
- 180 Z. Y. Peng and Y. Q. Shen, *Polym.-Plast. Technol. Eng.*, 2011, **50**, 245–250.
- 181 J. Michalek, R. Hobzova, M. Pradny and M. Duskova, in *Biomedical Applications of Hydrogels Handbook*, ed. R. M. Ottenbrite, K. Park and T. Okano, Springer, New York, 2010, pp. 303–315.
- 182 S. Atzet, S. Curtin, P. Trinh, S. Bryant and B. Ratner, *Biomacromolecules*, 2008, **9**, 3370–3377.
- 183 S. J. Bryant, J. L. Cuy, K. D. Hauch and B. D. Ratner, *Biomaterials*, 2007, **28**, 2978.
- 184 S. M. Paterson, A. M. A. Shadforth, D. H. Brown, P. W. Madden, T. V. Chirila and M. V. Baker, *Mater. Sci. Eng., C*, 2012, **32**, 2536–2544.
- 185 Y. S. Casadio, D. H. Brown, T. V. Chirila, H.-B. Kraatz and M. V. Baker, *Biomacromolecules*, 2010, **11**, 2949–2959.
- 186 J. T. Zhang, R. Bhat and K. D. Jandt, *Acta Biomater.*, 2009, **5**, 488–497.



- 187 K. Varaprasad, S. Ravindra, N. N. Reddy, K. Vimala and K. M. Raju, *J. Appl. Polym. Sci.*, 2010, **116**, 3593–3602.
- 188 J. R. Santos, N. M. Alves and J. F. Mano, *J. Bioact. Compat. Polym.*, 2010, **25**, 169–184.
- 189 X.-Z. Zhang, X.-D. Xu, S.-X. Cheng and R.-X. Zhuo, *Soft Matter*, 2008, **4**, 385.
- 190 A. K. Andrianov and R. Langer, *Polyphosphazenes for Biomedical Applications*, John Wiley and Sons, 2009.
- 191 K. Y. Lee and D. J. Mooney, *Chem. Rev.*, 2001, **101**, 1869–1880.
- 192 H. R. Allcock, *Soft Matter*, 2012, **8**, 7521–7532.
- 193 C. Chun, S. M. Lee, C. W. Kim, K.-Y. Hong, S. Y. Kim, H. K. Yang and S.-C. Song, *Biomaterials*, 2009, **30**, 4752–4762.
- 194 T. Potta, C. Chun and S.-C. Song, *Biomaterials*, 2010, **31**, 8107–8120.
- 195 Y. Li, J. Rodrigues and H. Tomás, *Chem. Soc. Rev.*, 2012, **41**, 2193–2221.
- 196 G. G. Odian, *Principles of polymerization*, Wiley-Interscience, Hoboken, NJ, 2004.
- 197 C. N. Salinas and K. S. Anseth, *Macromolecules*, 2008, **41**, 6019–6026.
- 198 J. L. Iffkovits and J. A. Burdick, *Tissue Eng.*, 2007, **13**, 2369–2385.
- 199 A. D. Rouillard, C. M. Berglund, J. Y. Lee, W. J. Polacheck, Y. Tsui, L. J. Bonassar and B. J. Kirby, *Tissue Eng., Part C*, 2011, **17**, 173–179.
- 200 J. A. Burdick, A. J. Peterson and K. S. Anseth, *Biomaterials*, 2001, **22**, 1779–1786.
- 201 M. Malkoch, R. Vestberg, N. Gupta, L. Mespouille, P. Dubois, A. F. Mason, J. L. Hedrick, Q. Liao, C. W. Frank, K. Kingsbury and C. J. Hawker, *Chem. Commun.*, 2006, 2774–2776.
- 202 M. D. Brigham, A. Bick, E. Lo, A. Bendali, J. A. Burdick and A. Khademhosseini, *Tissue Eng., Part A*, 2008, **15**, 1645–1653.
- 203 S. Khetan, J. S. Katz and J. A. Burdick, *Soft Matter*, 2009, **5**, 1601–1606.
- 204 S. Ekici, P. Ilgin, S. Butun and N. Sahiner, *Carbohydr. Polym.*, 2011, **84**, 1306–1313.
- 205 A. M. Kloxin, A. M. Kasko, C. N. Salinas and K. S. Anseth, *Science*, 2009, **324**, 59–63.
- 206 X. Dai, X. Chen, L. Yang, S. Foster, A. J. Coury and T. H. Jozefiak, *Acta Biomater.*, 2011, **7**, 1965–1972.
- 207 A. Morelli and F. Chiellini, *Macromol. Chem. Phys.*, 2010, **211**, 821–832.
- 208 M. Guvendiren and J. A. Burdick, *Nat. Commun.*, 2012, **3**, 792.
- 209 K. Matyjaszewski, K. L. Beers, A. Kern and S. G. Gaynor, *J. Polym. Sci., Part A: Polym. Chem.*, 1998, **36**, 823–830.
- 210 J. A. Yoon, S. A. Bencherif, B. Aksak, E. K. Kim, T. Kowalewski, J. K. Oh and K. Matyjaszewski, *Chem.-Asian J.*, 2011, **6**, 128–136.
- 211 J. A. Yoon, J. K. Oh, W. Li, T. Kowalewski and K. Matyjaszewski, in *Hydrogel Micro and Nanoparticles*, Wiley-VCH Verlag GmbH & Co. KGaA, 2012, pp. 169–186.
- 212 B. D. Fairbanks, M. P. Schwartz, A. E. Halevi, C. R. Nuttallman, C. N. Bowman and K. S. Anseth, *Adv. Mater.*, 2009, **21**, 5005–5010.
- 213 H. C. Kolb, M. G. Finn and K. B. Sharpless, *Angew. Chem., Int. Ed.*, 2001, **40**, 2004–2021.
- 214 J. E. Moses and A. D. Moorhouse, *Chem. Soc. Rev.*, 2007, **36**, 1249–1262.
- 215 C. R. Becer, R. Hoogenboom and U. S. Schubert, *Angew. Chem., Int. Ed.*, 2009, **48**, 4900–4908.
- 216 C. A. Deforest, E. A. Sims and K. S. Anseth, *Chem. Mater.*, 2010, **22**, 4783–4790.
- 217 S. Q. Liu, P. L. Ee, C. Y. Ke, J. L. Hedrick and Y. Y. Yang, *Biomaterials*, 2009, **30**, 1453–1461.
- 218 C. A. DeForest, B. D. Polizzotti and K. S. Anseth, *Nat. Mater.*, 2009, **8**, 659–664.
- 219 J. F. Lutz and Z. Zarafshani, *Adv. Drug Delivery Rev.*, 2008, **60**, 958–970.
- 220 M. Malkoch, R. Vestberg, N. Gupta, L. Mespouille, P. Dubois, A. F. Mason, J. L. Hedrick, Q. Liao, C. W. Frank, K. Kingsbury and C. J. Hawker, *Chem. Commun.*, 2006, 2774.
- 221 C. M. Nimmo and M. S. Shoichet, *Bioconjugate Chem.*, 2011, **22**, 2199–2209.
- 222 V. V. Rostovtsev, L. G. Green, V. V. Fokin and K. B. Sharpless, *Angew. Chem., Int. Ed.*, 2002, **41**, 2596–2599.
- 223 V. Crescenzi, L. Cornelio, C. Di Meo, S. Nardecchia and R. Lamanna, *Biomacromolecules*, 2007, **8**, 1844–1850.
- 224 G. Testa, C. Di Meo, S. Nardecchia, D. Capitani, L. Mannina, R. Lamanna, A. Barbetta and M. Dentini, *Int. J. Pharm.*, 2009, **378**, 86–92.
- 225 S. Piluso, B. Hiebl, S. N. Gorb, A. Kovalev, A. Lendlein and A. T. Neffe, *Int. J. Artif. Organs*, 2011, **34**, 192–197.
- 226 M. van Dijk, C. F. van Nostrum, W. E. Hennink, D. T. S. Rijkers and R. M. J. Liskamp, *Biomacromolecules*, 2010, **11**, 1608–1614.
- 227 M. G. Finn and V. V. Fokin, *Chem. Soc. Rev.*, 2010, **39**, 1231–1232.
- 228 J. A. Codelli, J. M. Baskin, N. J. Agard and C. R. Bertozzi, *J. Am. Chem. Soc.*, 2008, **130**, 11486–11493.
- 229 J. C. Jewett and C. R. Bertozzi, *Chem. Soc. Rev.*, 2010, **39**, 1272–1279.
- 230 J. Xu, T. M. Fillion, F. Prifti and J. Song, *Chem.-Asian J.*, 2011, **6**, 2730–2737.
- 231 J. Zheng, L. A. S. Callahan, J. Hao, K. Guo, C. Wesdemiotis, R. A. Weiss and M. L. Becker, *ACS Macro Lett.*, 2012, **1**, 1071–1073.
- 232 A. Sanyal, *Macromol. Chem. Phys.*, 2010, **211**, 1417–1425.
- 233 H.-L. Wei, Z. Yang, H.-J. Chu, J. Zhu, Z.-C. Li and J.-S. Cui, *Polymer*, 2010, **51**, 1694–1702.
- 234 C. M. Nimmo, S. C. Owen and M. S. Shoichet, *Biomacromolecules*, 2011, **12**, 824–830.
- 235 H. Tan, J. P. Rubin and K. G. Marra, *Macromol. Rapid Commun.*, 2011, **32**, 905–911.
- 236 M. L. Blackman, M. Royzen and J. M. Fox, *J. Am. Chem. Soc.*, 2008, **130**, 13518–13519.
- 237 J. C. Jewett and C. R. Bertozzi, *Chem. Soc. Rev.*, 2010, **39**, 1272–1279.
- 238 N. K. Devaraj, R. Weissleder and S. A. Hilderbrand, *Bioconjugate Chem.*, 2008, **19**, 2297.

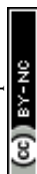


- 239 R. Pipkorn, W. Waldeck, B. Diding, M. Koch, G. Mueller, M. Wiessler and K. Braun, *J. Pept. Sci.*, 2009, **15**, 235–241.
- 240 D. S. Liu, A. Tangpeerachaikul, R. Selvaraj, M. T. Taylor, J. M. Fox and A. Y. Ting, *J. Am. Chem. Soc.*, 2012, **134**, 792–795.
- 241 C. E. Hoyle and C. N. Bowman, *Angew. Chem., Int. Ed.*, 2010, **49**, 1540–1573.
- 242 M. J. Kade, D. J. Burke and C. J. Hawker, *J. Polym. Sci., Part A: Polym. Chem.*, 2010, **48**, 743–750.
- 243 A. Gress, A. Völkel and H. Schlaad, *Macromolecules*, 2007, **40**, 7928–7933.
- 244 A. Dondoni, *Angew. Chem., Int. Ed.*, 2008, **47**, 8995–8997.
- 245 B. D. Fairbanks, M. P. Schwartz, A. E. Halevi, C. R. Nuttelman, C. N. Bowman and K. S. Anseth, *Adv. Mater.*, 2009, **21**, 5005–5010.
- 246 H. Shih and C. C. Lin, *Biomacromolecules*, 2012, **13**, 2003–2012.
- 247 S. B. Anderson, C. C. Lin, D. V. Kuntzler and K. S. Anseth, *Biomaterials*, 2011, **32**, 3564–3574.
- 248 Y. Lei and T. Segura, *Biomaterials*, 2009, **30**, 254–265.
- 249 A. D. Baldwin and K. L. Kiick, *Polym. Chem.*, 2013, **4**, 133–143.
- 250 C. L. McGann, E. A. Levenson and K. L. Kiick, *Macromol. Chem. Phys.*, 2013, **214**, 203–213.
- 251 G. N. Grover, J. Lam, T. H. Nguyen, T. Segura and H. D. Maynard, *Biomacromolecules*, 2012, **13**, 3013–3017.
- 252 I. Migneault, C. Dartiguenave, M. J. Bertrand and K. C. Waldron, *BioTechniques*, 2004, **37**, 790–806.
- 253 R. M. Broyer, E. Schopf, C. M. Kolodziej, Y. Chen and H. D. Maynard, *Soft Matter*, 2011, **7**, 9972–9977.
- 254 L. Zhao, L. Zhu, F. Liu, C. Liu, D. Shan, Q. Wang, C. Zhang, J. Li, J. Liu, X. Qu and Z. Yang, *Int. J. Pharm.*, 2011, **410**, 83–91.
- 255 M. M. Abdel-Mottaleb, N. D. Mortada, A. A. El-Shamy and G. A. Awad, *Drug Dev. Ind. Pharm.*, 2009, **35**, 311–320.
- 256 H. Hosseinkhani, M. Hosseinkhani, A. Khademhosseini and H. Kobayashi, *J. Controlled Release*, 2007, **117**, 380–386.
- 257 J. N. Hunt, K. E. Feldman, N. A. Lynd, J. Deek, L. M. Campos, J. M. Spruell, B. M. Hernandez, E. J. Kramer and C. J. Hawker, *Adv. Mater.*, 2011, **23**, 2327–2331.
- 258 D.-Y. Ji, T.-F. Kuo, H.-D. Wu, J.-C. Yang and S.-Y. Lee, *Carbohydr. Polym.*, 2012, **89**, 1123–1130.
- 259 Y. H. Lin, H. F. Liang, C. K. Chung, M. C. Chen and H. W. Sung, *Biomaterials*, 2005, **26**, 2105–2113.
- 260 M. Matyash, F. Despang, R. Mandal, D. Fiore, M. Gelinsky and C. Ikonomidou, *Tissue Eng., Part A*, 2012, **18**, 55–66.
- 261 B. A. Aguado, W. Mulyasasmita, J. Su, K. J. Lampe and S. C. Heilshorn, *Tissue Eng., Part A*, 2012, **18**, 806–815.
- 262 M. J. Nugent and C. L. Higginbotham, *Eur. J. Pharm. Biopharm.*, 2007, **67**, 377–386.
- 263 K. Rajagopal, M. S. Lamm, L. A. Haines-Butterick, D. J. Pochan and J. P. Schneider, *Biomacromolecules*, 2009, **10**, 2619–2625.
- 264 M. C. Branco, D. J. Pochan, N. J. Wagner and J. P. Schneider, *Biomaterials*, 2010, **31**, 9527–9534.
- 265 Z. Li and T. J. Deming, *Soft Matter*, 2010, **6**, 2546.
- 266 M. J. Glassman, J. Chan and B. D. Olsen, *Adv. Funct. Mater.*, 2012, **23**, 1182–1193.
- 267 S. Koutsopoulos, L. D. Unsworth, Y. Nagai and S. Zhang, *Proc. Natl. Acad. Sci. U. S. A.*, 2009, **106**, 4623–4628.
- 268 Y. Nagai, L. D. Unsworth, S. Koutsopoulos and S. Zhang, *J. Controlled Release*, 2006, **115**, 18–25.
- 269 C. T. S. W. P. Foo, J. S. Lee, W. Mulyasasmita, A. Parisi-Amon and S. C. Heilshorn, *Proc. Natl. Acad. Sci. U. S. A.*, 2009, **106**, 22067–22072.
- 270 Y. Liu, B. Liu, J. J. Riesberg and W. Shen, *Macromol. Biosci.*, 2011, **11**, 1325–1330.
- 271 K. L. Kiick, *Soft Matter*, 2008, **4**, 29–37.
- 272 N. Yamaguchi, L. Zhang, B. S. Chae, C. S. Palla, E. M. Furst and K. L. Kiick, *J. Am. Chem. Soc.*, 2007, **129**, 3040–3041.
- 273 S. H. Kim and K. L. Kiick, *Macromol. Rapid Commun.*, 2010, **31**, 1231–1240.
- 274 D. S. Benoit, A. R. Durney and K. S. Anseth, *Tissue Eng.*, 2006, **12**, 1663–1673.
- 275 Z. Zhang, J. Ni, L. Chen, L. Yu, J. Xu and J. Ding, *Biomaterials*, 2011, **32**, 4725–4736.
- 276 C. R. Nuttelman, A. M. Kloxin and K. S. Anseth, in *Tissue Eng*, ed. J. P. Fisher, Springer-Verlag Berlin, Berlin, 2006, vol. 585, pp. 135–149.
- 277 S. Sahoo, C. Chung, S. Khetan and J. A. Burdick, *Biomacromolecules*, 2008, **9**, 1088–1092.
- 278 A. D. Baldwin and K. L. Kiick, *Bioconjugate Chem.*, 2011, **22**, 1946–1953.
- 279 A. M. Kloxin, M. W. Tibbitt, A. M. Kasko, J. A. Fairbairn and K. S. Anseth, *Adv. Mater.*, 2010, **22**, 61–66.
- 280 D. R. Griffin and A. M. Kasko, *J. Am. Chem. Soc.*, 2012, **134**, 13103–13107.
- 281 Y. S. Jo, J. Gantz, J. A. Hubbell and M. P. Lutolf, *Soft Matter*, 2008, **5**, 440–446.
- 282 N. A. Peppas, J. Z. Hilt, A. Khademhosseini and R. Langer, *Adv. Mater.*, 2006, **18**, 1345–1360.
- 283 P. J. Martens, S. J. Bryant and K. S. Anseth, *Biomacromolecules*, 2003, **4**, 283–292.
- 284 N. C. Hunt, A. M. Smith, U. Gbureck, R. M. Shelton and L. M. Grover, *Acta Biomater.*, 2010, **6**, 3649–3656.
- 285 K. J. Lampe, K. B. Bjugstad and M. J. Mahoney, *Tissue Eng., Part A*, 2010, **16**, 1857–1866.
- 286 F. Lee, J. E. Chung and M. Kurisawa, *J. Controlled Release*, 2009, **134**, 186–193.
- 287 S. J. Buwalda, L. Calucci, C. Forte, P. J. Dijkstra and J. Feijen, *Polymer*, 2012, **53**, 2809–2817.
- 288 R. S. Ashton, A. Banerjee, S. Punyani, D. V. Schaffer and R. S. Kane, *Biomaterials*, 2007, **28**, 5518–5525.
- 289 J. X. Tan, X. Y. Wang, H. Y. Li, X. L. Su, L. Wang, L. Ran, K. Zheng and G. S. Ren, *Int. J. Cancer*, 2011, **128**, 1303–1315.
- 290 J. Patterson and J. A. Hubbell, *Biomaterials*, 2010, **31**, 7836–7845.
- 291 M. C. Giano, D. J. Pochan and J. P. Schneider, *Biomaterials*, 2011, **32**, 6471–6477.
- 292 L. Li, Z. Tong, X. Jia and K. L. Kiick, *Soft Matter*, 2013, **9**, 665–673.
- 293 D. Seliktar, A. H. Zisch, M. P. Lutolf, J. L. Wrana and J. A. Hubbell, *J. Biomed. Mater. Res., Part A*, 2004, **68**, 704–716.





- 294 V. W. Wong, K. C. Rustad, M. G. Galvez, E. Neofytou, J. P. Glotzbach, M. Januszyk, M. R. Major, M. Sorkin, M. T. Longaker and J. Rajadas, *Tissue Eng., Part A*, 2010, **17**, 631–644.
- 295 C. Yang, L. Xu, Y. Zhou, X. M. Zhang, X. Huang, M. Wang, Y. Han, M. L. Zhai, S. C. Wei and J. Q. Li, *Carbohydr. Polym.*, 2010, **82**, 1297–1305.
- 296 J. Patterson, R. Siew, S. W. Herring, A. S. Lin, R. Guldberg and P. S. Stayton, *Biomaterials*, 2010, **31**, 6772–6781.
- 297 J. Kim, I. S. Kim, T. H. Cho, K. B. Lee, S. J. Hwang, G. Tae, I. Noh, S. H. Lee, Y. Park and K. Sun, *Biomaterials*, 2007, **28**, 1830–1837.
- 298 M. Patenaude and T. Hoare, *ACS Macro Lett.*, 2012, **1**, 409–413.
- 299 J. N. Brantley, K. M. Wiggins and C. W. Bielawski, *Science*, 2011, **333**, 1606–1609.
- 300 D. P. Jones, J. L. Carlson, P. S. Samiec, P. Sternberg, Jr., V. C. Mody, Jr., R. L. Reed and L. A. Brown, *Clin. Chim. Acta*, 1998, **275**, 175–184.
- 301 J. M. Estrela, A. Ortega and E. Obrador, *Crit. Rev. Clin. Lab. Sci.*, 2006, **43**, 143–181.
- 302 R. Franco, O. J. Schoneveld, A. Pappa and M. I. Panayiotidis, *Arch. Physiol. Biochem.*, 2007, **113**, 234–258.
- 303 A. Sanyal, *Macromol. Chem. Phys.*, 2010, **211**, 1417–1425.
- 304 H. L. Wei, J. Yang, H. J. Chu, Z. Yang, C. C. Ma and K. Yao, *J. Appl. Polym. Sci.*, 2011, **120**, 974–980.
- 305 K. C. Koehler, D. L. Alge, K. S. Anseth and C. N. Bowman, *Biomaterials*, 2013, **34**, 4150–4158.
- 306 G. Pasparakis, T. Manouras, P. Argitis and M. Vamvakaki, *Macromol. Rapid Commun.*, 2012, **33**, 183–198.
- 307 B. D. Fairbanks, S. P. Singh, C. N. Bowman and K. S. Anseth, *Macromolecules*, 2011, **44**, 2444–2450.
- 308 A. Skardal, S. F. Sarker, A. Crabbe, C. A. Nickerson and G. D. Prestwich, *Biomaterials*, 2010, **31**, 8426–8435.
- 309 N. Fomina, C. L. McFearn, M. Sermsakdi, J. M. Morachis and A. Almutairi, *Macromolecules*, 2011, **44**, 8590–8597.
- 310 C. K. Choi, M. T. Breckenridge and C. S. Chen, *Trends Cell Biol.*, 2010, **20**, 705–714.
- 311 M. P. Lutolf, P. M. Gilbert and H. M. Blau, *Nature*, 2009, **462**, 433–441.
- 312 A. L. Berrier and K. M. Yamada, *J. Cell Physiol.*, 2007, **213**, 565–573.
- 313 L. H. Romer, K. G. Birukov and J. G. Garcia, *Circ. Res.*, 2006, **98**, 606–616.
- 314 H. Studenovska, P. Vodicka, V. Proks, J. Hlucilova, J. Motlik and F. Rypacek, *J. Tissue Eng. Regener. Med.*, 2010, **4**, 454–463.
- 315 M. Zhou, A. M. Smith, A. K. Das, N. W. Hodson, R. F. Collins, R. V. Ulijn and J. E. Gough, *Biomaterials*, 2009, **30**, 2523–2530.
- 316 I. Jun, K. M. Park, D. Y. Lee, K. D. Park and H. Shin, *Macromol. Res.*, 2011, **19**, 911–920.
- 317 M. S. Weiss, B. P. Bernabe, A. Shikanov, D. A. Bluver, M. D. Mui, S. Shin, L. J. Broadbelt and L. D. Shea, *Biomaterials*, 2012, **33**, 3548–3559.
- 318 R. O. Hynes, *Cell*, 2002, **110**, 673–687.
- 319 R. Liddington and M. Ginsberg, *J. Cell Biol.*, 2002, **158**, 833–839.
- 320 C. A. DeForest and K. S. Anseth, *Nat. Chem.*, 2011, **3**, 925–931.
- 321 J. W. Lee, Y. J. Park, S. J. Lee, S. K. Lee and K. Y. Lee, *Biomaterials*, 2010, **31**, 5545–5551.
- 322 S. P. Zustiak, R. Durbal and J. B. Leach, *Acta Biomater.*, 2010, **6**, 3404–3414.
- 323 R. Ayala, C. Zhang, D. Yang, Y. Hwang, A. Aung, S. S. Shroff, F. T. Arce, R. Lal, G. Arya and S. Varghese, *Biomaterials*, 2011, **32**, 3700–3711.
- 324 B. Alberts, A. Johnson, J. Lewis, M. Raff, K. Roberts and P. Walter, *Molecular Biology of the Cell*, Garland Science, 4th edn, 2002.
- 325 A. J. Ridley, M. A. Schwartz, K. Burridge, R. A. Firtel, M. H. Ginsberg, G. Borisy, J. T. Parsons and A. R. Horwitz, *Science*, 2003, **302**, 1704–1709.
- 326 M. P. Schwartz, B. D. Fairbanks, R. E. Rogers, R. Rangarajan, M. H. Zaman and K. S. Anseth, *Integr. Biol.*, 2010, **2**, 32–40.
- 327 D. Guarnieri, A. De Capua, M. Ventre, A. Borzacchiello, C. Pedone, D. Marasco, M. Ruvo and P. A. Netti, *Acta Biomater.*, 2010, **6**, 2532–2539.
- 328 P. Tayalia and D. J. Mooney, *Adv. Mater.*, 2009, **21**, 3269–3285.
- 329 A. Zieris, K. Chwalek, S. Prokoph, K. R. Levental, P. B. Welzel, U. Freudenberg and C. Werner, *J. Controlled Release*, 2011, **156**, 28–36.
- 330 C. C. Lin and K. S. Anseth, *Proc. Natl. Acad. Sci. U. S. A.*, 2011, **108**, 6380–6385.
- 331 I. Konstantinova, G. Nikolova, M. Ohara-Imaizumi, P. Meda, T. Kucera, K. Zarbalis, W. Wurst, S. Nagamatsu and E. Lammert, *Cell*, 2007, **129**, 359–370.
- 332 R. G. Wylie, S. Ahsan, Y. Aizawa, K. L. Maxwell, C. M. Morshead and M. S. Shoichet, *Nat. Mater.*, 2011, **10**, 799–806.
- 333 S. E. Kendall, J. Najbauer, H. F. Johnston, M. Z. Metz, S. Li, M. Bowers, E. Garcia, S. U. Kim, M. E. Barish and K. S. Aboody, *Stem Cells*, 2008, **26**, 1575–1586.
- 334 D. P. Cross and C. Wang, *Pharm. Res.*, 2011, **28**, 2477–2489.
- 335 X. Zhao, S. Jain, H. B. Larman, S. Gonzalez and D. J. Irvine, *Biomaterials*, 2005, **26**, 5048–5063.
- 336 X. Li, X. Liu, W. Zhao, X. Wen and N. Zhang, *Acta Biomater.*, 2012, **8**, 2087–2095.
- 337 J. C. Garbern, E. Minami, P. S. Stayton and C. E. Murry, *Biomaterials*, 2011, **32**, 2407–2416.
- 338 T. Diab, E. M. Pritchard, B. A. Uhrig, J. D. Boerckel, D. L. Kaplan and R. E. Guldberg, *J. Mech. Behav. Biomed. Mater.*, 2011, **11**, 123–131.
- 339 M. W. Tibbitt, B. W. Han, A. M. Kloxin and K. S. Anseth, *J. Biomed. Mater. Res., Part A*, 2012, **100**, 1647–1654.
- 340 S. A. Oh, H. Y. Lee, J. H. Lee, T. H. Kim, J. H. Jang, H. W. Kim and I. Wall, *Tissue Eng., Part A*, 2012, **18**, 1087–1100.
- 341 T. R. Hoare and D. S. Kohane, *Polymer*, 2008, **49**, 1993–2007.
- 342 L. Wei, C. Cai, J. Lin and T. Chen, *Biomaterials*, 2009, **30**, 2606–2613.



- 343 F. Guilak, D. M. Cohen, B. T. Estes, J. M. Gimble, W. Liedtke and C. S. Chen, *Cell Stem Cell*, 2009, **5**, 17–26.
- 344 A. J. Engler, M. A. Griffin, S. Sen, C. G. Bonnemann, H. L. Sweeney and D. E. Discher, *J. Cell Biol.*, 2004, **166**, 877–887.
- 345 F. Rehfeldt, A. E. X. Brown, M. Raab, S. S. Cai, A. L. Zajac, A. Zemel and D. E. Discher, *Integr. Biol.*, 2012, **4**, 422–430.
- 346 B. Trappmann, J. E. Gautrot, J. T. Connelly, D. G. T. Strange, Y. Li, M. L. Oyen, M. A. C. Stuart, H. Boehm, B. Li, V. Vogel, J. P. Spatz, F. M. Watt and W. T. S. Huck, *Nat. Mater.*, 2012, **11**, 642–649.
- 347 O. Chaudhuri and D. J. Mooney, *Nat. Mater.*, 2012, **11**, 568–569.
- 348 H. N. Chia, M. Vigen and A. M. Kasko, *Acta Biomater.*, 2012, **8**, 2602–2611.
- 349 K. G. Robinson, T. Nie, A. D. Baldwin, E. C. Yang, K. L. Kiick and R. E. Akins, Jr., *J. Biomed. Mater. Res., Part A*, 2012, **100**, 1356–1367.
- 350 B. C. Isenberg, P. A. Dimilla, M. Walker, S. Kim and J. Y. Wong, *Biophys. J.*, 2009, **97**, 1313–1322.
- 351 O. V. Sazonova, K. L. Lee, B. C. Isenberg, C. B. Rich, M. A. Nugent and J. Y. Wong, *Biophys. J.*, 2011, **101**, 622–630.
- 352 A. A. Chen, S. R. Khetani, S. Lee, S. N. Bhatia and K. J. Van Vliet, *Biomaterials*, 2009, **30**, 1113–1120.
- 353 J. A. Wood, N. M. Shah, C. T. McKee, M. L. Houghbanks, S. J. Liliensiek, P. Russell and C. J. Murphy, *Biomaterials*, 2011, **32**, 5056–5064.
- 354 M. J. Poellmann, P. A. Harrell, W. P. King and A. J. W. Johnson, *Acta Biomater.*, 2010, **6**, 3514–3523.
- 355 M. Guvendiren and J. A. Burdick, *Biomaterials*, 2010, **31**, 6511–6518.
- 356 K. A. Kilian, B. Bugarija, B. T. Lahn and M. Mrksich, *Proc. Natl. Acad. Sci. U. S. A.*, 2010, **107**, 4872–4877.
- 357 J. L. Young and A. J. Engler, *Biomaterials*, 2011, **32**, 1002–1009.
- 358 H. Wang, S. M. Haeger, A. M. Kloxin, L. A. Leinwand and K. S. Anseth, *PLoS One*, 2012, **7**, e39969.
- 359 A. M. Kloxin, J. A. Benton and K. S. Anseth, *Biomaterials*, 2010, **31**, 1–8.
- 360 M. T. Frey and Y. L. Wang, *Soft Matter*, 2009, **5**, 1918–1924.
- 361 S. Raghavan, R. A. Desai, Y. Kwon, M. Mrksich and C. S. Chen, *Langmuir*, 2010, **26**, 17733.
- 362 M. Guvendiren and J. A. Burdick, *Adv. Healthcare Mater.*, 2013, **2**, 155–164.
- 363 S. S. Rao, S. Bentil, J. DeJesus, J. Larison, A. Hissong, R. Dupais, A. Sarkar and J. O. Winter, *PLoS One*, 2012, **7**, e35852.
- 364 J. S. Choi and B. A. Harley, *Biomaterials*, 2012, **33**, 4460–4468.
- 365 K. Bott, Z. Upton, K. Schrobback, M. Ehrbar, J. A. Hubbell, M. P. Lutolf and S. C. Rizzi, *Biomaterials*, 2010, **31**, 8454–8464.
- 366 G. D. Nicodemus, S. C. Skaalure and S. J. Bryant, *Acta Biomater.*, 2011, **7**, 492–504.
- 367 N. Huebsch, P. R. Arany, A. S. Mao, D. Shvartsman, O. A. Ali, S. A. Bencherif, J. Rivera-Feliciano and D. J. Mooney, *Nat. Mater.*, 2010, **9**, 518–526.
- 368 S. A. Ruiz and C. S. Chen, *Stem Cells*, 2008, **26**, 2921–2927.
- 369 S. Khetan and J. A. Burdick, *Biomaterials*, 2010, **31**, 8228–8234.
- 370 M. Ehrbar, A. Sala, P. Lienemann, A. Ranga, K. Mosiewicz, A. Bittermann, S. C. Rizzi, F. E. Weber and M. P. Lutolf, *Biophys. J.*, 2011, **100**, 284–293.
- 371 Q. Guo, X. Wang, M. W. Tibbitt, K. S. Anseth, D. J. Montell and J. H. Elisseeff, *Biomaterials*, 2012, **33**, 8040–8046.
- 372 N. Gjorevski and C. M. Nelson, *Integr. Biol.*, 2010, **2**, 424–434.
- 373 C. M. Nelson, M. M. Vanduijn, J. L. Inman, D. A. Fletcher and M. J. Bissell, *Science*, 2006, **314**, 298–300.
- 374 A. M. Kloxin, K. J. Lewis, C. A. Deforest, G. Seedorf, M. W. Tibbitt, V. Balasubramaniam and K. S. Anseth, *Integr. Biol.*, 2012, **4**, 1540–1549.
- 375 S. H. Lee, J. J. Moon, J. S. Miller and J. L. West, *Biomaterials*, 2007, **28**, 3163–3170.
- 376 H. J. Kong, T. R. Polte, E. Alsberg and D. J. Mooney, *Proc. Natl. Acad. Sci. U. S. A.*, 2005, **102**, 4300–4305.
- 377 N. D. Huebsch and D. J. Mooney, *Biomaterials*, 2007, **28**, 2424–2437.
- 378 A. T. Metters, C. N. Bowman and K. S. Anseth, *J. Phys. Chem. B*, 2000, **104**, 7043–7049.
- 379 M. A. Rice, J. Sanchez-Adams and K. S. Anseth, *Biomacromolecules*, 2006, **7**, 1968–1975.
- 380 K. M. Schultz and E. M. Furst, *Soft Matter*, 2012, **8**, 6198–6205.
- 381 D. C. Appleyard, S. C. Chapin, R. L. Srinivas and P. S. Doyle, *Nat. Protoc.*, 2011, **6**, 1761–1774.
- 382 K. M. Schultz, A. D. Baldwin, K. L. Kiick and E. M. Furst, *ACS Macro Lett.*, 2012, **1**, 706–708.
- 383 C. Franck, S. A. Maskarinec, D. A. Tirrell and G. Ravichandran, *PLoS One*, 2011, **6**, e17833.
- 384 N. Gjorevski and C. M. Nelson, *Biophys. J.*, 2012, **103**, 152–162.
- 385 B. N. Giepmans, S. R. Adams, M. H. Ellisman and R. Y. Tsien, *Science*, 2006, **312**, 217–224.
- 386 S. Gobaa, S. Hoehnel, M. Roccio, A. Negro, S. Kobel and M. P. Lutolf, *Nat. Methods*, 2011, **8**, 949–955.
- 387 S. Alimperti, P. Lei, J. Tian and S. T. Andreadis, *Gene Ther.*, 2012, **19**, 1123–1132.
- 388 M. W. Tibbitt, A. M. Kloxin, K. U. Dyamenahalli and K. S. Anseth, *Soft Matter*, 2010, **6**, 5100.
- 389 A. L. Boyle and D. N. Woolfson, *Chem. Soc. Rev.*, 2011, **40**, 4295–4306.
- 390 M. W. Tibbitt, A. M. Kloxin, L. A. Sawicki and K. S. Anseth, *Macromolecules*, 2013, **46**, 2785–2792.

